

AMERICAN UNIVERSITY OF BEIRUT

DEVELOPMENT OF NOVEL METAL ORGANIC
FRAMEWORKS BASED CATALYSTS FOR BIO-FUEL
PRODUCTION

by
GHEWA ALI ALSABEH

A thesis
submitted in partial fulfillment of the requirements
for the degree of Master of Arts
to the Department of Chemistry
of the Faculty of Arts and Sciences
at the American University of Beirut

Beirut, Lebanon
October 2020

AMERICAN UNIVERSITY OF BEIRUT

DEVELOPMENT OF NOVEL METAL ORGANIC
FRAMEWORKS BASED CATALYSTS FOR BIO-FUEL
PRODUCTION

by
GHEWA ALI ALSABEH

Approved by:



Dr. Mohamad Hmadeh, Associate Professor
Department of Chemistry

Advisor



Dr. Tarek Ghaddar, Professor
Department of Chemistry

Member of Committee



Dr. Pierre Karam, Associate Professor
Department of Chemistry

Member of Committee

Date of thesis/dissertation defense: October 13, 2020

AMERICAN UNIVERSITY OF BEIRUT

DEVELOPMENT OF NOVEL ORGANIC FRAMEWORKS BASED CATALYSTS FOR BIO-FUEL PRODUCTION

Student Name: ___ AlSabeh _____ Ghewa _____ Ali _____
Last First Middle

Master's Thesis Master's Project Doctoral Dissertation

I authorize the American University of Beirut to: (a) reproduce hard or electronic copies of my thesis, dissertation, or project; (b) include such copies in the archives and digital repositories of the University; and (c) make freely available such copies to third parties for research or educational purposes.

I authorize the American University of Beirut, to: (a) reproduce hard or electronic copies of it; (b) include such copies in the archives and digital repositories of the University; and (c) make freely available such copies to third parties for research or educational purposes

after:

One ---- year from the date of submission of my thesis, dissertation, or project.

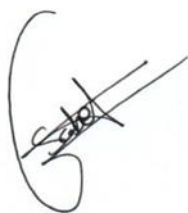
Two ---- years from the date of submission of my thesis, dissertation, or project.

Three years from the date of submission of my thesis, dissertation, or project.

___ Ghewa Ali AlSabeh _____ October 15, 2020 _____

Signature

Date



ACKNOWLEDGMENTS

I would like to start my words by thanking the one who I will never be able to return his favor no matter what, my advisor Dr. Mohamad Hmadeh. Being a member of his team was a great opportunity that I am very grateful to, and I consider myself blessed for. Over the past three years, he wasn't only a mentor, but also a backbone and a friend. He was always there for me, guiding me patiently in my research, increasing my curiosity, and encouraging me to become not only a better version of myself but also the future scientist I wish to be. I would also like to express my great appreciation and earnest gratitude for my committee members, Dr. Pierre Karam, and Dr. Tarek Ghaddar, for their on-point feedback, important comments and constructive suggestions, that I wouldn't be able to fulfill my thesis without. I also want to thank Dr. Hmadeh, Dr. Ghaddar another time and Dr. Saliba for their very strong recommendation letters they have sent for my PhD application, that I wouldn't be able to pursue my PhD without. In addition, a great thanks for the Central Research Science Laboratory (CRSL), to Ms. Rania Shatila and Mr. Joan Younes in particular, for their time and efforts in training me, and solving my countless problems with the machines.

A warm thanks goes to my lab mate, friends and colleagues, who I shared with the greatest and toughest moments of my last three years: Asma, Mahmoud, Rawan, Zeinab, Manal, Salah, Zahraa, Rawan, Patrick, and Meghrie. Last but not least, my greatest acknowledgement goes to my family, especially to my parents and sisters. I am very thankful for their unconditional love and support, for the details they took care of, for always making me feel that I am the only one existing in this universe, for their encouragement to pursue my dreams, and for always being there for me, no matter what.

AN ABSTRACT OF THE THESIS OF

Ghewa AlSabeH for

Master of Science

Major: Chemistry

Title: Development of Novel Metal Organic Frameworks Based Catalysts for Bio-Fuel Production

The global energy demand is dramatically increasing, and the dependence is on petroleum fossil fuels. Liquid biofuels, such as ethanol and biodiesel, are considered great alternatives to fossil fuels in the transportation sector. Butyl levulinate which is produced through the esterification reaction of butanol and levulinic acid in the presence of a catalyst, is considered as one of the most promising fossil fuel substitutes. The conventional catalyst for this reaction is sulphuric acid, which is known to be corrosive, environmentally hazardous, and hard to recover and recycle. In this work, Metal Organic Frameworks known as MOFs are employed as heterogeneous catalysts for butyl levulinate production. MOFs are a new class of porous crystalline solids consisting of metal ions linked to organic ligands via strong coordination bonds and arranged in extended networks. Their extraordinary characteristics including large surface area, stability, presence of accessible metal sites, and high porosity give them great potentials in various fields ranging from catalysis, gas separation, to adsorption. The thrust of this research project is to understand the relation between the synthesis, composition, structure and properties of the catalyst materials. To this end, MOF-74 which could incorporate different metals (e.g. Mg, Zn, Mn, Co, and Ni) are synthesized and fully characterized by XRD, TGA, SEM, IR and BET measurements. Their catalytic activity in the esterification to butyl levulinate is further investigated by detecting the produced ester on GC. Moreover, MOF catalysts will be loaded by magnetic nanoparticles to produce magnetic metal organic framework composites (MFCs). The resulting MFCs will be used to enhance the separation process from the reaction media. This work sheds light on the effect of designing MOFs' structures to serve as efficient catalysts for the production of esters that are of industrial relevance in the biofuel sector.

CONTENTS

ACKNOWLEDGMENTS	v
AN ABSTRACT OF THE THESIS OF	vi
CONTENTS.....	vii
ILLUSTRATIONS	ix
TABLES	xi
CHAPTER I LITERATURE REVIEW	1
A. OVERIEW	1
B. Energy Consumption and the Deviation toward Renewables.....	2
C. Biofuels and Biofuel Additives.....	3
1. Bioethanol and Biodiesel	3
2. Levulinic Acid (LA).....	5
3. Butyl Levulinate (BL)	6
D. Catalysts for Esterification Reactions	7
1. Homogenous Catalysts.....	7
2. Heterogenous Catalysts	7
E. Metal Organic Frameworks (MOFs)	9
1. Overview	9
2. Synthetic Routes of MOFs	11
3. Properties of MOFs	15
4. Acidity in MOFs	20
5. Applications of MOFs.....	25
6. Structure of MOF-74.....	30
F. Magnetic Framework Composites (MFCs)	31
G. Objectives.....	35
CHAPTER II MATERIALS AND METHODS.....	38
A. Synthesis of MOF-74	38
1. Solvothermal MOFs	38
2. Cu-MOF-74.....	39
B. Synthesis of Magnetic Framework Composites (MFCs).....	40
1. Synthesis of Magnetite (Fe ₃ O ₄) Magnetic Nanoparticles (NPs)	40

2.	MFCs.....	40
C.	Room Temperature MOFs.	41
1.	RT-Zn-MOF-74	41
2.	Mixed Metals (RT-Zn/Mn-MOF-74, and RT-Co/Mg-MOF-74).....	41
D.	Characterization Techniques.....	41
1.	Powder X-Ray Diffraction	41
2.	Thermogravimetric analysis.....	41
3.	Scanning Electron Microscopy	42
4.	Brunauer–Emmett–Teller (BET) surface area measurement.....	42
5.	Atomic Adsorption Spectroscopy	42
E.	Esterification Reaction of Butyl Levulinate (BL).....	42
F.	Gas Chromatography Sampling (GC).....	43
G.	Catalyst Recycling	46
CHAPTER III RESULTS AND DISCUSSIONS		47
A.	Powder X-Ray Diffraction (PXRD).....	47
B.	Thermogravimetric analysis (TGA).....	49
C.	Atomic Adsorption (AA)	52
D.	Scanning Electron Microscopy (SEM)	52
E.	Brunauer–Emmett–Teller (BET)	56
F.	Esterification Reaction of Butyl Levulinate	59
1.	Different Solvothermal MOFs	60
2.	Catalyst Recycling	64
3.	Nano-Scaled Room Temperature MOFs.....	66
4.	Magnetic Framework Composites (MFCs).....	67
G.	Mechanism of Esterification Reaction	69
H.	Discussion of Results	69
CHAPTER IV CONCLUSION AND FUTURE WORK.....		73
REFERENCES		78

ILLUSTRATIONS

Figure

1.1 Derivatives of Levulinic Acid.....	5
1.2 The metal ions and the organic linkers making the extended MOF structure.....	10
1.3 The progress in the synthesis of MOFs with high surface areas.....	16
1.4 (A) Various secondary building units showing the different metal oxide clusters. (B) Different organic linkers. H4DOBDC = 2,5-Dihydroxyterephthalic acid; H3BTC = Benzene-1,3,5-tricarboxylic acid; H3THBTS = 2,4,6-Trihydroxybenzene-1,3,5-trisulfonic acid; H2BPDC = 4,4'-Biphenyldicarboxylic acid; DCDPBN = 6,6'-Dichloro-4,4'-di(pyridin-4-yl)-[1,1'-binaphthalene]-2,2'-diol; H3BTB = 1,3,5-Tris(4-carboxyphenyl)benzene; ADP = Adipic acid; H4ADB = 5,5'-(Diazene-1,2-diyl)diisophthalic acid; TIPA = Tris(4-(1H-imidazol-1-yl)phenyl)amine; H3ImDC = 4,5-Imidazoledicarboxylic acid.....	19
1.5 Lewis acidic site (unsaturated metal center) made by the loss of oxygen from a solvent molecule.....	21
1.6 Various Brønsted sites in MOFs.....	23
1.7 (A) Crystal structure of MOF-74, shown along the c axis, revealing the 1D honeycomb-like pores. (B) Coordination mode of the metal atom showing the rod-like secondary building unit. Color code: metal: cyan, oxygen: purple, and carbon: blue....	31
1.8 (A) Embedding and (B) mixing procedures for preparing MFCs.....	34
Scheme 1 Esterification reaction setup.....	35
Scheme 2 Great magnetic separation of the MFC from the reaction medium.....	36
2.1 Synthetic route for producing MOF-74 samples.....	39
2.2 Calibration curve based on Y and X ratios.....	45
3.1 PXRD patterns of (A) solvothermal synthesized MOFs, (B) MFCs, and (C) room temperature synthesized MOFs.....	48
3.2 TGA curves for (A) solvothermal synthesized MOFs, (B) MFCs, and (C) room temperature synthesized MOFs.....	50
3.3 SEM images of (A) Zn-MOF-74, (B) Mn-MOF-74, (C) Ni-MOF-74, (D) Co-MOF-74, (E) Mg-MOF-74, and (F) Cu-MOF-74.....	53
3.4 SEM images of magnetite Fe ₃ O ₄	53
3.5 SEM images of (A) Zn-MOF-74 free of any nanoparticles, (B) MFC1, (C) MFC2, and (D) MFC3, taken at different scales.....	54

3.6 EDX mapping for (A) MFC1, (B) MFC2 and (C) MFC3. Color code: green dots represent Zn element, and red dots represent Fe element.....	55
3.7 SEM images of nano-scaled MOFs (A) RT-Zn-MOF-74, (B) RT-Zn/Mn-MOF-74 and (C) RT-Co/Mg-MOF-74.	56
3.8 N ₂ isotherms for (A) solvothermal MOFs, (B) MFCs and (C) room temperature MOFs.	57
3.9 Conversion of butyl levulinate for the different catalysts as function of time (hour).....	61
3.10 Butyl levulinate conversion under the effect of different Zn-MOF-74 loading.....	62
3.11 Butyl levulinate conversion under the effect Zn-MOF-74 at different temperatures.	63
3.12 (A) PXRD pattern of Zn-MOF-74 before and after testing. (B) butyl levulinate conversion after two regeneration cycles.....	64
3.13 Butyl levulinate conversion with the catalysis of nano-scaled MOFs.....	67
3.14 Conversion to butyl levulinate with the various composites and the magnetite nanoparticles.....	68
3.15 Conversion to butyl levulinate under 5 wt% of the tested samples.....	71
4.1 (A) PXRD and (B) SEM of MW-AUBM1.....	75
4.2 SEM images of (A) MW-MIL-88B and (B) MW-Ti-MOF-74.....	75
4.3 Conversion Percentage for MW-MIL-88B compared to Zn-MOF-74.....	76

TABLES

Table	
2.1 Metal salts used for synthesizing the used MOFs.....	39
2.2 Calibration curve standards and their corresponding peak area (average over 3 runs).....	44
3.1 BET surface areas and pore volumes for the tested catalysts.	59
3.2 Various catalyst used for butyl levulinate synthesis.....	71

CHAPTER I

LITERATURE REVIEW

A. OVERVIEW

Day by day, the global energy need is increasing dramatically with enormous dependence on petroleum derived fuels constituting around three quarters of the energy mix.¹ Taking into consideration the environmental deterioration, economical restrictions, and gradual depletion of fossil resources caused by excessive usage of fossil fuels, the world is now directed toward establishing a more sustainable energy system through exploring new environmentally friendly chemicals that are able to satisfy the energy demand serving as biofuel or biofuel additives.² Recently, new investigations have been sought worldwide to study chemical or biological conversion of biomass into fuels and raw materials³ in which n-butyl levulinate is one of these explored chemicals. Butyl levulinate is an ester that it is characterized by fuel like properties and it can be obtained by the esterification reaction of levulinic acid and butanol in the presence of suitable acid catalyst, usually sulphuric acid.⁴

As mentioned before, the esterification reaction is catalysed by acid catalysts in which homogenous ones are commonly used such as sulphuric acid. However, their disadvantages are so many in a way that the shift to other catalysts is a need. On the other hand, heterogenous catalysts are being explored for esterification reactions due to their better properties. Some of these investigated catalysts include zeolites, metal oxides, and resins.⁵⁻⁷

Recently, a new class of porous materials is being explored for catalysis and it is expressed by metal organic frameworks (MOFs).⁸ MOFs are porous crystalline solids composed of inorganic metal cluster connected to organic linkers via strong coordination bonds and arranged in extended networks.⁹⁻¹⁰ Because of their unprecedented characteristics, MOFs grabbed the attention in the field of material chemistry, and are widely used in enormous applications especially in the catalysis field due to their ability of incorporating active sites into their metal clusters, organic linkers, or porous network.¹¹ Extra functionality can be accessed to the MOFs through the addition of magnetic nanoparticles (magnetite) to them in a way they become what's known by magnetic framework composite (MFC) with special magnetic properties making their recovery easily attained.¹² Our project is to explore an isorecticular series of MOF-74 as acid catalysts for the esterification to butyl levulinate starting from levulinic acid and butanol.

B. Energy Consumption and the Deviation toward Renewables

Accompanied with the nowadays modernization, worldwide development and high living standards, the energy needs are drastically expanding.¹ The need's satisfaction is based on existing finite energy sources in which fossil fuels are considered the most dominating ones such as petroleum products, coal, and natural gases. These fuels are of non-renewable nature, have elevated importing prices and high energy costs because of their limited amounts, in addition to causing ecological deterioration as a result of emitting greenhouse gases. Based on this, the shift to finding sustainable energy sources has been the public's stimulus.¹³ An appropriate alternative

must be renewable, eco-friendly, and cost-effective to solve the energy problem.¹⁴ However, up till today, there doesn't exist a full alternative to fossil fuels. Several countries are trying to nourish the renewable energy uses through their regulations. For example, the European Union (EU) has customized a 2020 grand in which every EU member state must share a minimum of 10% renewable energy through transportations.

Because of their low cost, diesel fuels are more abundant than gasoline engines even though they are higher in particulate matter, carbon monoxide, and nitrogen oxide (NO_x) emissions.¹⁵ As a result, controlling the exhaust emissions is crucial in light of protecting the environment with strict gas regulations. This can be achieved by certain fuel modifications including decreasing sulfur content, reducing aromatics, raising cetane number, increasing the volatility of the fuel, or blending the diesel with oxygenates.¹⁵ Oxygenated fuels are the fuels having oxygen atoms in their formula. When they are added to diesel fuels, they improve combustion efficiency by increase the fuel burning, increase power production, and decreases the exhaust emission of polluting gases.¹⁶ Biofuels (bioethanol, biodiesel...) and alkyl levulinate such as methyl, ethyl and butyl levulinate originating from levulinic acid are examples of oxygenated compounds that succeeded in being great fuel additives.¹⁷

C. Biofuels and Biofuel Additives

1. Bioethanol and Biodiesel

Biofuels are the fuels used for transportation and derived from biomass materials such as ethanol, and biodiesel. They can be used independently as fuel materials, but they are usually used as additives for petroleum fuels (diesel, and gasoline). While

blending, the usage of non-renewable fuels decreases the consumption of them, leading to shrinking the amount of imported crude oil. Moreover, biodiesel and ethanol are cleaner fuels that, when burned, don't release polluting gases. Ethanol is characterized by its high-octane number resulting in great spark-ignition engine fuel, whereas, diesels are known for their high cetane number thus being good engine fuels.¹⁸

Ethanol, an alcohol of molecular formula C_2H_5OH , is obtained through fermentation of simple sugars resulting from vegetables materials (glucose, fructose...). Recently, it is commercially obtained from the sugar of the grains, like corn, sorghum, and barley. In addition, it is also produced from sugar beets, rice, cassava, potato skins, tree bark and the like. It is noteworthy to mention that corn is the main constituent for deriving ethanol fuel in the United States. Speaking about numbers, the worldwide ethanol production increased tremendously from 4 billion gallons in 1990, to 26.6 billion gallons in 2016.¹⁹ Nowadays, approximately all of the sold gasoline in the US has around 10% ethanol by volume.²⁰

Biodiesel is another commonly used biofuel that is generated from oily plants such as oil palm, sunflower, or soybean and from animal sources (Beef and sheep tallow).²¹ They are the monoalkyl esters of the fatty acids originating from sustainable biolipids. Biodiesels are used in diesel engines since they burn like petroleum diesel and has higher productivity than gasoline. In addition, the HHVs (higher heating values) of biodiesels (39-41 MJ/kg) are considered high and very close to that of petroleum (43 MJ/kg). In addition to ethanol and biodiesel, other biofuels like methanol, butanol, and dimethyl ether, are still developing in the field.²¹

2. Levulinic Acid (LA)

4-Oxypentanoic acid or Levulinic acid (LA), is a versatile basic chemical that is derived from acid catalyzed degradation of polysaccharides such as cellulose, and has been recognized as one of the top chemistry building blocks by the United States Department of Energy in 2004 and 2010,²² in addition to its extraordinary role in biofuel generation.²³

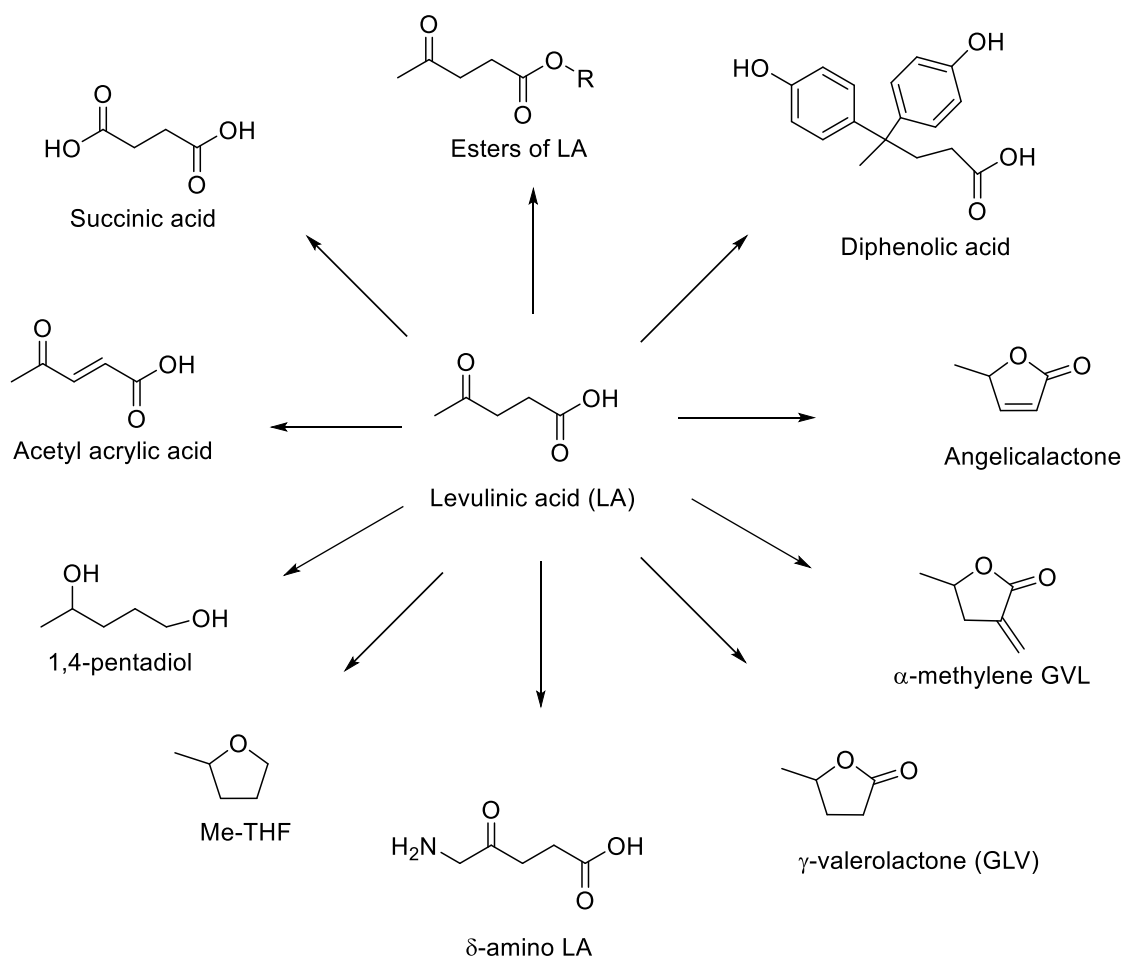


Figure 1.1 Derivatives of Levulinic Acid.

Because it contains more than one functional group (carbonyl and carboxyl group) as shown in **Figure 1.1**, several compounds can be produced from levulinic acid other than levulinate esters such as acrylic acid, δ -amino levulinic acid, γ -valerolactone,

2-methyltetrahydrofuran, α angelica lactone, 1,4-pentanediol, β -acetylacrylic acid, and other chemicals that can be used in various industrial fields.²⁴⁻²⁶

Moreover, LA undergoes chemical reactions that yield compounds that are useful in electronics, plasticizers, pharmaceuticals, batteries, adsorbents, coating polymers, fuels, herbicides and so much more.²⁷⁻²⁸

3. *Butyl Levulinate (BL)*

n-Butyl levulinate (BL) is one of levulinate esters that is produced by the esterification reaction of Levulinic acid with n-butanol. It has been recognized as a multipurpose feedstock that is used widely in the organic synthesis, plasticizing agents' production, , and flavoring industry.²⁹

Because of its fuel like properties, n-butyl levulinate has been investigated to be used as a fragrance gasoline and diesel fuel additive because of its ability to boost conductivity of the diesel fuel, its lubricity, and diminish emissions in addition to its low toxicity, and mild flow property. Moreover, butyl levulinate boils within the diesel range, and has a steady flash point that is high enough to suit the requirements of diesel fuels.²³

Speaking about fuel properties, the cetane number is a measure of the diesel's value and performance. It indicates the ability of autoignition of the fuel when placed in the engine, in a way that higher octane numbers mean better fuel burning.³⁰ Another used indicator for the fuel properties is the octane number, that rates the quality of its combustion. Same to cetane number, higher octane ratings, the better the fuel performance. The difference between the two is that cetane number refers to the diesel, whereas octane number is related to gasoline. BL has very low cetane number (less than

15) in which regular cetane number of diesel ranges from 48 to 50. However, cetane improver additives, such as 2-ethylhexyl nitrate, can be added to the ester before being mixed with the diesel. Moreover, it has high blending octane number (near 100) that increases the performance of the gasoline engines.³¹

Even though the literature focused the most on the production of ethyl levulinate among other levulinate esters, recent studies have shown that BL has more potentials when it comes to diesel blending.³²⁻³³

D. Catalysts for Esterification Reactions

1. Homogenous Catalysts

Generally, mineral acids like sulfuric acid and hydrofluoric acid are the conventional used catalysts in the reactions of obtaining alkyl levulinates such as butyl levulinate.³⁴ However, the usage of such homogenous catalysts has many drawbacks because of their non-eco-friendly nature where they cause reactor corrosion in addition to the fact that they are hard to be regenerated. Moreover, they are separated through neutralization by washing the reaction mixture with water that leads to wastewater generation and biodiesel loss because of water.³⁴ As a result, the amount of required catalysts will be higher which increases the costs of production. Consequently, the shift to new green heterogenous catalysts for biodiesel development has been an urging need.

2. Heterogenous Catalysts

In general, a catalyst must be specific, selective, and able to yield high amounts of biodiesel. Concerning solid catalysts, they should be highly stable, porous, of high

surface area, cost affordable and most importantly possessing enormous acid sites. Recently, heterogenous catalysts were able to prove themselves in industrial fields because of their unique catalytic advantageous when compared to their homogenous analogue. For example, a solid catalyst doesn't lead to corrosion and is easily removed from the reaction medium without wastewater regeneration and biodiesel loss. Add to that, many of them have the ability to be regenerated preserving the same catalysis activity, and thus used for many times rather than once as in homogenous catalysis making them not only eco-friendly but also cost effective. Nevertheless, heterogenous catalysts are still inferior to homogenous catalysts when it comes to their performance.

Numerous heterogenous catalysts have been developed for the esterification reaction of butyl levulinate from levulinic acid and butanol, such as zeolites,⁴ heteropoly acids,³⁵ silicas,³⁶ ion exchange resins,³⁷ and other catalysts. However, these catalysts are exposed to loss of active sites through leaching, large mass transfer resistance, and small catalytic activity.

Zeolites are the most available and used heterogenous catalysts, they have proved their success in the field and have been employed directly after their synthesis in the 1960s.³⁸ Massive studies have been conducted on the investigation of zeolites as catalysts in gas, and liquid-phase reactions leading to the accumulation of huge data amounts reported in the literature.³⁹⁻⁴⁰ Moreover, they have been used in wide ranging petrochemical industries, reduction of car flue gas, and considered promising materials of high potentials in biomass transformations.^{4, 41-43} Their strong acid strength, high chemical and thermal stability, in addition to their high suitability to nearly all types of catalysis make them superior to other conventional catalysts.⁴⁴ However, their low surface area and low prediction design for new emerging materials are major drawbacks,

and their great sensitivity makes them susceptible to deactivation due to permanent adsorption or steric blockage of large products. Moreover, the micropores of zeolites cause certain diffusion limitations of the reacting materials and/or produced ones in the liquid-phase reactions. With all these downsides, it was a necessity to find alternative heterogenous catalysts to replace zeolites. Because of their large porosity, their rich metal content and their tunability, metal organic frameworks (MOFs) were the perfect candidates for the job, where they were able to surpass all other competing heterogenous catalysts.

E. Metal Organic Frameworks (MOFs)

1. Overview

Reticular chemistry, the chemistry concerned with sewing molecular building blocks by robust linkages to form highly fashioned and extended frameworks, is expanding in a spectacular manner for the last 25 years.⁴⁵⁻⁴⁶ This chemistry allowed the discovery of new class of crystalline hybrid materials, in which the precise and controlled metal organic frameworks (MOFs) are at the basis of it. In a simple way, MOFs are the highly ordered class of crystalline porous materials consisting of metal ion “joints” in the form of secondary building unit (SBU), strongly linked to organic linkers “struts”, and expanded in all directions forming extended coordination networks as represented in **Figure 1.2**.⁴⁷

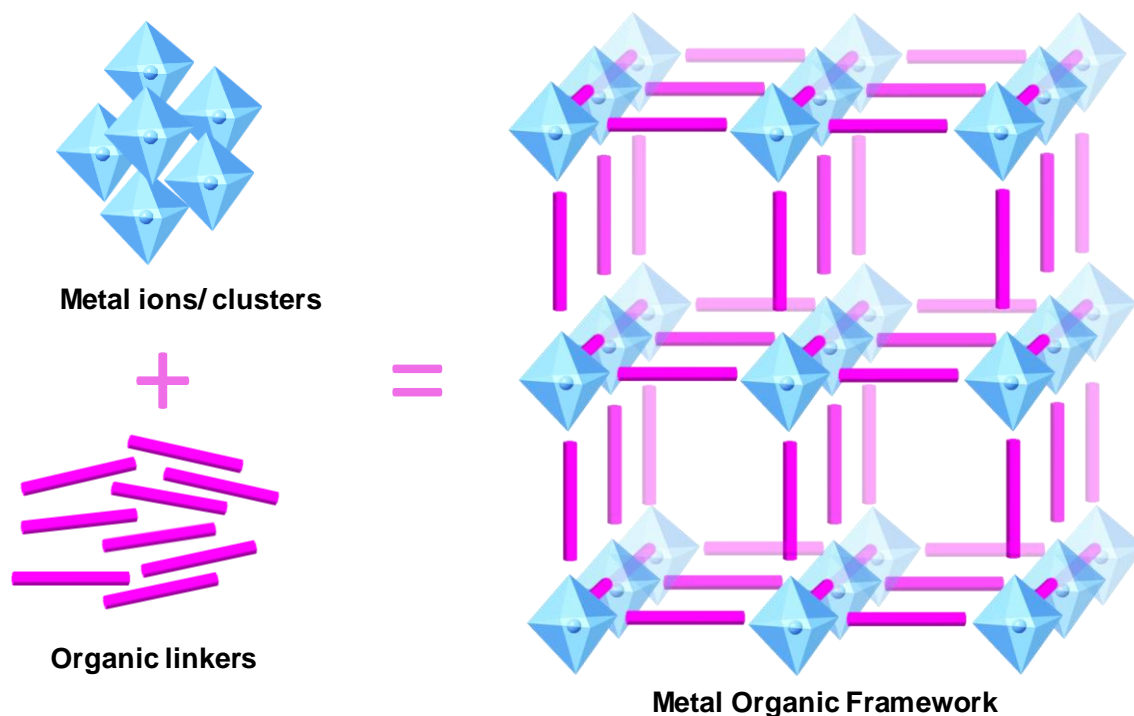


Figure 1.2 The metal ions and the organic linkers making the extended MOF structure.

MOFs have been known for their tremendous ultrahigh internal surface area (extending up to $14600 \text{ m}^2 \cdot \text{g}^{-1}$),⁴⁸ extraordinary porosity (reaching 90% void), open metal sites, and high chemical and thermal stability (between $250 \text{ }^\circ\text{C}$ and $600 \text{ }^\circ\text{C}$) owing to the nature of their strong bonds.^{47, 49} These characteristics, along with their accessible tunability due to the outstanding extent of variability for both the inorganic and organic counterparts,⁵⁰ allow MOFs to withstand great potentials for a variety of applications in diverse fields especially for environmental and energy purposes. For example, MOFs have been used as efficient adsorbents for water decontamination from toxic elements such as selenites⁵¹, phosphates⁵², and arsenate,⁵³⁻⁵⁴ in addition to being noticeable storage materials for gases (hydrogen, methane),⁵⁵⁻⁵⁶ and promising candidate for drug delivery.⁵⁷ Additional applications include biochemical imaging, selective separation, conductivity, and chemical sensing.⁵⁸⁻⁶⁰

2. *Synthetic Routes of MOFs*

Several synthetic routes for MOF production have been reported.⁶¹ However, solvothermal and hydrothermal syntheses are the most common procedures used to prepare MOFs, in which dissolved metal salts and organic linkers are mixed and held at elevated temperatures, at time ranging from few hours to several days.⁶² To control the synthesis time and the morphology of the crystals, alternative synthetic methods have been developed, such as microwave-assisted,⁶³ mechanochemical,⁶⁴ electrochemical,⁶⁵ sonochemical,⁶⁶ slow evaporation⁶⁷ and reaction diffusion methods.⁶⁸⁻⁶⁹

a. Solvothermal Synthesis

After being dissolved and mixed in the appropriate solvent or combination of solvents, the metal salts and the organic linkers are transferred into vials or sealed tubes, then placed under conventional electric heating. The difference between hydrothermal and solvothermal is the used solvent; it is water for hydrothermal reactions, and organic solvents (such as N,N-Dimethyl formamide (DMF), N,N-Diethyl formamide (DEF), methanol, ethanol, acetonitrile ...) ⁷⁰⁻⁷¹ for solvothermal ones. Based on the reaction temperature, that is the one of the main components in this synthesis, two ranges are noticed, solvothermal and non-solvothermal. In brief, when the temperature is above the solvent boiling point, the reaction is solvothermal, and needs to be done under pressure in a closed vessel such as Teflon autoclaves.⁷²⁻⁷³ On the contrary, non-solvothermal reactions are those of temperature lower than the boiling point of the solvent and taking place under ambient pressure in simple containers like scintillation vials.⁷² The latter ones include those made at room temperature or at high temperatures.

b. Microwave-Assisted Synthesis

This route is effective because of its ability to generate elevated and consistent heating throughout the system, in addition to yielding MOFs in a very short time.⁷⁴⁻⁷⁵ It depends on the direct interaction taking place between the electromagnetic radiations and mobile electric charges that can be electrons/ions in the solid, or polar solvent/ions in the solution. In the solid, the produced electric current will lead to heat production because of the solid resistance; whereas, in the solution, polar particles line up in an electromagnetic field, and change their direction. With the suitable frequency, the particles will collide, and energy will be released in the form of kinetic energy leading to an increase in the temperature of the system.⁷⁴ What makes this synthetic path special is its ability to control the system pressure and temperature, and to monitor MOF nucleation rate.⁷⁵⁻⁷⁶ Increasing the nucleation rate and heating the solvents directly allowed the MW assisted synthesis to concentrate on producing nanoscale MOFs, increasing their crystallization rate, and enhancing their purity.

c. Mechanochemical Synthesis

Mechanochemical synthesis takes place in a solvent-free conditions where the intramolecular bonds are ruptured because of the applied mechanical action, and then chemical transformations are allowed to take place.⁷⁷ Mechanochemistry has been applied for so long in different chemical syntheses, such organic, inorganic, polymer and pharmaceuticals synthesis.⁷⁸⁻⁸⁰ In 2006, the first crystalline single-phase MOF was produced using this synthetic route, by simply grinding isonicotinic acid and copper acetate together with the use of steel ball without any solvent.⁸¹ Several factors make MOF mechanochemical synthesis an interesting route; environmental effect is the first

and most important one. Being able to carry the reaction at room temperature and in solvent free environment, avoiding the necessity of using harmful organic solvents, gives this route its eco-friendly touch.⁸⁰ Besides, in some reactions, metal oxides can substitute metal salts, leading to the production of only water as side product.⁸² Furthermore, it allows shortening the reaction time from several hours to less than one hour, along with quantitative yielding of MOFs with generally small particle size.⁸³

d. Electrochemical Synthesis

In 2005, scientists at BASF reported the first electrochemically synthesized MOF,⁶⁵ in which the metal salts were replaced by metal ions excluding the usage of anions such as sulfate, chloride, nitrate, and perchlorate of dangerous concern when produced in large amounts.⁸⁴ Replacing metal salts, metal ions are continuously added to the reaction via anodic dissolution, where a conducting salt or an electrolyte with the dissolved organic ligands are presented.⁸⁵ In order to prevent the deposition of the metal on the cathode, protic solvents are used, but this will lead to the production of H₂. To prevent this, it is recommended to replace the protic solvents with other chemicals that can be favorably reduced such as acrylonitrile, acrylic, or maleic esters.⁸⁶ Moreover, being compared to regular batch synthetic procedures at the industrial level, electrochemical synthesis yields higher amounts of MOFs under mild conditions and in a short time.⁸⁷

e. Sonochemical Synthesis

Sonochemistry is the chemistry of applying highly energetic ultrasonic radiations to a reaction medium.⁸⁸ It is a fast, energy-efficient method used for producing MOFs in a green environment at room temperature.⁸⁹⁻⁹⁰ Ultrasound's

frequency ranges between 20 kHz (upper acoustical human hearing limit) and 10 MHz. Having such a high wavelength, even larger than the dimensions of the molecules, makes the reason behind inducing the chemical reaction a process different than the interactions between the reagent's molecules and ultrasound. This process is called cavitation process, in which the ultrasound affects the liquid and as a result of their interaction, cyclic alternating compression areas of high pressure, and refraction areas of low pressure appear in the liquid. Since the pressure decreases in the refraction area (low pressure) and becomes lower than the vapor pressure of the reagents and/ or the solvent, cavities (tiny bubbles) are created. These bubbles start to increase in size as result of the diffusion of the volume of the solute into the bubble volume eventually ending with the accumulation of ultrasonic energy. When the maximum size of the bubbles is attained, they collapse because of their instability. This cavitation procedure that consists of the three mentioned steps (bubble creation, expansion, and collapse) induces high energy release through the formation of "hot spots", within the bubbles. These spots of elevated temperatures (around 5000K), and pressures (around 1000 bar), cause the formation of excessive crystallization nuclei.⁹⁰

f. Slow-Evaporation Method

This process resembles solvothermal method, where the metal salt and the organic linker are dissolved in the solvent and mixed together. Then the solvent is allowed to evaporate at room temperature, leaving behind the produced MOF. This method is perfect for room temperature synthesis, but it takes more time than other methods; therefore, it is preferred to use solvents with low boiling points to increase the solubility of the reacting materials.

g. Reaction diffusion Framework (RDF)

RDF represents a facile and fast synthesis method that takes place at room temperature by constructing a precipitation system in a tube. The metal salt solution constitutes the outer electrolyte and diffuses into the agar medium as inner electrolyte solution where the linkers are present. The synthesis of MOFs and ZIFs using this method is advantageous for many reasons: (i) it is carried out efficiently at room temperature without using thermal treatment or aging processes, (ii) it is scalable where gram scales can be obtained by simply using larger reactor, (iii) it permits the preparation of solid solution and generation of a spatial doping gradient along the tubular reactor, and (iii) it easily provides control over the particle size and morphology. Examples of MOFs synthesized through this method include MOF-199, ZIF-8, and ZIF-67.⁶⁸

3. *Properties of MOFs*

As mentioned before, a MOF is constructed from the assembly of metal ions and organic linkers. Because of these long organic ligands, an empty space is included within the structure, allowing them to have the potentials of being permanently porous materials. In the 1990s, the porosity of these MOFs was studied and proved to be permanent after measuring carbon dioxide and nitrogen sorption isotherms on zinc MOF.⁹¹ In 1999, the synthesis of first rigid and extremely porous MOF-5 was reported, characterized by 61% void space, and a 2320 m²/g Brunauer-Emmett-Teller (BET) surface area⁹² which exceeded that of zeolites and activated carbon.⁹³ Increasing the surface area requires enhancing the storage space with respect to the weight of the substance. Using longer linkers increases the storage capacity as well as the number of

adsorption sites' however, it exposes the framework for growing interpenetrating structures (more than one framework) because of the resulted large space. To prevent this, MOFs whose topology prevents interpenetration are made since it necessitates the other framework to have another topology.⁹⁴ In addition, it is important to keep in mind that the pore diameter must remain in the micropore range (less than 2 nm), through the careful choice of the organic linkers while maximizing the BET surface area, since the geometric surface areas resulting from the MOF structure and the BET surface areas calculated from the sorption isotherms are analogous.⁹⁵ In 2004, MOF-177 was proved to have the MOFs' largest surface area, of BET area equals to 3780 m²/g and 83% porosity.⁹⁴ After this, the value doubled in 2010 to become 4530 m²/g and 6240 m²/g and porosity of 90% and 89% for MOF-200 and MOF-210 respectively.⁹⁶ The progress of the highest BET surface area over the years is shown in **Figure 1.3**.

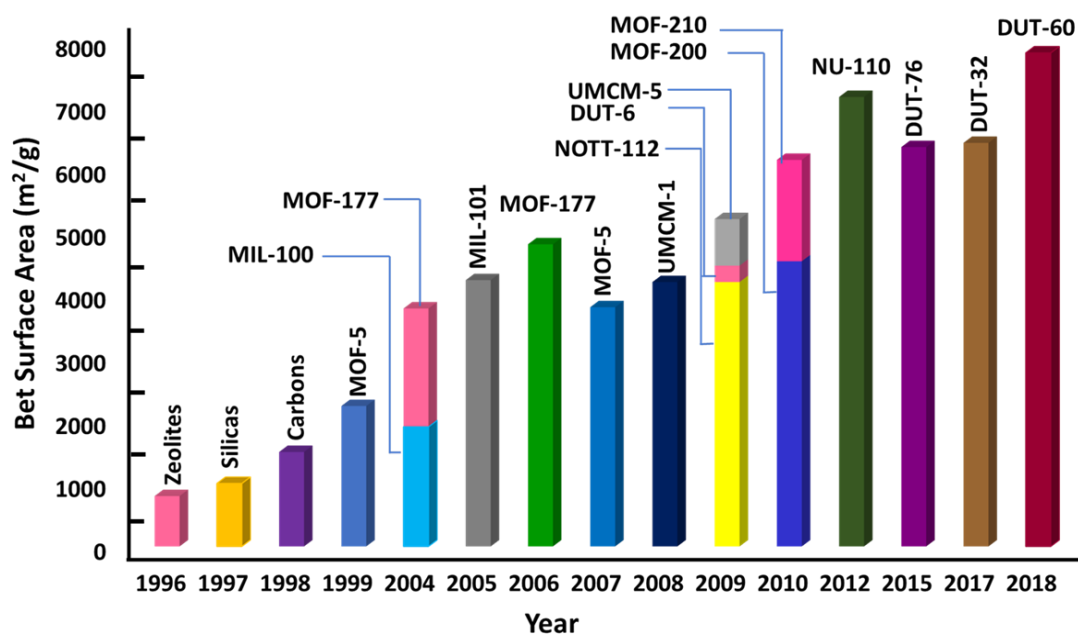


Figure 1.3 The progress in the synthesis of MOFs with high surface areas.^{50, 97}

Furthermore, adsorption sites inside the pores had been discovered through a study made on MOF-5 loaded with argon or nitrogen gas; these sites were the SBU, faces and edges of the linker.⁹⁶ By revealing the source of high porosity, this study not only allowed the creation of MOFs with higher porosities, but also proved the effect of extended alkyne-based tritopic linkers instead of phenylene-based on increasing the adsorption sites' number and thus the surface area.⁹⁸ This was proved with NU-110 (Northwestern University) MOF whose linker is characterized with such edges and showed a surface area of 7140 m²/g which remained the highest reported surface area⁴⁸ till 2018 where DUT-60 (University of Technology) broke the record with a 7839 m²/g BET surface area.⁹⁷ Furthermore, varying the length of the incorporated linkers lead to easily change the pore sizes of the MOFs from the angstrom scale to the nano level,⁵⁶ and the functionalization of the pore walls can also be attained through ligand design.

Because of the strength of the bonds composing MOFs, like C-C, C-O, C-H, and M-O, MOFs are thermally stable within a temperature range of 250 to 500 °C.⁵⁶ Preparing chemically stable MOFs has always been a hard task because of their vulnerability while being exposed to solvents for long time periods. ZIF-8 (zeolitic imidazolate framework-8) was the first chemically stable MOF, that remained unchanged after treating it in boiling methanol, benzene, and water for a period up to one week, as well as in boiling concentrated base (NaOH) for 24 hours.⁹⁹ Other examples on chemically stable MOFs include UiO-66 (University of Oslo), MOF-525, MOF-545 and so on.

The diversity of the organic linkers and the metal clusters resulted in the presence of a massive library encountering them. Few examples of some linkers and clusters are shown in **Figure 1.4**, where different assembly of them leads to a wide

variety of different MOFs. Extra diversity is added to the mixed-metal MOFs that can encounter up to 10 different metals retaining the same topology.¹⁰⁰⁻¹⁰¹ Another composition variety extend to reach the linkers leading to mixed-linker MOFs permitting the modification is the structure of MOFs.¹⁰² Based on this tunability, preferred topologies can be chosen and MOFs with the best structural design are made.¹⁰³ In addition, postsynthetic modification has achieved tremendous results with changing the reactivity of MOFs and their active sites.¹⁰⁴ With all the tunability in the chemistry of MOFs, it wasn't a long time before their Lewis and Brønsted acidic properties were studied.

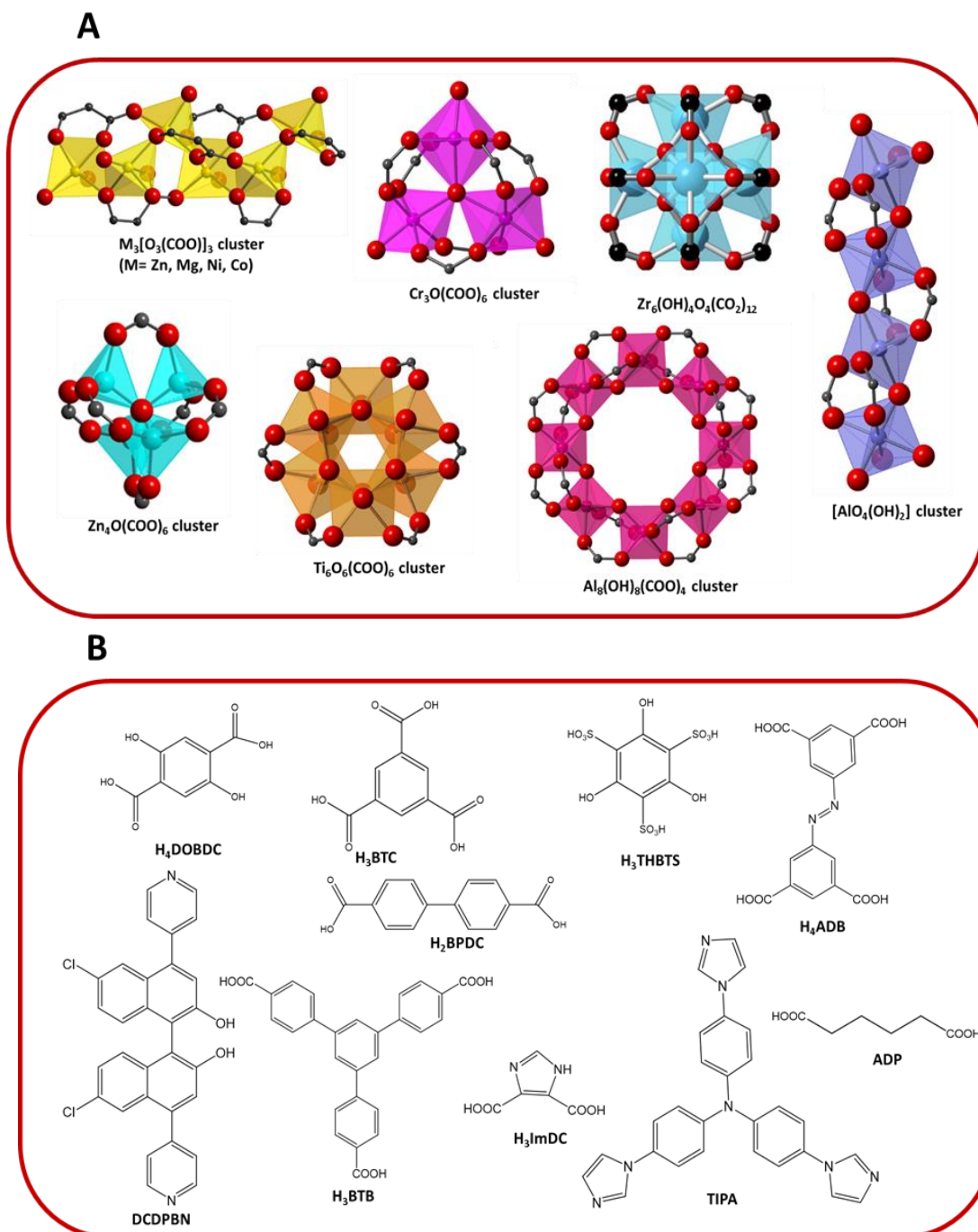


Figure 1.4 (A) Various secondary building units showing the different metal oxide clusters. (B) Different organic linkers. H_4DOBDC = 2,5-Dihydroxyterephthalic acid; H_3BTC = Benzene-1,3,5-tricarboxylic acid; H_3THBTS = 2,4,6-Trihydroxybenzene-1,3,5-trisulfonic acid; H_2BPDC = 4,4'-Biphenyldicarboxylic acid; DCDPBN = 6,6'-Dichloro-4,4'-di(pyridin-4-yl)-[1,1'-binaphthalene]-2,2'-diol; H_3BTB = 1,3,5-Tris(4-carboxyphenyl)benzene; ADP = Adipic acid; H_4ADB = 5,5'-(Diazene-1,2-diyl)diisophthalic acid; TIPA = Tris(4-(1H-imidazol-1-yl)phenyl)amine; H_3ImDC = 4,5-Imidazoledicarboxylic acid.

Even though the research on MOF is now directed toward gaining extra functionality through synthesizing dynamic magnetic MOFs¹⁰⁵ (having stimuli-responsive magnetic building blocks), an innovative movement of integrating MOFs with other active materials like micro- and nano-particles is initiated. For example, luminescent core-shell quantum dots were incorporated within MOFs (such as MOF-5),¹⁰⁶ as well as silica nanoparticles that acted as a nucleating agent for MOF growth.¹⁰⁷ Metal nanorods,¹⁰⁸ metal nanoparticles,¹⁰⁹⁻¹¹⁰ graphene,¹¹¹ and magnetic beads¹¹² are other examples of active nanoparticles that were combined with MOFs to produce extremely porous composites with special engineering and additional characteristics. In particular, combining MOFs with magnetic nanoparticles leads to the formation of magnetic framework composites (MFCs).

4. Acidity in MOFs

Lewis acids acts as catalysts for various organic reactions by exposing the functional groups of the reagents to nucleophilic attack through withdrawing the electron density from them.¹¹³ Lewis acids MOFs were investigated for the first time as Lewis acidic catalysts for the aldehyde cyanosilylation reaction.¹¹⁴ The Lewis acid positions are the unsaturated open metal sites, that were bonded to solvent molecules before activation and had these molecules removed by heating or evacuation upon activation without the framework collapse as illustrated by **Figure 1.5**. Examples on such MOFs include MOF-74, HKUST-1(Hong Kong University of Science and Technology) and MIL-101 (Matériaux de l'Institut Lavoisier) that proved to be active catalysts for several reactions such as citronellal cyclization, Knoevenagel condensation, isomerization of α -pinene oxide, cyanosilylation of aldehydes, and organic compounds

oxidations.¹¹⁵ It is noteworthy to mention that MOFs having no open sites can still perform as Lewis acids due to the accessibility of the metal center.

In addition to having already synthesized Lewis acid sites, externally functional groups is another tool to introduce Lewis acidity into the MOFs.^{11, 115} For example, Feng and his co-workers were able to integrate Lewis acidic linkers (Metal-tetrakis(4-carboxyphenyl) porphyrin (M-TCPP) linkers) into UiO-66 framework via one-pot approach.¹¹⁶ The resulted composite preserved the structure, stability, and design. Defect engineering is another method used to generate Lewis acidic sites within MOFs.¹¹⁷ Zr-based MOF UiO-66 has attracted attention in this field because of the high tunability of its defect's concentration, and the ability to even remove defected positions. For instance, Trickett and his co-workers worked on missing linker defects on UiO-66 MOFs;¹¹⁸ whereas, Cliffe and his co-workers focused on the defect dispersion and the nanoscale disorder within these MOFs.¹¹⁹ Moreover, post-synthetic metalation succeeded in boosting MOFs with additional metal sites and Lewis acidity in case the linkers contain functional groups like thiol and hydroxyl groups.¹⁰⁴

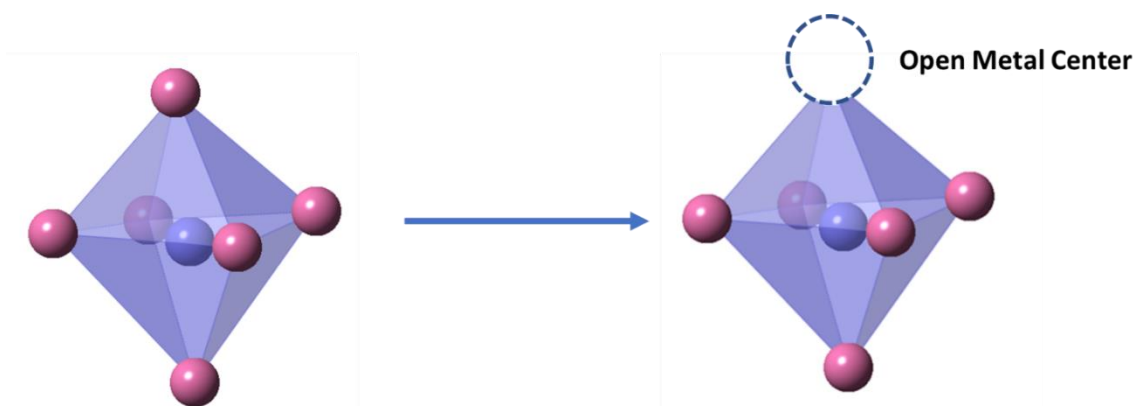


Figure 1.5 Lewis acidic site (unsaturated metal center) made by the loss of oxygen from a solvent molecule.

With all the massive work done on studying Lewis acidic MOFs, a new motion toward studying Brønsted acidic MOFs began to emerge. This is a challenging process since the heterogeneity of acid sites in the solid samples along with the absence of acid-base equilibrium make it hard to characterize Brønsted acidity within these samples. Moreover, being able to introduce high acidity to the MOFs, exceeding that of sulfuric acid, is a very difficult procedure in general. Introducing acidic sites to the MOFs can occur either through one-pot synthesis or post-synthetic modification, and in both cases, the acidic protons affect the construction or the stability of the framework.¹²⁰ Nevertheless, the extraordinary tunable nature of MOFs has allowed the chance to address such drawbacks: MOF heterogeneity within order, multivariate chemistry, post synthetic modifications, and ordered MOF assembly that led to better understanding and withstanding of MOFs' Brønsted acidity.¹²¹

Brønsted acidity allowed MOFs to be proton donor, and thus gave them the advantage of being used as efficient catalysts for esterification reactions. As shown in **Figure 1.6**, it can be introduced into the MOF structure through three different methods.¹²¹ The first is by encapsulating the Brønsted acidic groups into the pores of the MOFs, that will be connected with the inner through fragile intermolecular interactions. This can occur with a two-step synthesis route (post synthetic modification), in which the MOF is made in the first step, then the Brønsted acid molecules are impregnated within the pores. However, this can be done also through one-step synthetic approach, in which the guest molecules exist at the same time of MOF formation; in other words, these acidic groups are mixed with MOF precursors (metal ion and the linker). For example, H_2SO_4 and H_3PO_4 were successfully impregnated as guest molecules within MIL-101,¹²² even though the PXRD pattern lacked any diffraction peaks when the acids

were presented; however, the crystalline structure was restored once the acids were washed away assuring MOF integrity. Another example includes the use of highly acidic polyoxometalates (POMs), that proved to be efficient guest molecules within the MOFs.¹²³ Since their large size exceeds the pore openings of the MOFs, they can be encapsulated only through the one-step synthetic approach while synthesizing the MOFs, otherwise they can't pass through the pore openings in post synthetic modification). This combination of POMs within the MOFs proved to show better catalytic efficiency in chemical reactions.¹²⁴

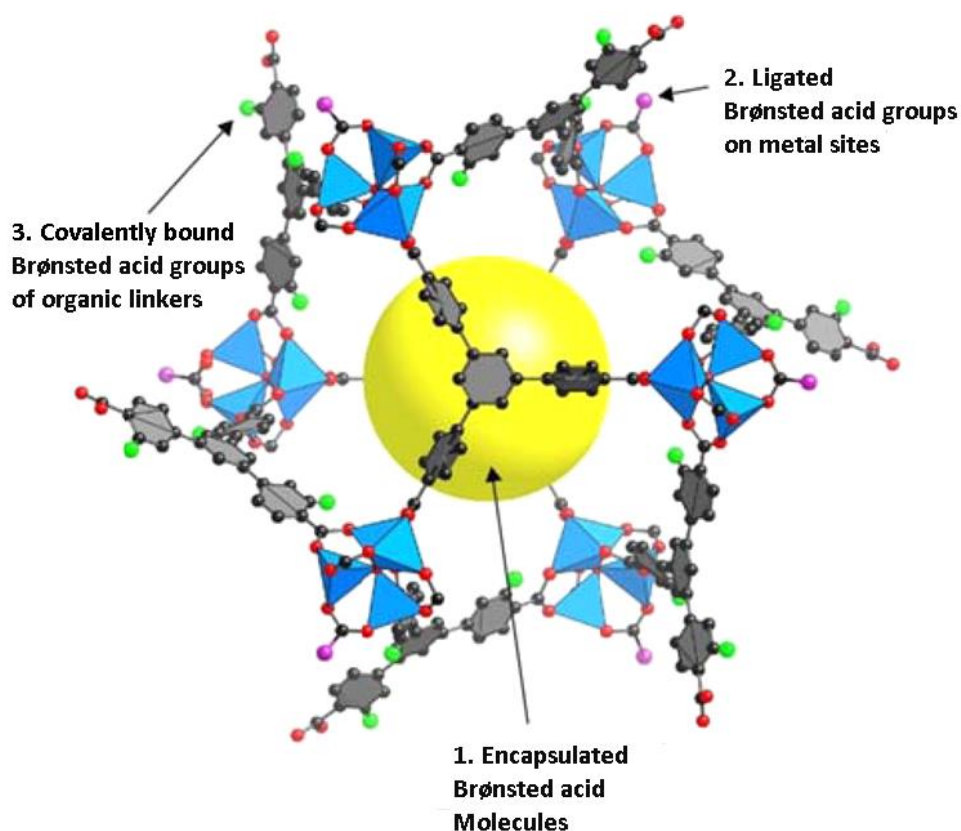


Figure 1.6 Various Brønsted sites in MOFs.⁵⁰

The second approach includes ligating the Brønsted acidic molecules onto the metal sites by using linkers having acidic groups such as hydroxyl group in addition to oxalic acids, water, sulfuric acids, and alcohols. This takes place by interacting the metal ion with the solvent linker. In hydroxyl-based acidic MOFs, bridging of more than one metal to the hydroxyl group occurs. Examples include MIL-53(Ga), and MOF-69C that proved to be catalytically active in Friedel-Craft alkylation reactions because of their bridging hydroxyl groups.¹²⁵ The acidity strength of these systems relies on the bounded metal, and it decreases while bridging the same metal type. Therefore, MOFs with mixed metals inside the same SBU shows higher acidity. An alternative method includes introducing these linkers into vacant sites of the SBU upon post-synthetic modification as shown in UiO-66 MOF.¹²⁶ First, the MOF was synthesized with missing BDC linkers causing vacancies at the zirconium metal SBUs. Following this, oxalic acid/DMF solution was added in which the oxalic acids occupied these vacancies. As a result, only one carboxyl group from the oxalic acid became bounded to the SBU, while the other free carboxyl group was pointed to the inside of the pores, generating Brønsted acidity atmosphere.

The last and most used method to introduce Brønsted acidity is achieved through using linkers that already contain Brønsted acidic groups or introducing such groups to the linkers through post-synthetic modification. For example, Brønsted acidity was introduced for UiO-66 MOF through the usage of carboxylic acid functionalized linker ($\text{H}_2\text{BDC}-\text{COOH}$) instead of H_2BDC , or through using sulfonic acid.¹²⁷ Even though in the later linkers with full sulfonation caused crystallinity and pore network destruction, a 25% sulfonated linkers allowed the successful synthesis of UiO-66 with 50% of its conventional porosity.

5. *Applications of MOFs*

Because of their unique properties, MOFs have been used in several fields in wide variety of applications where some are listed below:

a. Drug Delivery

The public's interest is now shifted toward cancer diagnosis and cure because of the high rates of infections reaching for one person in each group of three.¹²⁸ As a result, drug delivery systems have been developed as effective treatment through delivering therapeutics to specific areas of the body. However, several drawbacks are recognized including non-controllable drug release, carrier accumulation, or even failed carrier breakdown.¹²⁹⁻¹³⁰ Conventional drug delivery systems (DDS) are either organic or inorganic systems. The organic systems can't control drug release although being highly biocompatible with the body; whereas, the inorganic ones are highly controllable but with much lower loading capacity.¹³¹ Because of the hybrid nature of MOFs encountering both organic and inorganic counterparts, they have been used as drug storage and delivery materials.¹³² Their unprecedented properties including predetermined structural design and postsynthetic modifications give the chance to enhance drug delivery properties including cell selectivity, low cytotoxicity, good drug loading, appropriate drug release, suitable degradation rates and colloidal stability, and cell internalization.¹³³⁻¹³⁴

The first iron-based MOF used for drug delivery was reported in 2006 by Ferey and his co-workers.¹³⁵ Following this, massive work has been done on MOFs as promising candidates in biomedicine.¹³⁶ Up to date, the most used MOFs are iron-based MOFs because of their high drug loading as a result to their high porosity, and the

biocompatibility of iron with human bodies.¹³⁷ Lately, zirconium-based MOFs have been investigated in healthcare applications, since Zr is a biocompatible metal where the human body contains (300 mg) and needs good amount of it (4.15 mg per day).¹³⁸ Moreover, Zr-MOFs are more mechanically and chemically stable than Fe-MOFs due to the strong nature of Zr-carboxylates interactions making them great candidates in the field.¹³⁹⁻¹⁴⁰

b. Gas Storage

Because of the increasing global energy needs, the shift is directed toward green sources for energy production such as hydrogen and methane gases. However, such gases are known for their storage in high pressure tanks that are not only dangerous but also expensive. Recently, MOFs have emerged as an alternative candidate for safely storing such gasses due to their high surface areas and extreme porosity.¹⁴¹

Hydrogen is an ecofriendly great competitor for energy production because of its high energy density and overwhelming fuel performance exceeding internal combustion engines, in addition to its green effect by being carbon free, and thus producing only water as a byproduct for combustion without any CO₂ emissions.¹⁴² Despite all of this, the lack of safely storage systems prevents its usage as a successful fuel source.¹⁴³ Because of their unique properties, MOFs have been the perfect and the most studied applicants for storing H₂ gas since 2003 where the first experiment on hydrogen adsorption on MOF-5¹⁴⁴ was successfully done up till today.¹⁴⁵⁻¹⁴⁷ They have shown better adsorption activity while compared to other porous materials. Examples on other MOFs include MIL-101, IRMOF-20, MOF-177, HKUST-1, and many others.¹⁴⁷

Despite all of this, H₂ gas storage is still restricted with low temperatures (77 K) due to the weak interactions between hydrogen and the MOFs.

Like hydrogen, methane is also a green gas that can yield energy more than petroleum oil because of its higher hydrogen to carbon ratio and thus lower carbon release. The first reported methane sorption on MOFs was reported by Kitagawa and his co-worker in 1997. Following this, in 2002, Yaghi's group studied the isorecticular MOFs for methane storage. Since then, several studies have been made investigating wide variety of MOFs for methane storage with capacities equivalent or superior to those of activated carbon.¹⁴⁸

The public concern toward the crisis of global warming has grabbed the attention to the vital problem of CO₂ emissions. As an alternative to the inefficient and expensive recent carbon dioxide capturing systems, porous solids have been of great interest especially metal organic frameworks functionalized with polar groups at their pores.¹⁴⁹ The literature is full of examples on MOFs with high CO₂ capturing capacities such as MOF-177, NU-110E, functionalized UiO-66 and so on.¹⁴⁹

c. Sensing

In the world of luminescence and sensing, MOFs are recognized as promising materials with very high potentials. The hybrid nature of MOF allows the implementation of functional organic and inorganic counterparts such as luminescent and magnetic SBU and conducting linkers. Lanthanide MOFs are the most used MOFs in the field because of the electron transition between d and f orbitals and the corresponding photon emission taking place in the lanthanide metal.¹⁵⁰ Moreover, Lanthanide MOFs are known for their exclusive luminescence properties such as high

duration and sharp line emissions, great Stokes shifts, and large luminescence quantum yield.¹⁵¹⁻¹⁵² The unique luminescent properties of Lanthanides along with the attracting characteristics of MOFs offer great potentials for designing new materials with boosted functionalities for specific sensing applications.¹⁵³

d. Decontamination of Water

Water pollution has grabbed the worldwide interest because of its threatening effect for the entire biosphere. The heavy metals presented in the water such as lead, mercury, arsenic, and selenium are toxic even when they are in low amounts. As a result, new technologies have been established to solve this issue including chemical precipitation, ion-exchange coagulation, filtration, and adsorption. However, the need for better and more cost-effective systems is still desirable. Within this frame of reference, MOFs are considered to be promising materials for water decontamination processes. For example, UiO-66, MIL-96, ZIF-8, MOF-74, AUBM-1 and so much more were used for arsenate removal and showed great results.^{54, 154-156}

In addition to heavy metals, organics like dyes and pesticides constitutes a serious concern because of their high stability and high toxicity even in trace amounts. MOFs have proved to be great adsorbents for these contaminants although the reported ones aren't as many as in other fields. Particularly, MOF-235 and MIL-100 showed very good results while adsorbing Methyl Orange dye and Methylene Blue.¹⁵⁵

e. Catalysis

MOFs are recognized as a perfect platform for heterogeneous catalysis, proving themselves with high conversions in wide variety of chemical reactions.¹⁵⁷⁻¹⁵⁸ Their frameworks contain intrinsic catalytic positions (such as Lewis acid metal sites,

organocatalytic components...) and their high surface area and crystallinity provide the chance to have plenty and well dispersed active sites. Because of the hybrid nature of MOFs, active sites can be functionalized on the organic linkers, metal nodes or within the pores. Furthermore, their easy structural tunability allows tailoring the active sites resulting in chemo, stereo, enantio-, or regioselectivities, and their robust framework prevents the aggregation or degradation of the reacting materials.¹⁵⁹

Literature is full of reports about MOFs used as catalysts for various organic reactions. Fujita used the unsaturated metal sites within the MOFs as heterogeneous catalysts for cyanosilylation reactions. Hu and Zhao studied the design and development of Lewis acidic MOFs, and their catalytic activity in hydrogenation and redox reactions. Fisher investigated benzaldehyde cyanosilylation under the catalysis of Lewis acidic sites in defected UiO-66. As noticed, the uncoordinated sites within the MOFs are the sites of catalytic interactions. Many catalysts have open metal sites such as HKUST-1, and MOF-74 who showed great catalytic potentials.¹⁶⁰

On the other hand, Brønsted basicity of the amine-functionalized linkers of CAU-1-NH₂ MOF allowed it to excellently catalyze Knoevenagel condensation reactions.¹⁶¹ In addition, MOFs were tested on isomerization reactions of allylic alcohols into saturated ketones by the group of Gascon and Llabrés i Xamena. The used catalyst showed analogous results with enhanced turnovers compared to the conventional used catalysts. Add to that, it was stable in air and moisture, in addition to being recyclable. The active sites within the pores have been also studied. A study was made on palladium nanoparticle loaded on iron-based MOF and tested as heterogeneous catalyst for nitroaromatics reduction to amine. It showed complete conversion, perfect recyclability, and absence of Pd leaching.¹⁶² Esterification reactions were also catalyzed

by MOFs for biomass conversions. For instance, Zr-based MOFs were used as efficient catalysts for the production of alkyl levulinates¹⁶³⁻¹⁶⁴ and butyl butyrate.¹⁶⁵

In addition to the previously mentioned reactions, MOFs have been also investigated as effective catalysts in Diels–Alder, epoxide formation and their ring opening to give alcohols, acetalization, Friedel-Crafts, polymerization, cyclization and oxidation reactions. Finally, photoactive MOFs have been used as photocatalysts for solar fuel production.¹⁶⁶

6. Structure of MOF-74

MOF-74 is one interesting class of MOFs because these MOFs are characterized by having open metal sites in their framework acting as Lewis acidic sites that are required for the development of acid heterogenous catalysis. These unsaturated metal centers result from the loss of the solvent molecule due to high energy activation of the MOF. Their structure is built up through joining the DOBDC linker (2,5-dihydroxyterephthalic acid) units with the metal. An extra unique trait of this framework is the ability of incorporating different metals (Mg, Zn, Mn, Co, Ni, Cu, and Cd) with the DOBDC keeping the same topology. Each metal is coordinated to two hydroxyl, three carboxyl, and a solvent molecule (D,D-dimethylformamide) to establish an extended 3D framework characterized by honeycomb-like pores (**Figure 1.7**) leading finally to the formation of 1D helical chains of cis-edge-linked metal-oxygen coordination octahedra¹⁵⁶.

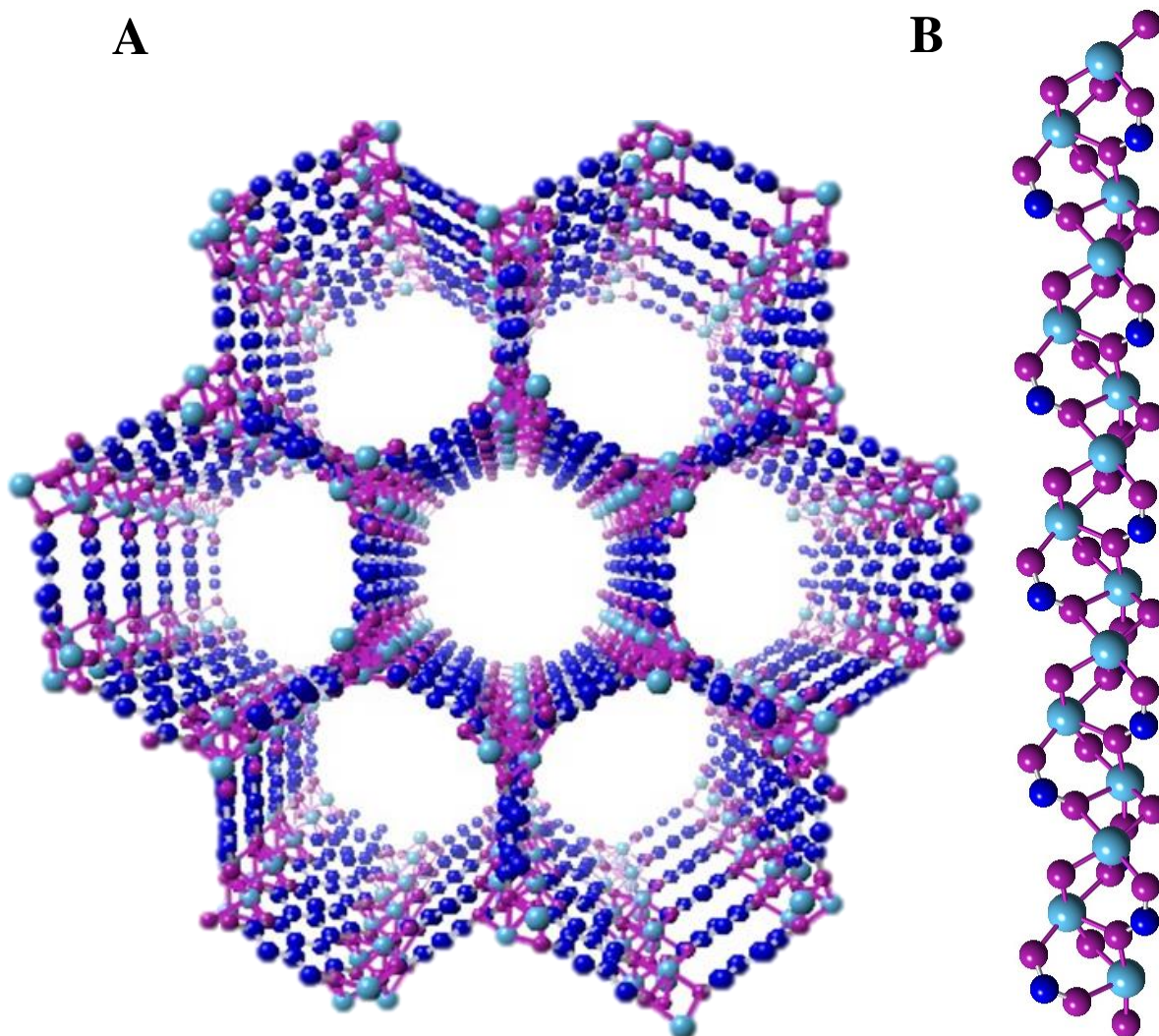


Figure 1.7 (A) Crystal structure of MOF-74, shown along the c axis, revealing the 1D honeycomb-like pores. (B) Coordination mode of the metal atom showing the rod-like secondary building unit. Color code: metal: cyan, oxygen: purple, and carbon: blue.

F. Magnetic Framework Composites (MFCs)

As stated above, magnetic framework composites (MFCs) are extremely porous materials resulting from the integration of magnetic nanoparticles with MOF crystals.¹⁰⁵ These composites with sophisticated architecture are known for their sensitivity toward external stimuli, thus being able to be easily separated when an external magnetic field

is applied.¹⁶⁷ Furthermore, MFCs are tunable since both MOFs and nanoparticles can be easily engineered, and infinite combinations of various nanoparticles and numerous MOF samples lead to unlimited number of resulting functional MFCs. In fact, this is an advantageous aspect, based on the application, a MOF can be chosen from the library and the magnetism of the nanoparticles can be tuned as wanted.¹⁶⁸

As a result, MFCs can be used in any “on demand” application. For example, they are widely used in biomedical fields especially for drug delivery because of the MOFs’ high surface area that permits the storing and releasing of drugs, in addition to the controlled nanoparticles’ magnetic properties.¹⁶⁹ Furthermore, certain nanoparticles (like iron oxide) have superparamagnetic characteristics that prevent any residual magnetization and avoiding any fatal blood vessel blockings because of uncontrolled accumulation.¹⁷⁰ Moreover, getting exposed to variable magnetic field causes localized heat within the composite that can be used in hyperthermal treatment to kill cancerous cells, and to simulate pharmaceuticals release.¹⁷¹ They are also used for sequestering contaminating substances found in polluted fluids, by simply allowing the adsorption of pollutants on the MFCs, and then separating the composites from the fluid through a magnet. In addition, they showed and still showing potentials in microfluidic circuits, in sensing, and in separation.¹⁷²

MFCs are also known in catalysis. In general, metal organic frameworks are recognized as effective catalysts for various chemical reactions,¹⁷³⁻¹⁷⁴ but the concern of removing them from the reaction medium with the minimal losses involves an extra effort with many extra purification steps. Fortunately, this problem doesn’t exist when it comes to MFCs, that can be separated rapidly and reused using an external magnetic field.¹⁷⁵

Depending on the type of connection between the nanoparticles and MOFs, different approaches for synthesizing MFCs exist, and all of them include the step of having a pre-made magnetic particles. The most two common methods are embedding, and mixing. In the embedding method shown in **Figure 1.8 (A)**, the magnetic nanoparticles are dispersed into the MOF mother liquor containing the inorganic precursors and organic linkers dissolved in the appropriate solvent. Following the mixing, sonication is done to guarantee a consistent spreading for the nanoparticles in the system, then heat-driven growth is carried out through hydrothermal or solvothermal procedures at high temperatures. The resulting MFC has a very similar if not the same morphology as the original MOF since both were prepared with the same protocol. However, controlling the MOF growth in such reactions is quietly hard, where the final medium will contain MFCs having unequal nanoparticles' distribution, MOF crystals that have no nanoparticles, and accumulated magnetic nanoparticles that are sensitive to the alternating magnetic field and cause overheating that might damage the MOF structure.¹²

However, in the mixing process represented in **Figure 1.8 (B)**, the MOFs and nanoparticles are made separately, and mixed with the help of sonication, to obtain stiff aggregated composites because of the electrostatic interactions.¹⁷⁶⁻¹⁷⁷

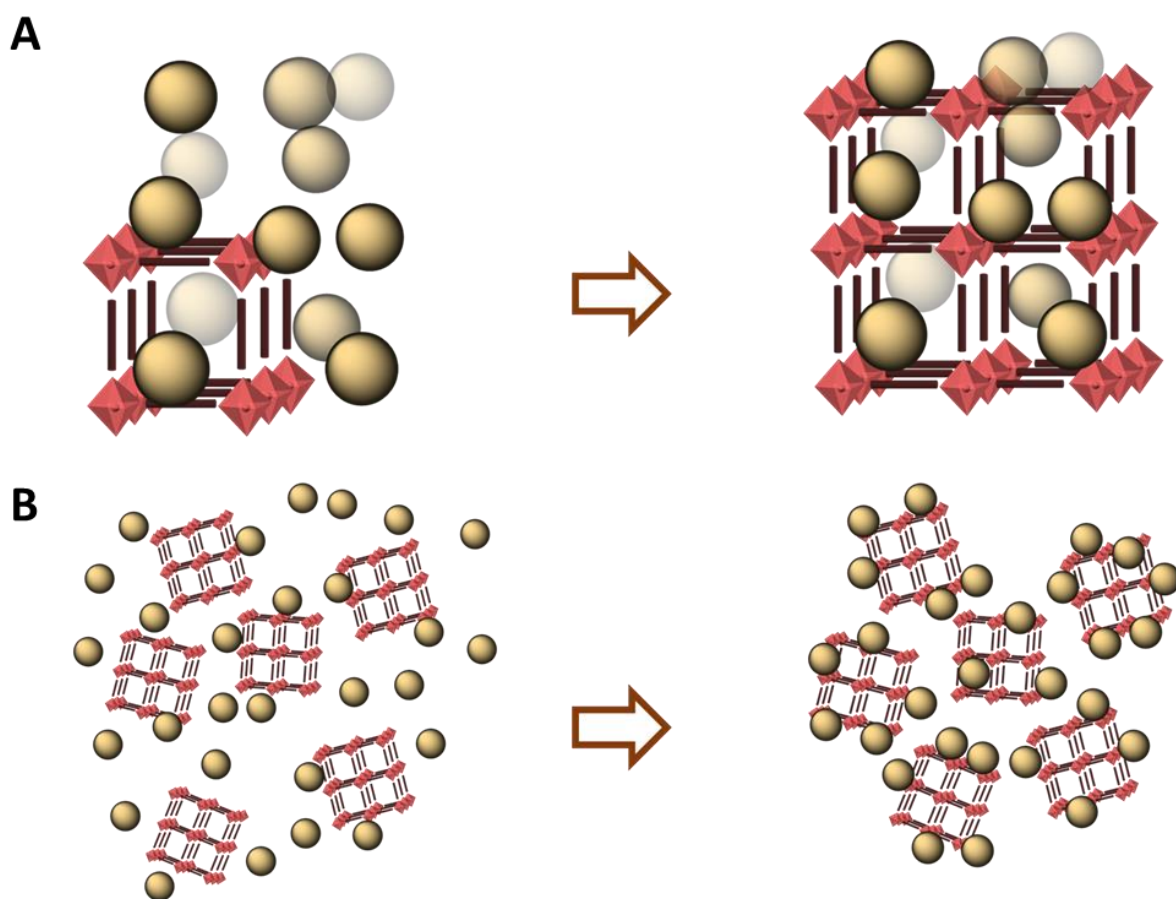


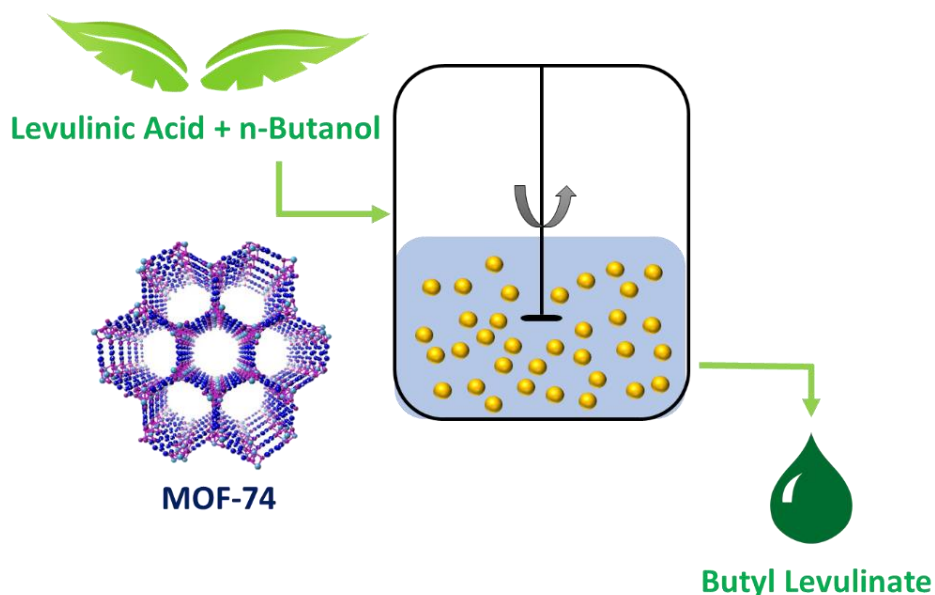
Figure 1.8 (A) Embedding and (B) mixing procedures for preparing MFCs.

Two other less common approaches exist, these are the layer-by-layer and encapsulation processes. Concerning the layer-by-layer procedure, the magnetic particles are designed with certain functional groups on their surface (carboxylic acids, amines...) ¹⁰⁷ in order to control the crystal growth, and for the well-organized synthesis of core-shell structures. Therefore, the MOF is allowed to develop layer-by-layer, ¹⁷⁸ and the final MFC has the tendency to retain the original shape of the magnetic nanoparticles. On the other hand, in the encapsulation method, the magnetic nanostructures are encapsulated within a certain material that is highly compatible to MOFs (carbonaceous substances, polymers...); subsequently, MOFs will grow around these complex nanostructures yielding the desired MFCs. Examples are the usage of

nanoparticles covered with polyvinylpyrrolidone (PVP) for controlled synthesis of ZIF (zeolitic imidazolate framework) materials,¹¹² and the use of carbon coated cobalt nanostructures for the growth of MOF-5.¹⁷⁹

G. Objectives

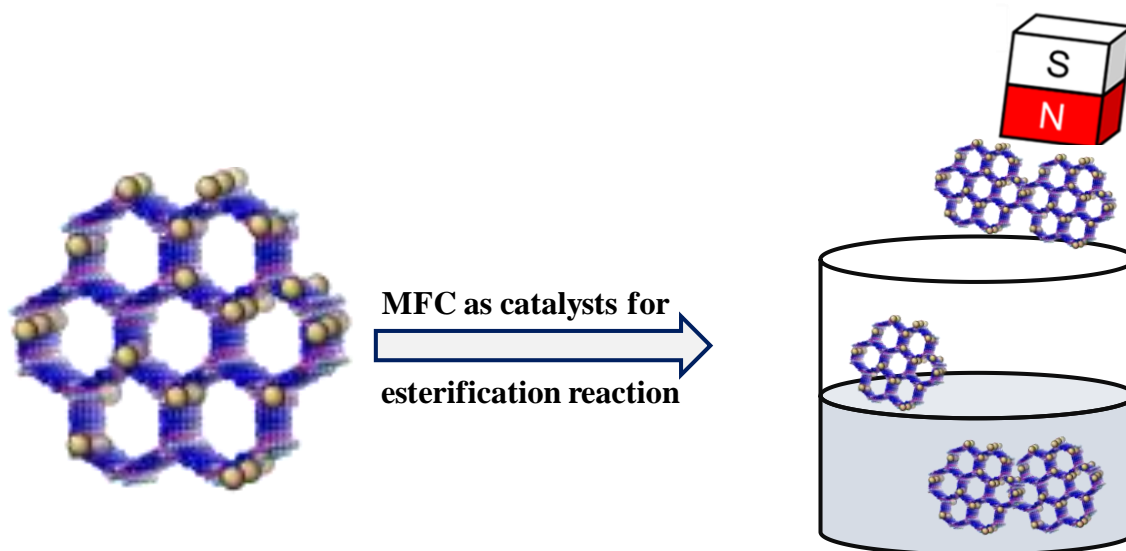
Because of the urging need for a sustainable eco-friendly energy, green catalysts are grabbing the world's attention and pushing the science toward optimizing the processes of biodiesel production. MOFs and MFCs are well known in the catalysis domain mainly because of their stability that is an indispensable property of the catalyst. In this work, various MOF-74 each incorporating different metals (Mg, Zn, Mn, Co, and Ni) were prepared solvothermally, characterized and tested as catalysts in the esterification reaction of levulinic acid into butyl levulinat in the presence of butanol.



Scheme 1 Esterification reaction setup.

In order to be able to separate the catalysts easily, magnetic framework composites (MFCs) were prepared-based on the best performing catalyst- by incorporating different

loadings of magnetite nanoparticles on the MOFs. These MFCs were characterized, tested on the same system, and compared with the previous results.



Scheme 2 Great magnetic separation of the MFC from the reaction medium.

In addition, in order to investigate the size effect of the catalyst on the reaction, nano-scaled MOFs were prepared (RT-Zn-MOF-74, RT-Co,Mg-MOF-74, and RT-Zn,Mn-MOF-74) by room temperature synthesis and were also tested and compared.

The impact of the catalysts' properties including their acid density, surface area, and particle size will be investigated and compared for a better understanding of their catalytic rule.

In specific, MOF-74 was chosen because of its open metal centers acting as strong Lewis acidic sites, high chemical and thermal stability, and its ability to incorporate different metals keeping the same topology. On the other hand, the choice of butyl levulinate ester was because of its fuel-like properties. In brief, it boils within the diesel range, has steady flash point, moderate flow property, and low toxicity. Furthermore, it

is ecofriendly, it increases conductivity and the lubricity when blended with gasoline and diesel.

In addition, further MOFs were synthesized and characterized: Cu-MOF-74, mono-wave assisted AUBM-1 (MW-AUBM-1), and mono-wave assisted MIL-88B. MIL-88B were tested on the same system for the sake of comparison with the studied MOF-74.

CHAPTER II

MATERIALS AND METHODS

All chemicals included in this study were purchased from Sigma-Aldrich and used directly as received.

A. Synthesis of MOF-74

1. Solvothermal MOFs

Zn-MOF-74 was synthesized based on a previously reported method in the literature.¹⁵⁶ In a 20 mL scintillation vial, 0.081 g of 2,5-dihydroxyterephthalic acid (DOBDC) and 0.190 g of $\text{Zn}(\text{NO}_3)_2 \cdot 6\text{H}_2\text{O}$ were dissolved in a solution containing 10 mL DMF, 1 mL of water, and 1 mL of ethanol. Following this, the mixture was placed in the oven at 120 °C for 24 h as shown in **Figure 2.1**. After being collected, the sample was washed with DMF over two days three times a day followed by methanol also for two days (three times a day). After being dried, the MOFs were activated in a vacuum oven at 120 °C overnight.

The same conditions were applied to synthesize the remaining MOFs (Mn-MOF-74, Ni-MOF-74, Co-MOF-74, and Mg-MOF-74) with the change in the metal salt type and amount as shown in **Table 2.1**

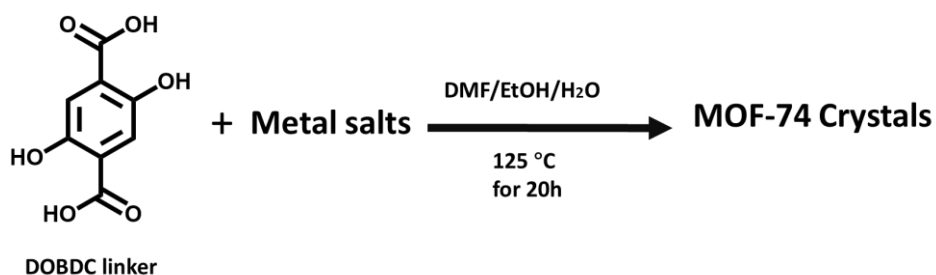


Figure 2.1 Synthetic route for producing MOF-74 samples.

Table 2.1 Metal salts used for synthesizing the used MOFs.

MOF	Metal Salt	Mass (g)
Zn-MOF-74	Zn(NO ₃) ₂ ·6H ₂ O	0.190
Mn-MOF-74	Mn(NO ₃) ₂ ·4H ₂ O	0.251
Ni-MOF-74	Ni(NO ₃) ₂ ·6H ₂ O	0.292
Co-MOF-74	Co(NO ₃) ₂ ·6H ₂ O	0.292
Mg-MOF-74	Mg(NO ₃) ₂ ·6H ₂ O	0.257

2. *Cu-MOF-74*

The MOF was prepared using a method from the literature.¹⁸⁰ In a 25 mL scintillation vial, 0.186 g of DOBDC and 0.500 g of trihydrated copper nitrate(II) were dissolved in a 20 mL DMF. After being dissolved, 1 mL of 2-propanol was added to form a clear greenish solution. This mixture was heated at 100 °C for 18 hours to give needle-shaped brownish crystals.

B. Synthesis of Magnetic Framework Composites (MFCs)

1. Synthesis of Magnetite (Fe_3O_4) Magnetic Nanoparticles (NPs)

They were synthesized according to the method found in the literature.¹⁸¹ In brief, citric acid trisodium salt dehydrate ($C_6H_5Na_3O_7 \cdot 2H_2O$, 294 mg, 1mmol), sodium hydroxide (NaOH, 160mg, 4mmol), and sodium nitrate ($NaNO_3$, 17mg, 0.2 mmol) were dissolved in 19 mL deionized water in 50 mL round bottom flask. The mixture was then heated to 100 °C under reflux where it formed a pellucid solution. Following this, 1 mL of 2 M $FeSO_4 \cdot 7H_2O$ (556 mg, 2mmol) solution was added into the mixture rapidly, and the mixed solution was kept at 100 °C for 1 h. After being cooled at room temperature, the mixture was washed through de-ionized water for four times over 2 day, then the particles were dried overnight.

2. MFCs

Fe_3O_4 nanoparticles were added to the Zn-MOF-74 by means of a one-pot solvothermal strategy previously reported.¹² Three different batches of MFCs of different nanoparticles loadings were prepared. In particular, in a 20 mL scintillation vial, 0.038 g of DOBDC and 0.18 g of $Zn(NO_3)_2 \cdot 6H_2O$ were dissolved in 16 mL of a 14:1:1 (v/v/v) mixture of DMF–ethanol- H_2O . Following this, 5, 10, and 20 mg of dried Fe_3O_4 nanoparticles were added to each of the vials constituting MFC1, MFC2, and MFC3. Then the vials were heated at 125 °C for 20h in the oven. Following this, it was cooled down at room temperature. The resulting samples were washed at activated same as the pre-synthesized MOFs.

C. Room Temperature MOFs.

1. *RT-Zn-MOF-74*

The MOF was prepared using a reported method.¹⁵⁶ In a 50 mL beaker, 0.081 g of DOBDC and 0.190 g of $\text{Zn}(\text{NO}_3)_2 \cdot 6\text{H}_2\text{O}$ were dissolved in a solution containing 5 mL DMF, 600 μL water, and 600 μL ethanol. After mixing, the solution was placed on a magnetic stirrer before adding 300 μL of triethylamine (TEA) and keeping the reaction on the magnetic stirrer for another 1h at room temperature. Following this, the precipitates were collected by centrifugation, washed and activated in the same manner as pre-synthesized MOFs.

2. *Mixed Metals (RT-Zn/Mn-MOF-74, and RT-Co/Mg-MOF-74)*

The two MOFs were prepared same as RT-Zn-MOF-74 was prepared, but instead of using 0.19 g of $\text{Zn}(\text{NO}_3)_2 \cdot 6\text{H}_2\text{O}$, 0.095 g of $\text{Zn}(\text{NO}_3)_2 \cdot 6\text{H}_2\text{O}$ and 0.080 g of $\text{Mn}(\text{NO}_3)_2 \cdot 4\text{H}_2\text{O}$ were used for synthesizing RT-Zn/Mn-MOF-74, and 0.093 g of $\text{Co}(\text{NO}_3)_2 \cdot 6\text{H}_2\text{O}$ and 0.082 g of $\text{Mg}(\text{NO}_3)_2 \cdot 6\text{H}_2\text{O}$ were mixed to prepare RT-Co/Mg-MOF-74.

D. Characterization Techniques

1. *Powder X-Ray Diffraction*

Powder x-ray diffraction (PXRD) patterns of the MOF samples were collected with a Bruker D8 advance x-ray diffractometer (Bruker AXS GmbH, Karlsruhe, Germany, working at 40 kV and current 40 mA, 2θ range: 5-50°, increment: 0.01°) using Cu $K\alpha$ radiation ($k=1.5418 \text{ \AA}$).

2. *Thermogravimetric analysis*

Thermogravimetric analysis (TGA) was performed with a Netzsch TG 209 F1 Libra apparatus under air flow from 30 to 800 °C at a heating rate of 11 K·min⁻¹.

3. *Scanning Electron Microscopy*

Scanning electron microscopy (SEM) imaging was done using a MIRA3 Tescan electron microscope after which the samples were coated with a thin layer (20 nm) of Platinum.

4. *Brunauer–Emmett–Teller (BET) surface area measurement*

N₂ adsorption-desorption isotherms were measured using a Quantachrome-NOVA 2200e-Surface Area and Pore Size Analyzer. The MOFs were degassed under nitrogen at a temperature of 120 °C for 12 hours.

5. *Atomic Adsorption Spectroscopy*

The concentrations of different metals in the samples were calculated using Atomic Absorption Spectroscopy (AAS) conducted with a Thermo Elemental Analyzer.

E. Esterification Reaction of Butyl Levulinate (BL)

Before being tested, the catalysts were placed in the vacuum oven at 120 °C overnight. The reaction was done in a 50 mL round-bottom flask in which 6.3 mL of butanol, 1 mL of levulinic acid (1:7 mole ratio of LA to butanol based on the literature) were mixed, and the proper loadings of the catalysts were added (5 weight percent of levulinic acid initial weight) at 120 °C. The catalyst loading will be shortened to wt%. the reaction proceeded under reflux using an oil bath placed on a magnetic hot plate at 500 rpm.

The reaction was conducted for 24 hours in which samples of 60 μL were collected from the reaction medium at 0, 2, 4, 6, 8 and 24 hours using an electronic pipette. The samples were diluted by adding them to 2 mL of n-heptane/octanol solution with a known octanol concentration. The diluted solution was then filtered using 0.2 μm PTFE filter to remove any catalyst particles present. The filtered samples were put in 1.5 mL GC for analysis.

After knowing the best performing catalyst, the reaction parameters (catalyst loading, and temperature) were studied to choose the best conditions. The catalyst amount was changed between 1, 2.5 and 5 wt% of the levulinic acid initial weight, which is equivalent to 11.34, 28.35 and 56.7 mg of catalyst respectively. Following this, the temperature was varied between 110, 120, and 125 $^{\circ}\text{C}$. The rest of the reactions (MFCs, room temperature MOFs) were performed under the best reaction parameters. Each reaction was repeated three times, and the average including the error bars was represented.

F. Gas Chromatography Sampling (GC)

The samples were analyzed using gas chromatography (Thermo Scientific, Trace GC Ultra, Gas Chromatograph), associated with a flame ionization detector (FID). The column used was Teknokroma capillary wax column (30 m X 0.32 mm X 0.25 μm). The inlet and detector temperatures were programmed to be 280 $^{\circ}\text{C}$. Hydrogen was used as the carrying gas, the volume injected was 1 μL , and the split ratio was 100:1.

While working with GC, it is essential to have an internal standard (IS) that ensures the proper calibration and accuracy of the standards and the precise running of

the machine. Herein, octanol is the used IS, and heptane is the solvent in which octanol and butyl levulinate were dissolved in for calibration and testing samples. The octanol concentration was 10 mg/mL (3.03 mL of octanol dissolved in 250 mL volumetric flask, followed by heptane till the line mark). A set of seven standards for butyl levulinate were prepared ranging from 0.05 g/mL to 0.25 g/mL based on the minimum and maximum conversion of LA to BL. Each standard was dissolved in the same amount of octanol/heptane solution as the samples were dissolved to have same systematic study. Each sample was tested three times and the average area for each one was represented. The concentrations of the standards and the peaks related to them are represented in **Table 2.2**; whereas the calibration curve representing them in terms of X and Y ratios is shown in **Figure 2.2**.

Table 2.2 Calibration curve standards and their corresponding peak area (average over 3 runs)

Standards	Octanol		Butyl Levulinate	
	Injected Concentration (mg/mL)	Average Peak Area	Injected Concentration (g/mL)	Peak Area
1	10	178063617	0.05	17514681
2	10	177370528	0.1	34560709
3	10	180321318	0.15	52034976
4	10	178114030.5	0.18	65023457.5
5	10	171568443.5	0.2	66311541.5
6	10	169842294.5	0.225	77601062.5
7	10	177373213.5	0.25	83298209.5

$$X_{ratio} = \frac{C_{is}}{C_s}$$

$$Y_{ratio} = \frac{PA_{is}}{PA_s}$$

In fact, X_{ratio} corresponds to the ratio of the concentration of the sample (C_{is}) to that of the standard (C_s), and Y_{ratio} is the ratio of the peak area of the sample (PA_{is}) to that of the standard (PA_s).

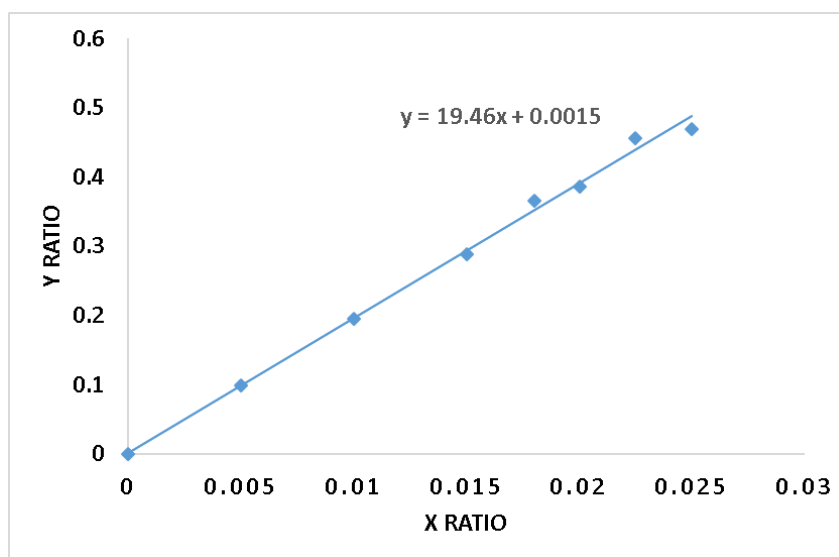


Figure 2.2 Calibration curve based on Y and X ratios.

Using the equation of the calibration curve and knowing the exact peaks of the IS and that of the ester, the concentration of the produced ester can be calculated through simple substitution in the equation.

G. Catalyst Recycling

The reaction medium containing the best performing catalyst among the studied MOFs was chosen. After centrifugation to separate the catalyst from the supernatant, the catalyst was washed with methanol 3 times, then dried at 100 °C in the vacuum oven overnight to be used for other two reactions. The samples were taken only at the beginning and at the end of the reaction (24 hour) for the sake of comparing the activity of the catalyst after being regenerated. Moreover, PXRD pattern of the regenerated MOF was collected to ensure that the crystallinity of the MOF is reserved.

CHAPTER III

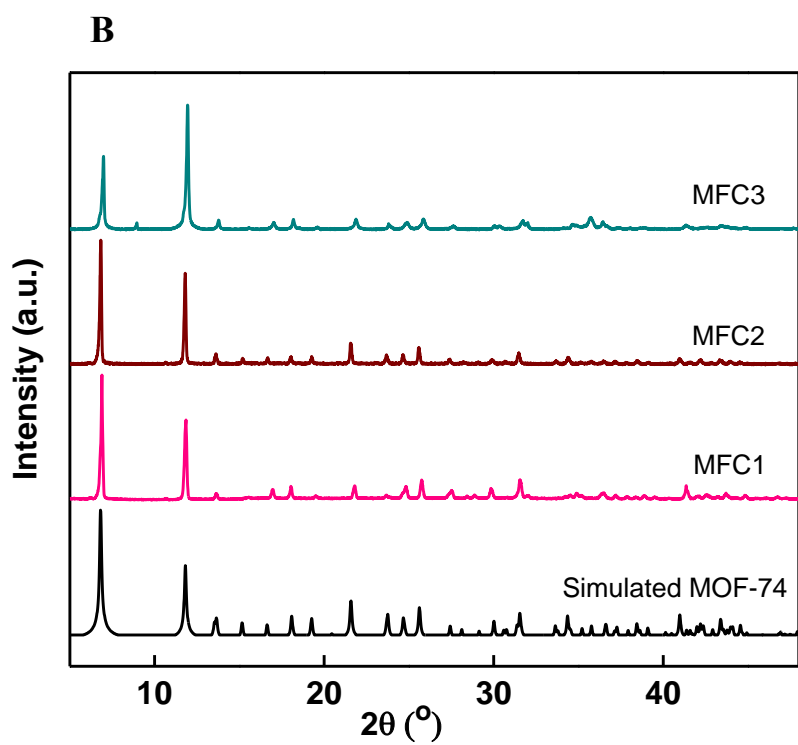
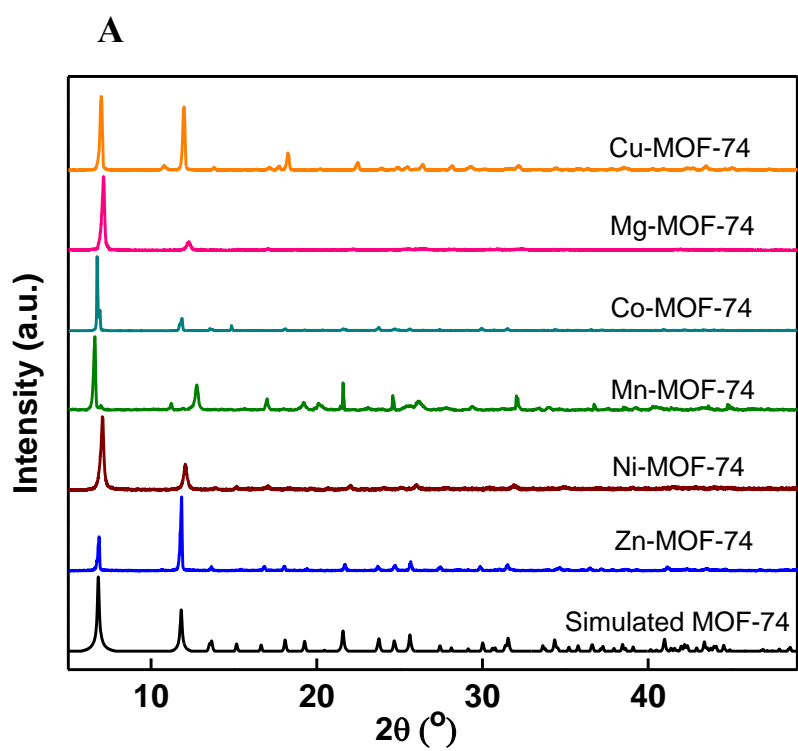
RESULTS AND DISCUSSIONS

A set of techniques were used to characterize the MOFs, these techniques are the following:

A. Powder X-Ray Diffraction (PXRD)

The experimental PXRD patterns of all solvo-thermally synthesized MOF-74 samples, and the various MFCs in addition to the room temperature synthesized MOFs are shown in **Figure 3.1 (A), (B) and (C)** respectively. The patterns are identical especially for the first two main peaks, with the exception of peak intensities that are linked to the variable orientation, and in great agreement with the simulated one reported in the literature assuring the high phase purity and crystallinity of the samples.¹⁸²

The peaks of the solvothermal synthesized MOFs and the MFCs are sharp narrow peaks different than that of the room temperature MOFs that are broader. This is explained by the fact that room temperature MOFs have nano-scaled particles (22.5 nm for RT-Zn-MOF74, 12 nm for RT-Co/Mg-MOF-74, and 19 nm for RT-Zn/Mn-MOF-74) whereas the size of solvothermal samples are in the micro range (144 μm for Zn-MOF-74).



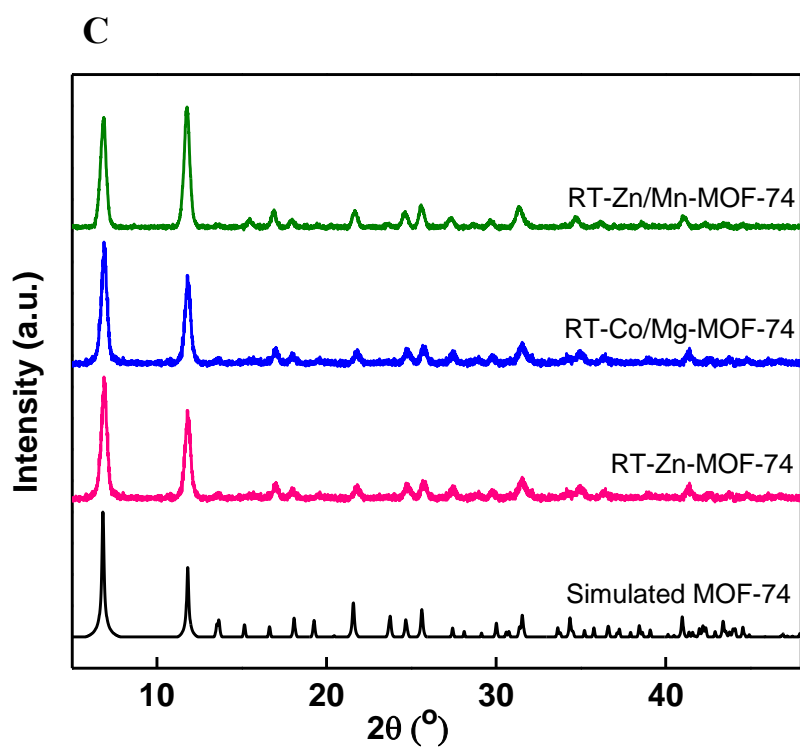
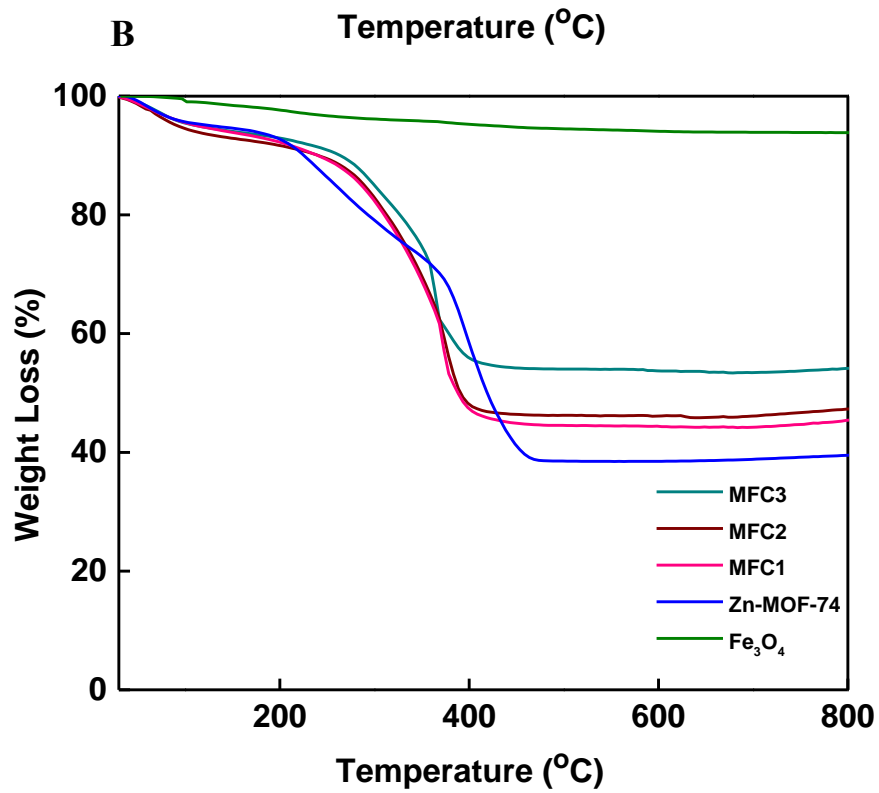
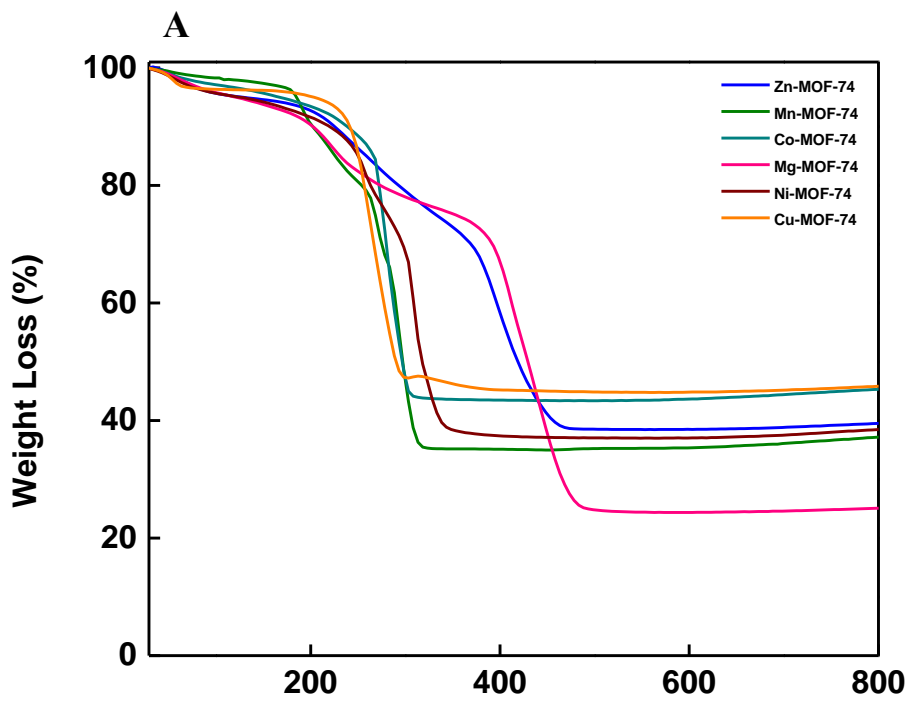


Figure 3.1 PXR D patterns of (A) solvothermal synthesized MOFs, (B) MFCs, and (C) room temperature synthesized MOFs.

B. Thermogravimetric analysis (TGA)

In order to investigate the thermal stability of the studied samples, TGA was performed and the resulting curves representing the weight loss as function of the temperature are represented in **Figure 3.2**.



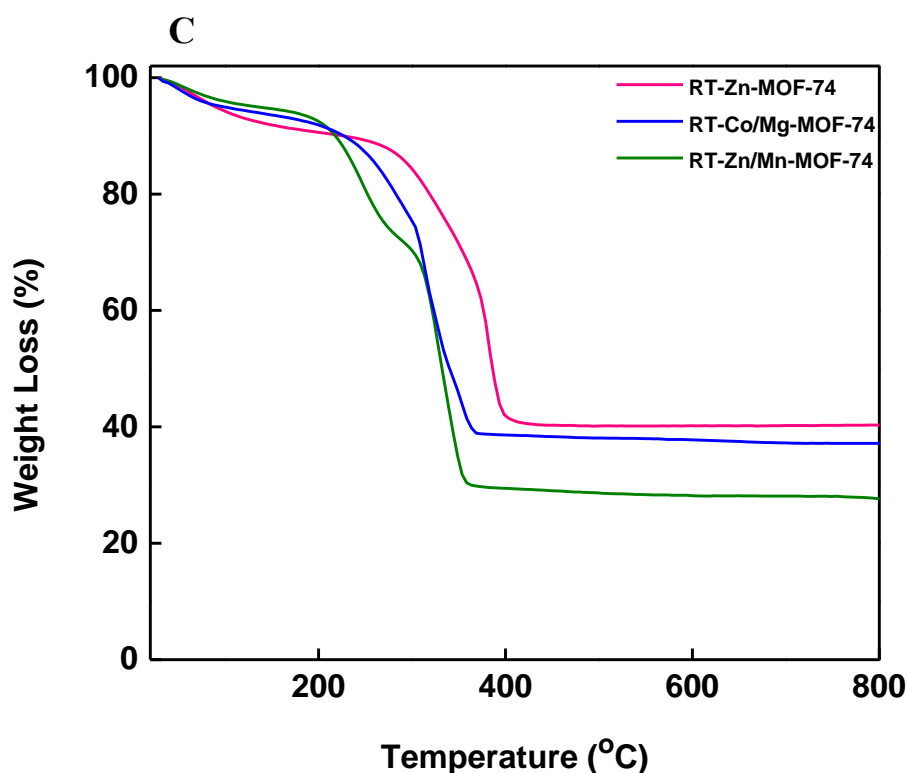


Figure 3.2 TGA curves for (A) solvothermal synthesized MOFs, (B) MFCs, and (C) room temperature synthesized MOFs.

In general, all the samples have similar thermal behavior, in which two main weight losses can be observed. The first one takes place below 200 °C, which corresponds to the evaporation of the water and other solvents. The second loss occurs between 200 to 500 °C, and it is attributed to the decomposition of the framework which agrees with the values reported in the literature. Beyond these temperatures, the remaining mass corresponds to the metal oxides formed.

Concerning **Figure 3.2 (B)**, the Fe₃O₄ nanoparticles showed negligible decrease in their weight loss throughout the entire process indicating their stability even at elevated temperatures. By comparing the remaining weight percent of the metal oxides for each sample at the end of the analysis, the percentage of the nanoparticles contained

within each composite can be calculated. The magnetite loading for each composite was found to be 6.16, 7.80 and 15.72 wt% for MFC1, MFC2 and MFC3 respectively.

C. Atomic Adsorption (AA)

To have the accurate percentage of iron found in the composites, the composites were dissolved in aqua regia followed by dilution with water, then the supernatants were investigated through AA spectroscopy. Iron concentrations were found to be 3.73, 7.16, 11.86 wt% for MFC1, MFC2 and MFC3 respectively.

Moreover, the room temperature mixed metals were analyzed by AA to calculate their metal percentages. Even though the samples were prepared by equal metal amounts, the actual percentages incorporated within the frameworks were completely different; RT-Zn/Mn-MOF-74 contained 80% zinc and 20% manganese, whereas RT-Co/Mg-MOF-74 contained 85% cobalt and 15% magnesium.

D. Scanning Electron Microscopy (SEM)

SEM images of the different samples were collected, and representative images were depicted in **Figure 3.3**. The images are unique and homogenous for each sample reflecting the purity of the studied MOFs and composites. All of the solvothermal MOFs showed the same rod-like structures with hexagonal aperture in agreement with the hexanol symmetry of the crystals except for the Ni-MOF-74 that had aggregated crystals in small rice-like structures. In addition, the difference in the particle sizes can be noticed in which Ni-MOF-74 was the smallest, followed by Mg, Cu, and Co-MOFs that showed similar sizes smaller than that of Mn, that is in return smaller than that of Zn sample.

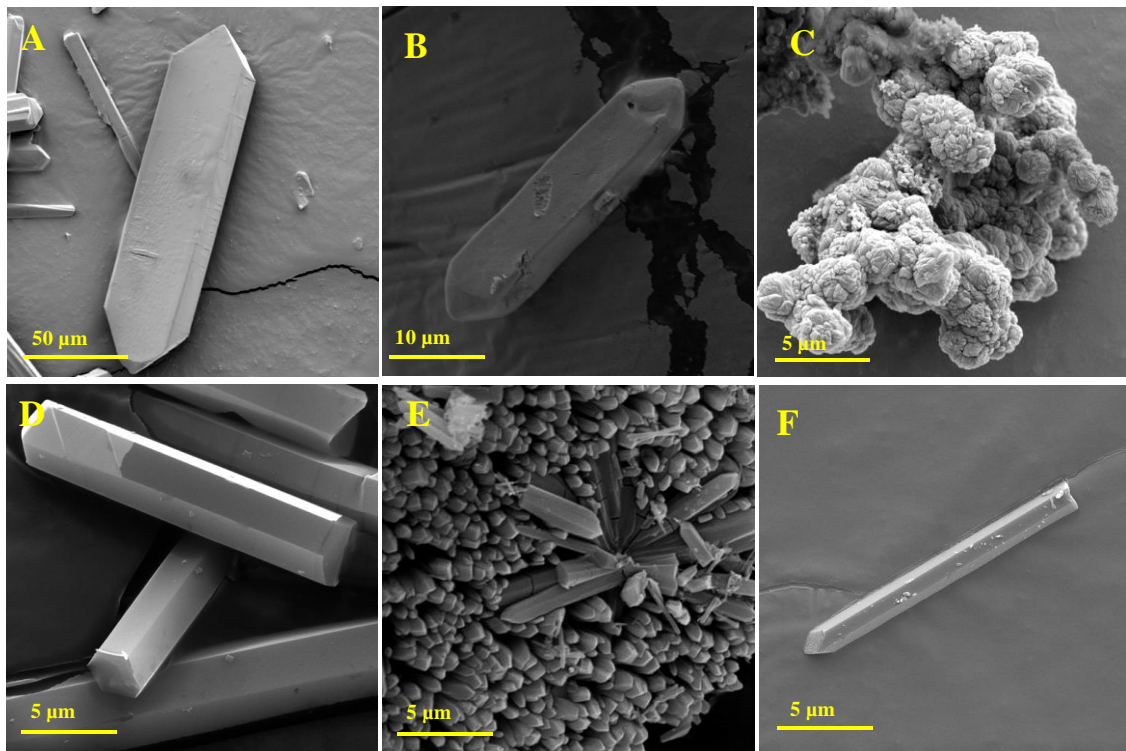


Figure 3.3 SEM images of (A) Zn-MOF-74, (B) Mn-MOF-74, (C) Ni-MOF-74, (D) Co-MOF-74, (E) Mg-MOF-74, and (F) Cu-MOF-74.

Following so, the morphologies of magnetic magnetite particles and the composites were studied and represented in **Figure 3.4** and **Figure 3.5** respectively.

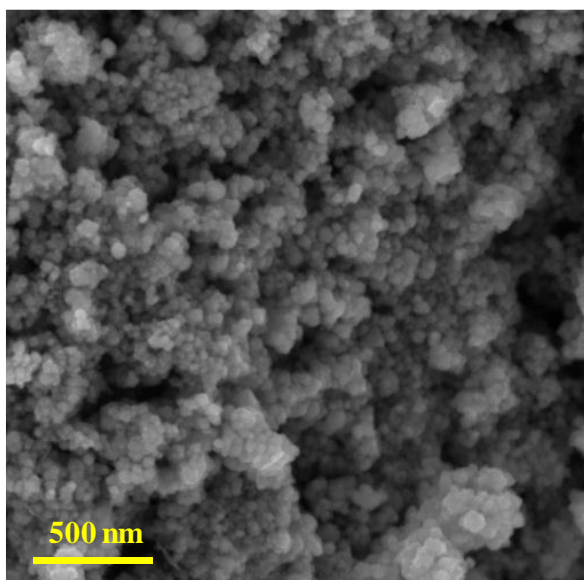


Figure 3.4 SEM images of magnetite Fe_3O_4 .

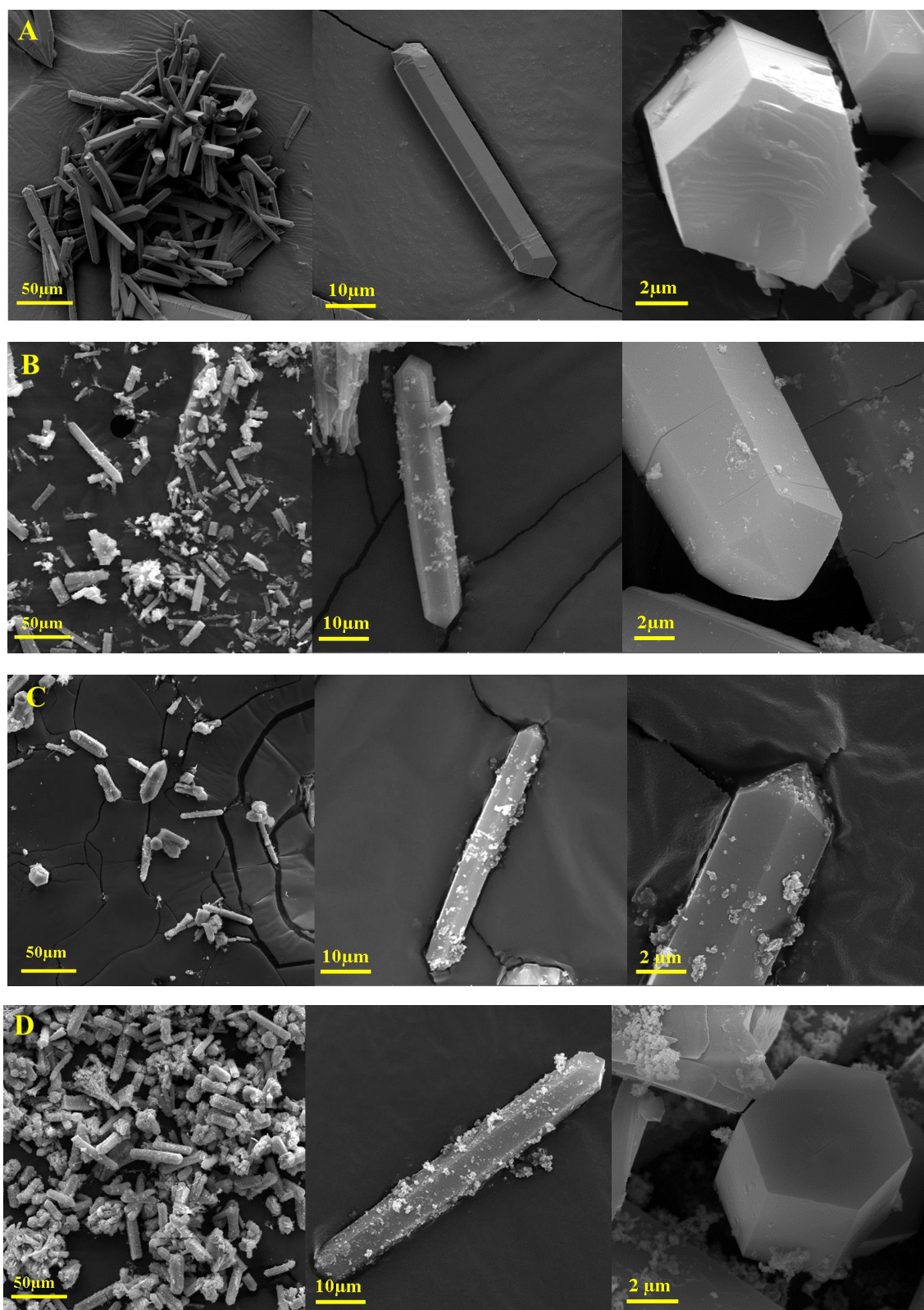


Figure 3.5 SEM images of (A) Zn-MOF-74 free of any nanoparticles, (B) MFC1, (C) MFC2, and (D) MFC3, taken at different scales.

All composites obtained retained the rod-like structure of solvothermal Zn-MOF-74. The only change was in the number of magnetic nanoparticles present where it increased while moving from MFC1 to MFC3. As expected, the nanoparticles' distribution wasn't homogenous, where certain areas contained magnetite aggregates, others had moderate amounts of particles and some had very low magnetite distribution.

Moreover, to confirm the presence of nanoparticles within the composites, the three samples were subjected to energy dispersive X-ray (EDX) mapping microanalysis. The results are shown in **Figure 3.6**. The results confirmed the presence of iron with the framework assuring the incorporation of magnetite with the crystals.

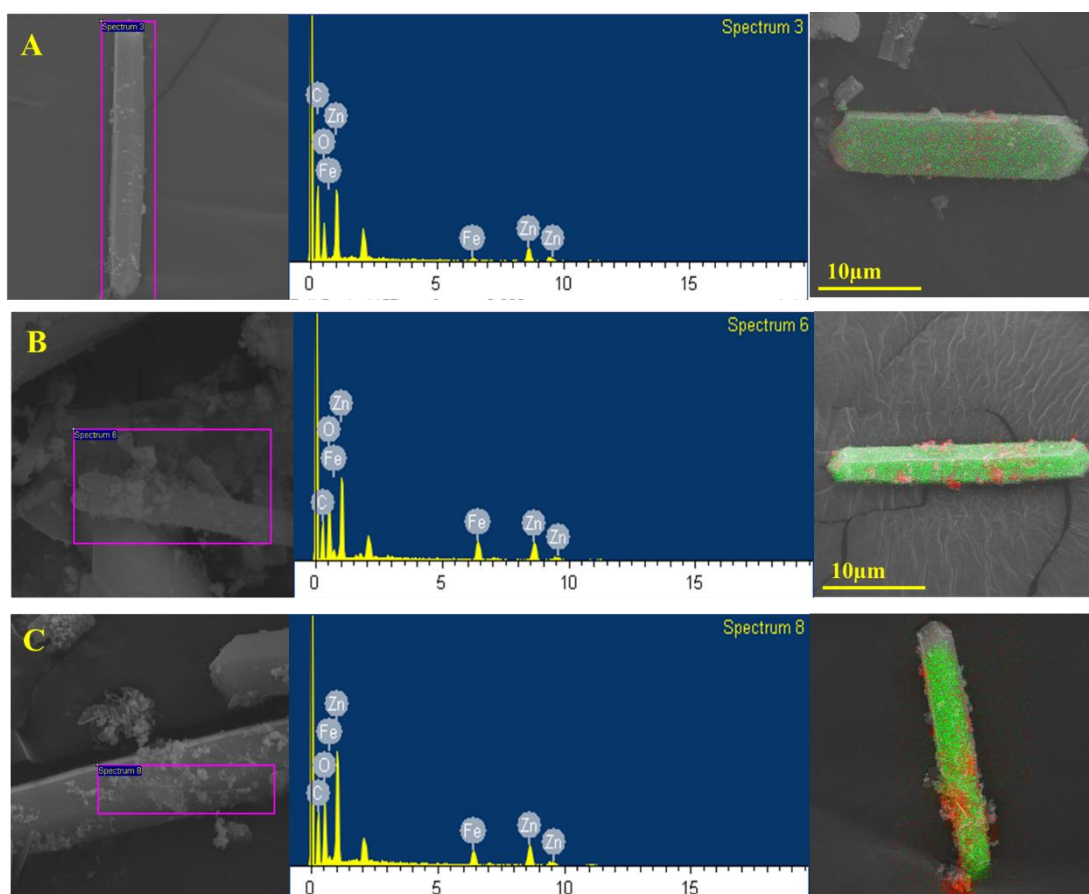


Figure 3.6 EDX mapping for (A) MFC1, (B) MFC2 and (C) MFC3. Color code: green dots represent Zn element, and red dots represent Fe element.

In addition, the morphology of room temperature MOFs was investigated and presented in **Figure 3.7**. Homogenous nano-scaled crystalline aggregated in the form of clusters are formed.

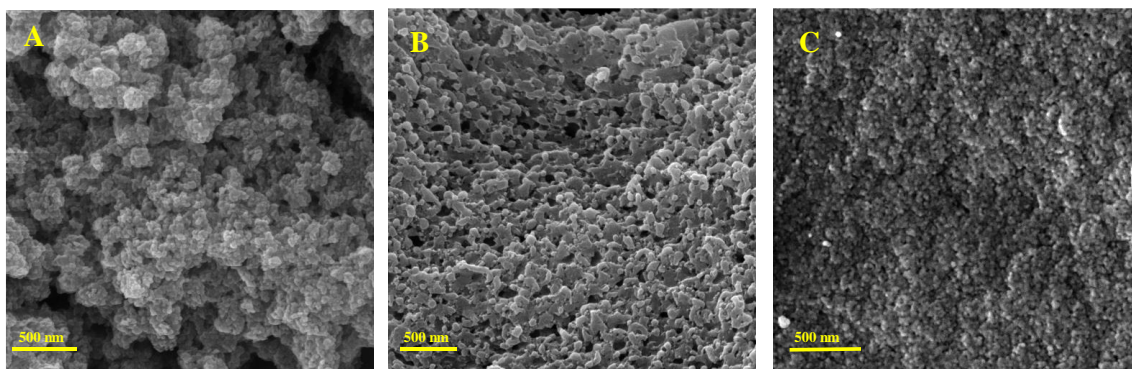
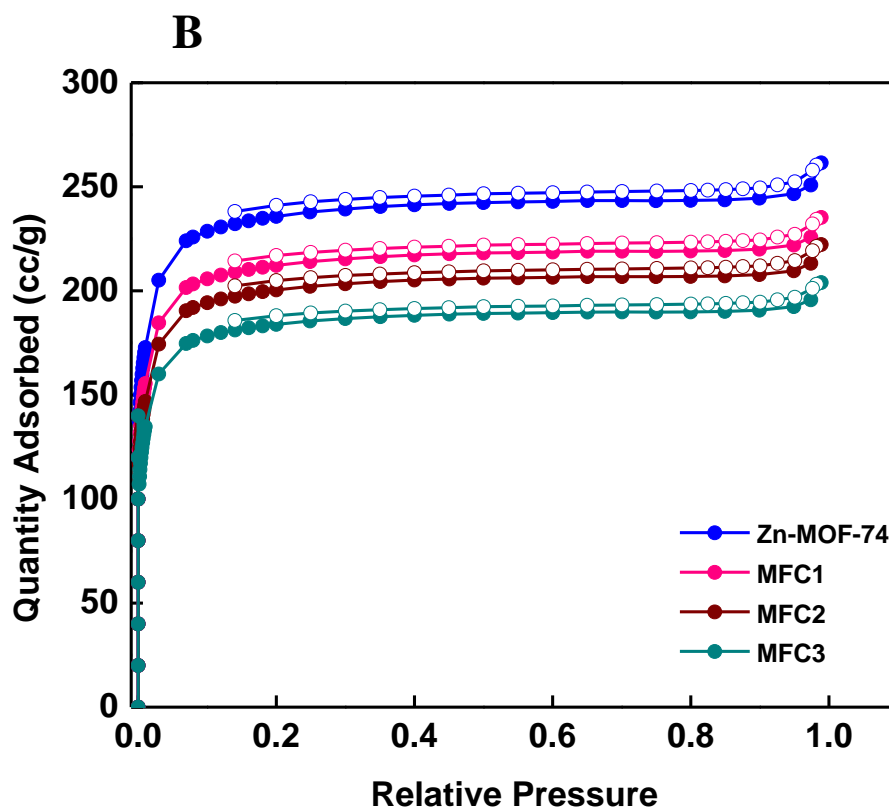
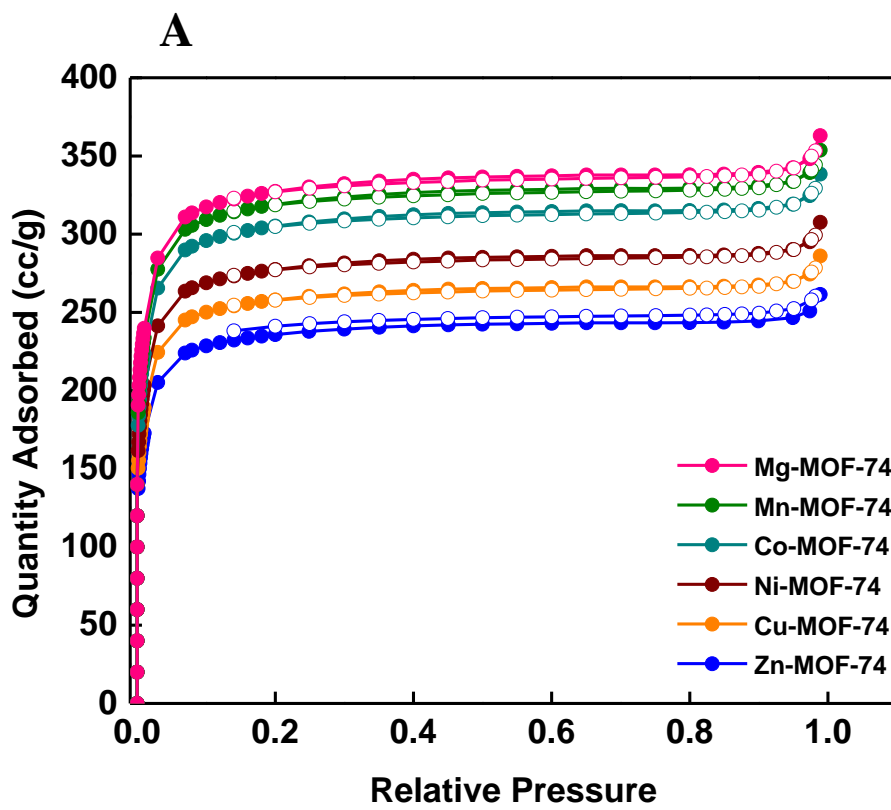


Figure 3.7 SEM images of nano-scaled MOFs (A) RT-Zn-MOF-74, (B) RT-Zn/Mn-MOF-74 and (C) RT-Co/Mg-MOF-74.

E. Brunauer–Emmett–Teller (BET)

The surface areas for the samples were evaluated by the BET method after their degassing at 120 °C. The nitrogen adsorption desorption isotherms are represented in **Figure 3.8**, and the BET surface area, and pore volume are summarized in **Table 3.1**.

All solvothermal MOFs and MFCs displayed type I isotherms, whereas the nano-scaled samples showed type IV. This is due to the use of triethylamine (TEA) while synthesizing the room temperature MOFs, that acts as an etching agent for the wall of the pores by coordinating to the metal cluster and thus giving the MOF the mesoporous character.



h

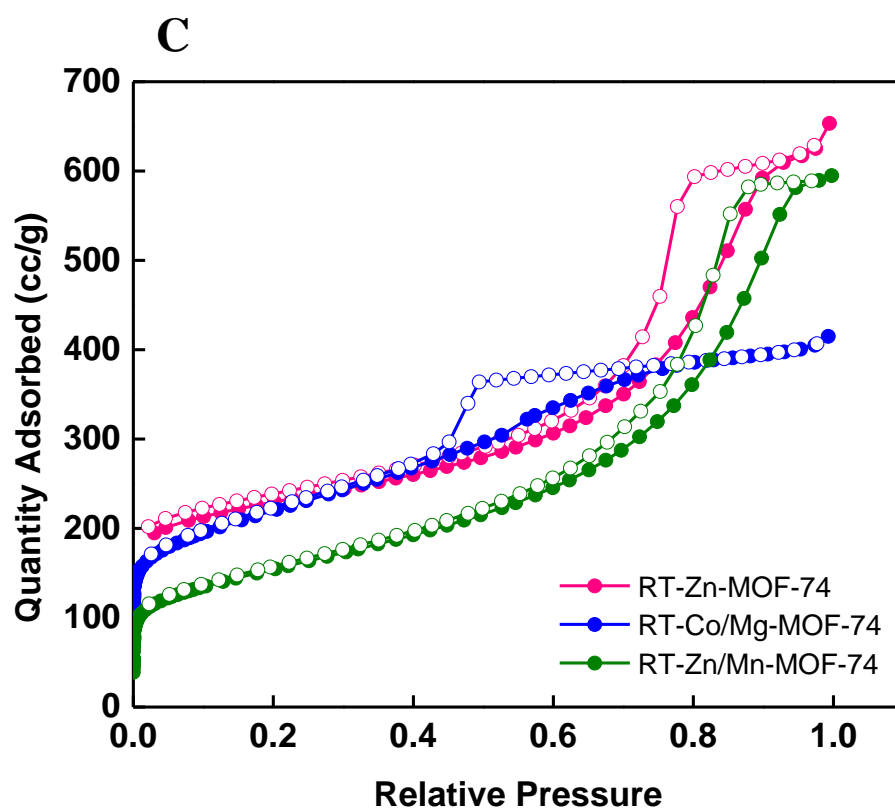


Figure 3.8 N₂ isotherms for (A) solvothermal MOFs, (B) MFCs and (C) room temperature MOFs.

Table 3.1 BET surface areas and pore volumes for the tested catalysts.

MOF	BET surface area (m²/g)	Pore volume (cm³/g)
Mg-MOF-74	1205	0.547
Mn-MOF-74	1174	0.533
Co-MOF-74	1123	0.510
Ni-MOF-74	1021	0.464
Cu-MOF-74	949	0.431
Zn-MOF-74	868	0.403
MFC1	781	0.363
MFC2	738	0.343
MFC3	677	0.315
RT-Zn-MOF-74	638	0.974
RT-Zn/Mn-MOF-74	371	0.912
RT-Mg/Co-MOF-74	582	0.630

F. Esterification Reaction of Butyl Levulinate

The esterification reaction of butyl levulinate starting from levulinic acid and butanol took place under the effect of different catalysts. All the catalysts were selective in a way that no byproducts beside butyl levulinate were formed. The conversion progress as a function of time was supervised and plotted.

1. Different Solvothermal MOFs

The first study included exploring the effect of the five solvothermal prepared MOFs (Mn-MOF-74, Ni-MOF-74, Co-MOF-74, Mg-MOF-74, and Zn-MOF-74) in comparison to each other and to the conventional used sulfuric acid (H₂SO₄) in addition the control reaction deprived of any catalyst (blank). In this study, 5 wt% catalyst loading (corresponding to 56.7 mg) were added to the reaction containing (6.3 mL butanol and 1 mL LA), and the reaction was allowed at a temperature of 120 °C. each run was repeated three times, and the results are shown in **Figure 3.9**.

As shown in **Figure 3.9**, all the MOFs showed relatively fast transformation in which the MOFs' activity followed a certain trend between the conventional sulfuric acid, and the no catalyst blank reaction. In the case of the blank, the formed ester is related to the autocatalysis of LA up to a certain level. By investigating the catalysts, sulfuric acid had the highest rate and conversion percentage (97%), followed by the Zn-MOF-74 that was the best among the MOFs with a 93% final conversion which is very slightly lower than sulfuric acid conversion, but over wider range of time (24 h instead of 4 h for H₂SO₄). After that, Mn-MOF-74 came the second-best performing MOF (78%), followed by Ni-MOF-74 as the third (74%), then Co-MOF-74 (72%), to finally end the series with Mg-MOF-74 of the lowest rate and conversion percentage (69%).

As the reaction proceeded, the rate gradually decreased with time until the reaction reached equilibrium after 24 h. This rate decline is attributed to the decrease in the reactants' concentrations, which is a kinetic factor, once decreases, the rate of the reaction decreases. Another factor can also be responsible for this drop, which is the blockage of the catalysts' active sites as a result to the increasing product amounts, that ends up by decreasing the MOFs' accessibility for the reagents.

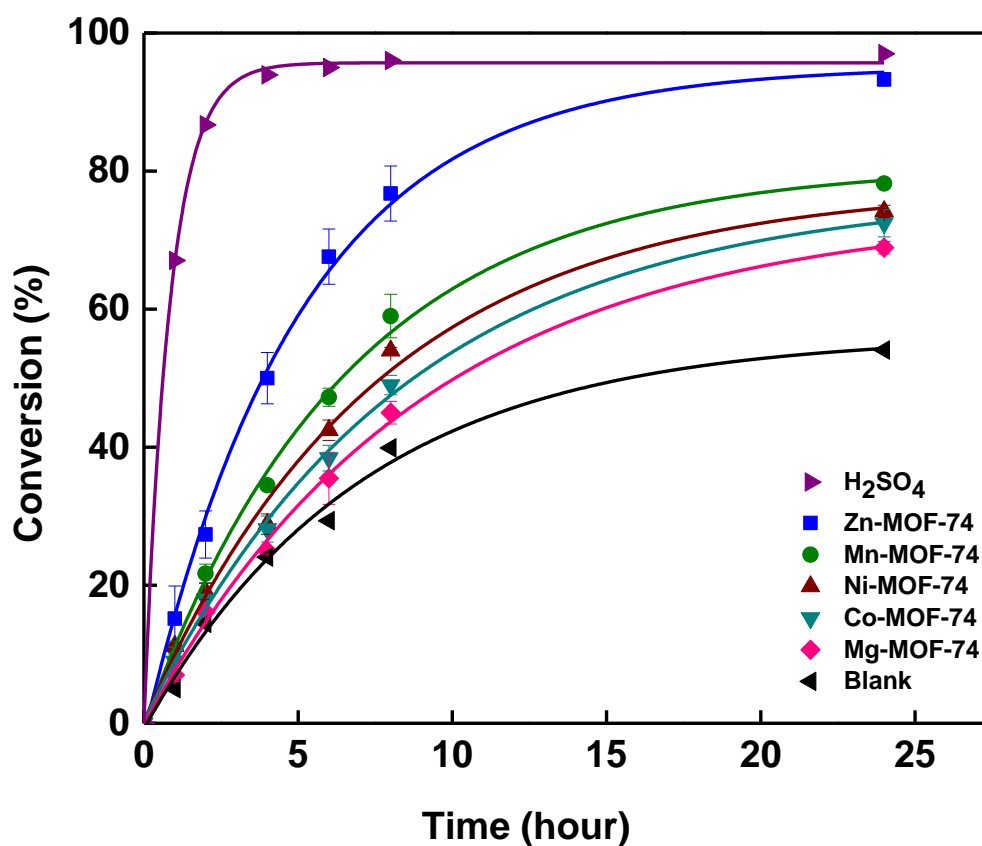


Figure 3.9 Conversion of butyl levulinate for the different catalysts as function of time (hour).

1. Changing Parameters

Following this, reaction parameters were studied to investigate the best temperature and loading for the esterification reaction. Therefore, the most performing catalyst was chosen (Zn-MOF-74), and three different loadings were used: 1, 2.5, and 5 wt% corresponding to 11.34, 28.35 and 56.7 mg. The obtained data are represented in **Figure 3.10**.

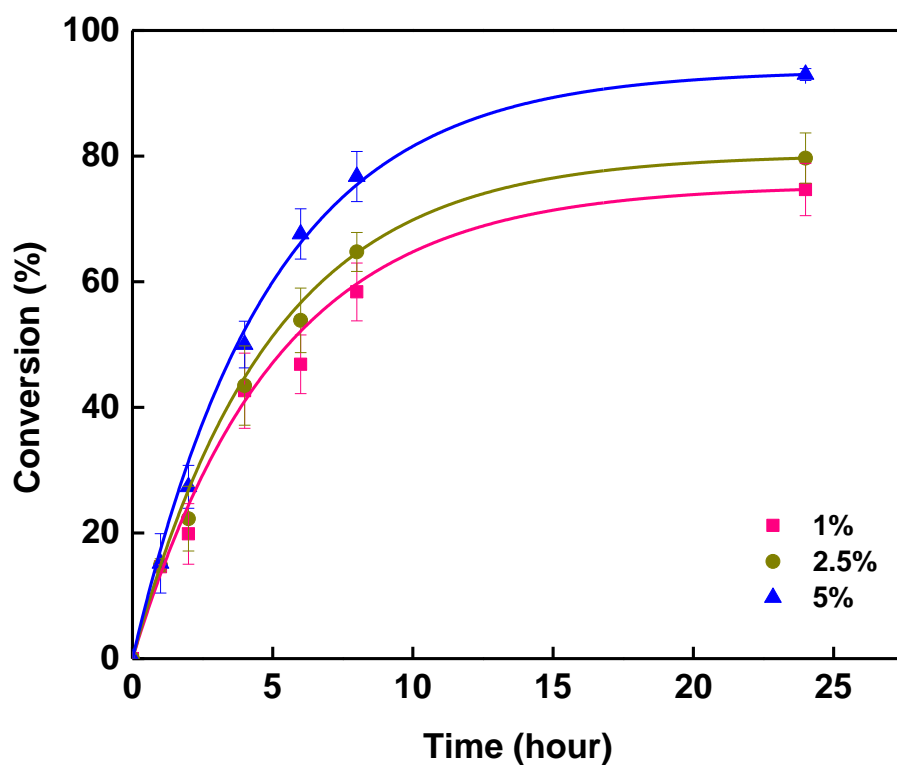


Figure 3.10 Butyl levulinate conversion under the effect of different Zn-MOF-74 loading.

The increase in the catalyst loading from 1 wt% to 5 wt% caused an increase in conversion rate and percentage from 76% to 93%. The explanation behind this behavior is the fact that increasing the loading leads to intensifying the number of active acid sites, that in return increases their accessibility for LA and butanol to form more butyl levulinate in faster way.

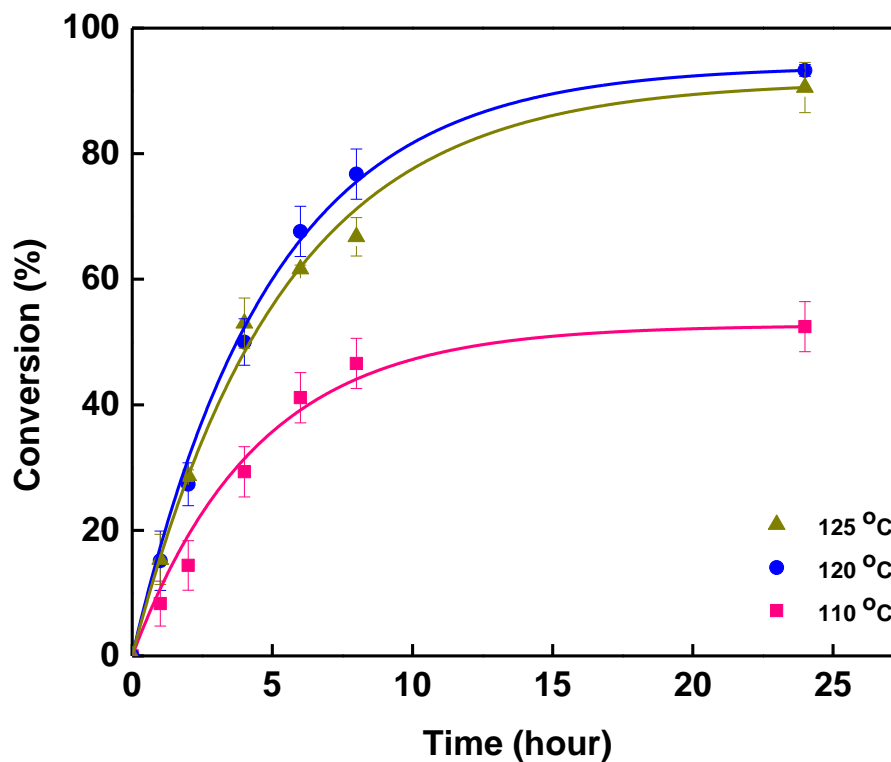


Figure 3.11 Butyl levulinate conversion under the effect Zn-MOF-74 at different temperatures.

Following this, temperature effect was studied under three different temperatures: 110, 120, and 125 °C and the results are shown in **Figure 3.11**. The lowest conversion rate and percentage were attributed to 110 °C, that increased to the maximum when the temperature increased to 120 °C, to further drop slightly at 125 °C. The system was under reflux, and the boiling point of butanol is around 118 °C, which means that the reaction necessitated such an elevated temperature to run normally. A temperature lower than butanol boiling point make the reaction slower with lower conversion and more needed time as observed. In addition, 120 °C is the closest temperature to the butanol boiling point making it the perfect choice for the process, whereas 125 °C showed lower conversions due to the troubles faced in the system that allowed the evaporation of some of the butanol leading to lower results.

Since higher conversion was obtained using 5 wt% loading at 120°C, these conditions will be used throughout the rest of the study.

2. Catalyst Recycling

While examining the reusability of a heterogenous catalyst, two main factors must be studied: activity and stability. Concerning stability, it can be studied by examining the PXRD pattern of the MOF after each recovery cycle, and the activity is studied through running the same used catalyst in a new esterification reaction.

Therefore, after each run, Zn-MOF-74 was separated from the reaction medium through centrifugation, then the MOF was washed and activated again to be ready for testing. First, PXRD pattern of the catalyst was investigated to assure that the MOF preserved its crystallinity and stability and the patterns are shown in **Figure 3.12 (A)**

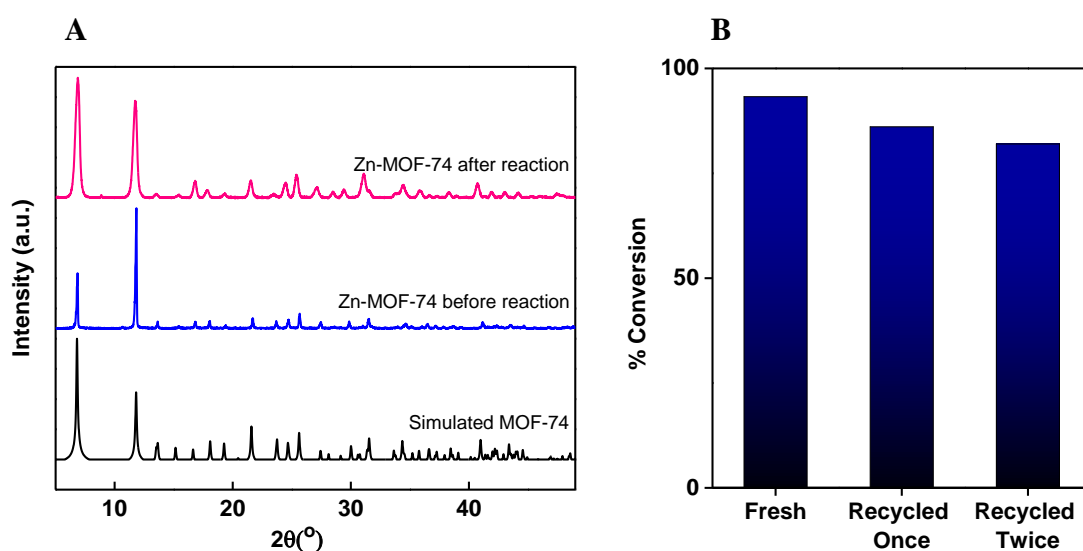


Figure 3.12 (A) PXRD pattern of Zn-MOF-74 before and after testing. **(B)** butyl levulinate conversion after two regeneration cycles.

As noticed, zinc MOF retained its crystallinity by having the same PXRD pattern before the reaction, where all the peaks were maintained confirming the rigidity and strength of the framework in addition to its suitability to be a perfect heterogenous catalyst. It is noteworthy to mention that the peaks of the post reaction PXRD were wider than those before, this can be due to the effect of the magnetic stirrer on the catalyst's morphology, in which continuous stirring leads to damaging the MOFs' morphology and thus decreasing their particle size.

After confirming the crystallinity, the activity of the samples must be studied and compared to the freshly used ones. **Figure 3.12 (B)** represents the conversion of levulinic acid to butyl levulinate using Zn-MOF-74 as fresh and as recovered over two cycles. By comparing the conversion percentages, it is observed that the catalyst presented minor activity loss which is due to the minor loss of the catalyst amount during regeneration. However, even after the third run, the conversion was still high (82%) and could be higher if the mass was preserved. Moreover, absence of any major deactivation was recorded, and this is a very crucial trait for heterogenous catalysts where its deactivation prevents it from being reused and being reused is one of the properties heterogenous catalysts surpass homogenous catalysts with. In fact, even if dealing with heterogenous catalysts is much more easier than dealing with homogenous ones, where the latter necessitates the refinement of the ester from the catalyst itself through separation units, but having to use new catalyst in every run isn't cost effective and leads to many economical losses.

Therefore, the stability, and high activity of Zn-MOF-74 allowed it to be a perfect candidate as a heterogenous catalyst for butyl levulinate production.

3. Nano-Scaled Room Temperature MOFs

Another important factor that could influence the esterification rate is the particle size of the catalyst. In general, large particle sizes cause reaction diffusion control as a result to impacting the mass transport characteristics. Moreover, as the particle size increases, the number of external active sites decreases. Therefore, in order to investigate this effect, nano-sized MOFs were synthesized at room temperature. In addition, mixed metal MOFs were also synthesized to investigate the effect of the different metals as well.

Because zinc MOF proved to be the best performing MOF, followed by manganese MOF, whereas magnesium and cobalt MOFs showed the lowest activity, three different room temperature MOFs were prepared. Pure zinc MOF (RT-Zn-MOF-74), mixed metal of the best two performing catalysts (RT-Zn/Mn-MOF-74), and the lowest performing two MOFs (RT-Co/Mg-MOF-74). These three samples were studied on the same system and the results are depicted in **Figure 3.13**.

Herein, three different observations can be made, the first concerns RT-Co/Mg-MOF-74 that showed the lowest conversion (64%) as expected, with a lower conversion rate and percentage than that of solvothermal Co-MOF-74 (72%) and Mg-MOF-74 (69%) even when the cobalt percentage was 85% with respect to the magnesium (15%). The second one is related to the activity of RT-Zn-MOF-74 and RT-Zn/Mn-MOF-74 that were almost the same but the latter should a little bit lower conversion that can be due to systematic error or to the fact that RT-Zn/Mn-MOF-74 contains around 20% Mn metal (lower activity than the zinc) compared to 80% Zn amount. Finally, the third observation is related to the fact that all these systems had very similar but little lower

conversions than the solvothermal Zn-MOF-74, even the room temperature pure zinc MOF of smaller size.

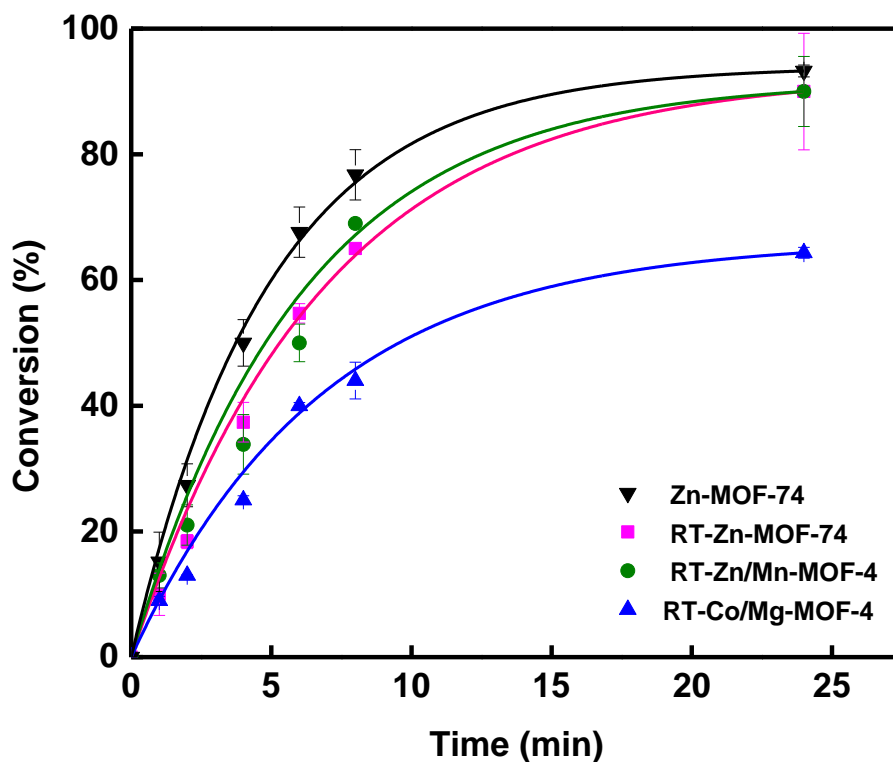


Figure 3.13 Butyl levulinate conversion with the catalysis of nano-scaled MOFs.

4. Magnetic Framework Composites (MFCs)

Because of the problem faced concerning the separation of the catalyst from the reaction medium, enhanced functionalization was done to the MOFs to make them magnetic for easier separation. This included the incorporation of previously synthesized magnetic nanoparticles (Fe_3O_4) within the framework of the best performing MOF, which is the solvothermal Zn-MOF-74, forming magnetic framework composites (MFCs) that allows the facile separation of it from the reaction medium through the usage of magnetic field.

Three composites were prepared of increasing magnetite's loading: MFC1, MFC2, and MFC3 in which MFC3 were the easiest to separate from the reaction medium. **Figure 3.14** represents the conversion percentage under the catalysis of these different composites in addition to the naked Fe_3O_4 nanoparticles.

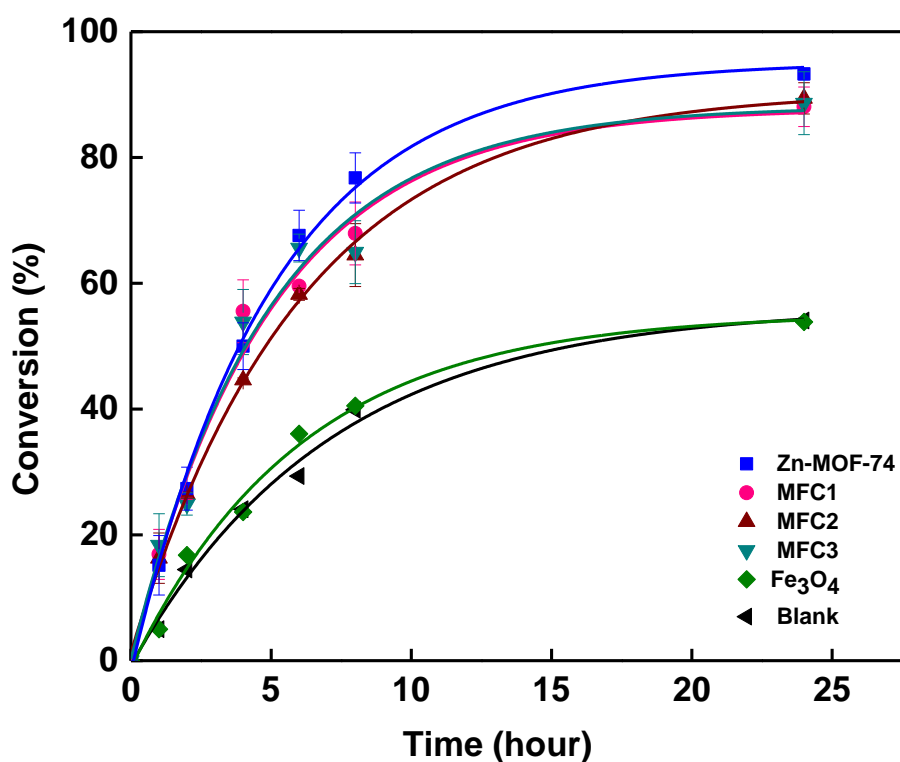


Figure 3.14 Conversion to butyl levulinate with the various composites and the magnetite nanoparticles.

Among themselves, the three composites had very close and almost overlapping results, and while comparing them with the Zn-MOF-74, they started almost identically with a slight difference in the final percentage. It is noteworthy to mention that the naked magnetite had no significant effect on the catalysis of the reaction assuring that the only catalytic active sites are those of the MOFs. The rate and percentage of

conversion were high for the studied composites, even with all the nanoparticles attached and embedded within the MOFs; therefore, it can be deduced that the magnetite facilitated the usage of the MOFs without blocking any of their active sites.

G. Mechanism of Esterification Reaction

As in all esterification reactions, the presence of an acidic catalyst acting as a proton donor is mandatory to efficiently produce levulinate esters. The first step in the mechanism is the protonation of the carboxylic acid by the acid catalyst; however, in the case of our reaction, the oxygen of the carboxyl group of levulinic acid would adsorb onto the acidic open metal site, thus increasing the electrophilicity of the carboxylic carbon atom. Following so, nucleophilic addition takes place in which butanol (lone pair of oxygen in particular) attacks the positively charged protonated carbon. After that water loss occurs preceded by proton transfer, resulting in an oxonium ion intermediate that will undergo deprotonation to release butyl levulinate.

H. Discussion of Results

In the first study where all solvothermal MOFs were compared with each other, a certain trend was followed: Zn-MOF-74 > Mn-MOF > Ni-MOF-74 > Co-MOF-74 > Mg-MOF-74. The main factor governing this trend is the acidity of the metals incorporated, in which Mg metal has the lowest acidity since it has belong to raw III elements, whereas the rest belong to raw IV elements, and as the number of energy levels increase, the acidity increase. In addition, within the same raw, the acidity increases as the atomic number increases, this explains the case of Ni, Co and Zn. However, Mn has lower atomic number than Co and Ni, yet it showed higher acidity,

indicating that the acidity of the metal wasn't the driving force in this case, but rather other properties that can be due to the BET surface area, particle size, distribution of the acidic sites on the sample, and so on. In addition, higher catalyst loading gave better results since it increased the acidic active sites, and a temperature close to the boiling point of the alcohol was the best suitable one since it allowed the evaporation and condensation of the reagents in the best way.

Concerning the nano-scaled MOFs synthesized through room temperature, it was noticed that all these MOFs showed close but lower results than the Zn-MOF-74. These observations assure that the catalytic activity is independent of the size of the particles and no diffusion control was observed. The conversion depends on the activity of the metal incorporated within, whereas the higher the acidity of the metal, the higher the conversion. However, it is important to mention that the conversion remains high in comparison to other catalyst, and the fact that these MOFs were synthesized at room temperature, thus decreasing the energy and the cost needed for their synthesis, making them perfect candidates for the job.

Moving to the composites, the high rate of conversion of MFCs even with the high magnetite loading, proved the effectiveness of using magnetite for a better catalyst separation without blocking any of the MOFs' active sites.

It is important to mention, that in all the studied samples, there were no relation between the BET surface area and the pore volume with the conversion activity indicating that the surface area isn't the driving force in this study.

The conversion to butyl levulinate under the effect of all the studied catalysts after 24 hours are represented in **Figure 3.15**. by comparing the results of this study with the catalysts of the same reaction reported previously in the literature in **Table 3.2**,

it can be noticed that the tested MOFs are among the best performing ones and gave high conversion with respect to the relatively moderate conditions.

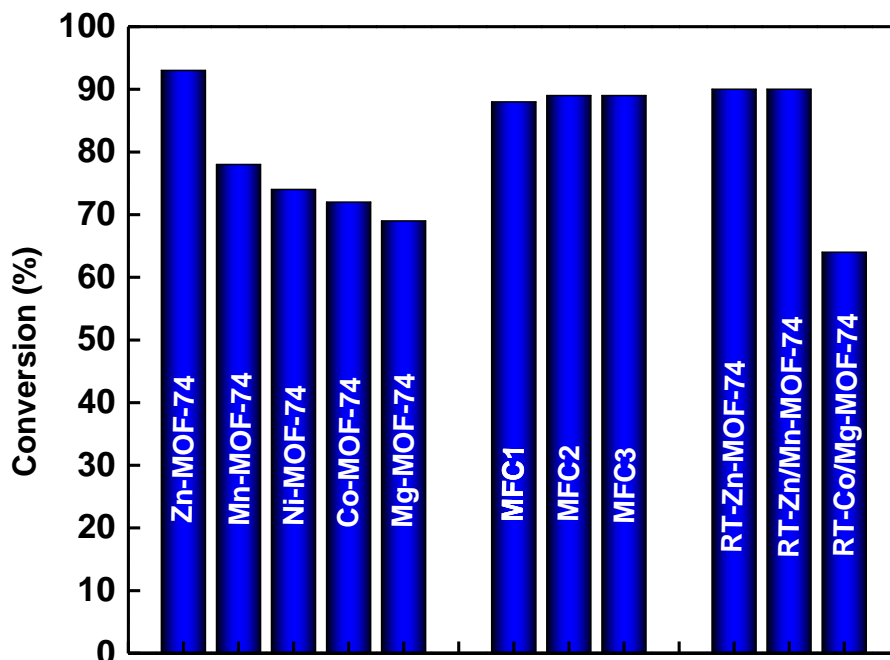


Figure 3.15 Conversion to butyl levulinate under 5 wt% of the tested samples.

Table 3.2 Various catalyst used for butyl levulinate synthesis.¹⁸³

Catalyst	Loading	Temperature (°C)	Yield (%)
ClO ₄ /SiO ₂ nanoporous solid acid	10 wt%	100	90
Tungsten oxide incorporated SBA-16	0.5 g	250	94
Amberlyst-15	20 wt%	124	97
Ammonium co-doped phosphotungstic acid	1.5 %	120	99
Micro/Meso-HZ-5 catalyst	20 wt%	120	96

H-Y catalyst	10 wt%	120	32.2
Bio-glycerol carbon-sulfonic-acid	derived 50 mg	reflux	44
Fe ₂ (SO ₄) ₃	3 mol%	60	90
UiO-66 and UiO-66-NH ₂	1.8 mol%	120	99
Modified titanate	15 wt%	120	82.7
P. cepacialipase	250 mg	45	36
Zn-MOF-74	5wt%	120	93

CHAPTER IV

CONCLUSION AND FUTURE WORK

This thesis has covered a full study on 11 MOF-74 catalysts tested as heterogenous catalysts for esterification reaction of levulinic acid and butanol to produce butyl levulinate, an eco-friendly, highly effective bio-additive fuel.

The relationship between the structure of the MOFs and their properties have been explored, to allow a better understanding of their catalytic performance in this eco-friendly cost-effective worldwide project.

In brief, 11 MOF-74 catalysts were synthesized where through solvothermal or room temperature conditions, then they were characterized to assure their high purity and crystallinity. Following so, these MOFs were tested as acid catalysts for the esterification reaction of butyl levulinate. Among the MOFs differing only in the metal cluster, zinc MOFs showed the highest activity, and magnesium MOFs showed the lowest. After that, the recyclability of the best performing catalyst was investigated, and great results were obtained for the stability and the catalytic activity of the sample, making it a perfect candidate for heterogenous catalysis.

The second study was related to the effect of particle size on the reaction conditions, so nano-scaled pure and mixed metal MOFs were prepared at room temperatures, the conversion was the highest for the pure zinc MOF (RT-Zn-MOF-74) among the nano-sized MOFs, and was very close for the solvothermal Zn-MOF-74. This is of great advantage, since these nanosized samples are prepared in a fast way (1 hour), and at room temperature, making them more cost-effective than the solvothermal

ones even with the slightly lower conversion. However, yielding lower conversions in lower rates assures that the particle size in this case isn't the driving force for the reaction.

After that, magnetic framework composites containing different magnetic nanoparticles loading were tested, to allow better separation of the catalyst from the reaction medium. The results were impressive, where high conversion yields were obtained, assuring the effectiveness of this composite, without any blockage of the MOFs' active sites by the nanoparticles aggregates.

MOFs have proved their uniqueness with all the high potentials they offer in the field of catalysis, that allows them to be the upcoming catalyst generation in the bio-fuel industry. This small research is the first step for a bigger future work, that includes studying new MOFs on the same system for the sake of comparison, and additional treatments for the MOFs, to enhance their acidity and thus their catalytic properties. In addition, further tests will be done, including acidity test, theoretical calculations, kinetic modeling for a better understanding to the mechanism of these reactions. This work is a great step toward our great aim in developing a worldwide eco-friendly environment.

In addition, micro-wave synthesized MOFs have been successfully developed that include MW-AUBM1, MW-MIL-88B and Ti-MOF-74 where they were partially characterized. PXRD and SEM of MW-AUBM1 are represented in **Figure 4.1 (A)**, and **Figure 4.1 (B)** respectively. SEM images of MW-MIL-88B and MW-Ti-MOF-74 are

shown in **Figure 4.2 (A)**, and **Figure 4.2 (B)** respectively. MW-MIL-88B has been tested on the same reaction to produce butyl levulinate, as shown in **Figure 4.3**, the conversion rate and percentage were high but not high enough to overcome Zn-MOF-74. However, MW-AUBM1, Ti-MOF-74 and Cu-MOF-74 will be tested on photocatalytic CO₂ reduction reactions in the future.

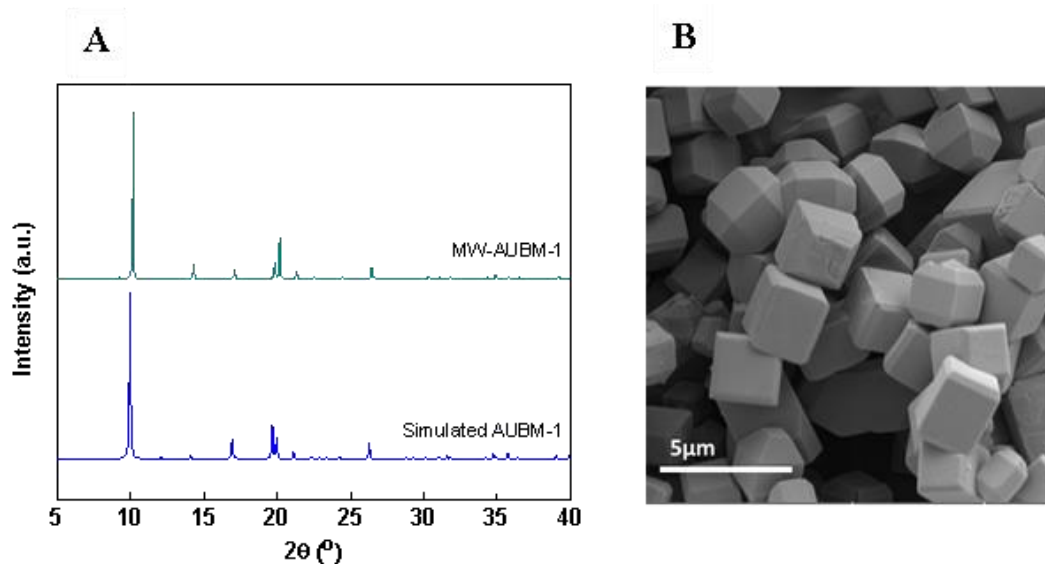


Figure 4.1 (A) PXRD and (B) SEM of MW-AUBM1.

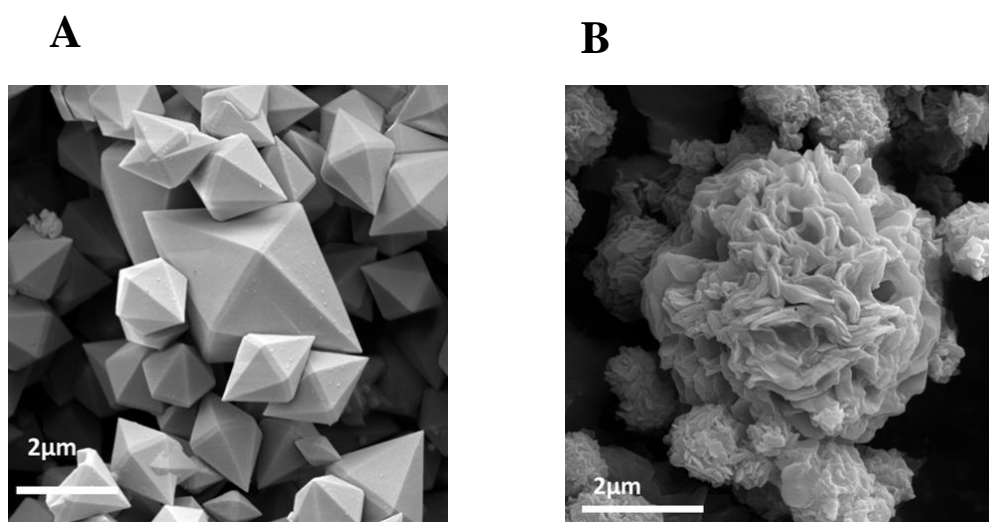


Figure 4.2 SEM images of (A) MW-MIL-88B and (B) MW-Ti-MOF-74.

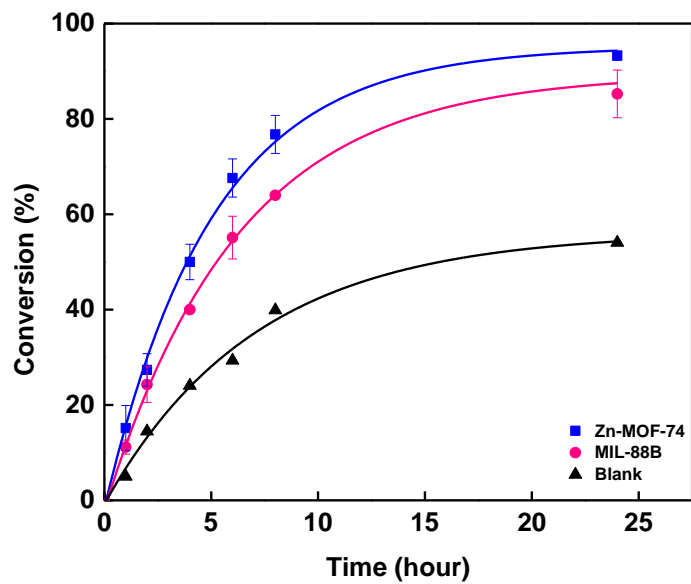


Figure 4.3 Conversion Percentage for MW-MIL-88B compared to Zn-MOF-74.

REFERENCES

1. Administration, E. I.; Office, G. P., *International Energy Outlook 2016, with Projections to 2040*. Government Printing Office: 2016.
2. Ragauskas, A. J.; Williams, C. K.; Davison, B. H.; Britovsek, G.; Cairney, J.; Eckert, C. A.; Frederick, W. J.; Hallett, J. P.; Leak, D. J.; Liotta, C. L., The path forward for biofuels and biomaterials. *Science* **2006**, *311* (5760), 484-489.
3. Govindaswamy, S.; Vane, L. M., Multi-stage continuous culture fermentation of glucose–xylose mixtures to fuel ethanol using genetically engineered *Saccharomyces cerevisiae* 424A. *Bioresour. Technol.* **2010**, *101* (4), 1277-1284.
4. Maheria, K. C.; Kozinski, J.; Dalai, A., Esterification of levulinic acid to n-butyl levulinate over various acidic zeolites. *Catal. Lett.* **2013**, *143* (11), 1220-1225.
5. Milina, M.; Mitchell, S.; Pérez-Ramírez, J., Prospectives for bio-oil upgrading via esterification over zeolite catalysts. *Catal. Today* **2014**, *235*, 176-183.
6. Avramidou, K. V.; Zaccheria, F.; Karakoulia, S. A.; Triantafyllidis, K. S.; Ravasio, N., Esterification of free fatty acids using acidic metal oxides and supported polyoxometalate (POM) catalysts. *Molecular Catalysis* **2017**, *439*, 60-71.
7. Kuzminska, M.; Backov, R.; Gaigneaux, E. M., Behavior of cation-exchange resins employed as heterogeneous catalysts for esterification of oleic acid with trimethylolpropane. *Applied Catalysis A: General* **2015**, *504*, 11-16.
8. Zhang, F.; Jin, Y.; Shi, J.; Zhong, Y.; Zhu, W.; El-Shall, M. S., Polyoxometalates confined in the mesoporous cages of metal–organic framework MIL-100 (Fe): efficient heterogeneous catalysts for esterification and acetalization reactions. *Chemical Engineering Journal* **2015**, *269*, 236-244.
9. Zhou, H.-C.; Long, J. R.; Yaghi, O. M., Introduction to Metal–Organic Frameworks. *Chemical Reviews* **2012**, *112* (2), 673-674.
10. Trickett, C. A.; Helal, A.; Al-Maythaly, B. A.; Yamani, Z. H.; Cordova, K. E.; Yaghi, O. M., The chemistry of metal–organic frameworks for CO₂ capture, regeneration and conversion. *Nature Reviews Materials* **2017**, *2*, 17045.
11. Liu, J.; Chen, L.; Cui, H.; Zhang, J.; Zhang, L.; Su, C.-Y., Applications of metal–organic frameworks in heterogeneous supramolecular catalysis. *Chem. Soc. Rev.* **2014**, *43* (16), 6011-6061.
12. Li, H.; Sadiq, M. M.; Suzuki, K.; Ricco, R.; Doblin, C.; Hill, A. J.; Lim, S.; Falcaro, P.; Hill, M. R., Magnetic Metal–Organic Frameworks for Efficient Carbon Dioxide Capture and Remote Trigger Release. *Advanced Materials* **2016**, *28* (9), 1839-1844.
13. Gallezot, P., Conversion of biomass to selected chemical products. *Chem. Soc. Rev.* **2012**, *41* (4), 1538-1558.
14. Hill, J.; Nelson, E.; Tilman, D.; Polasky, S.; Tiffany, D., Environmental, economic, and energetic costs and benefits of biodiesel and ethanol biofuels. *Proceedings of the National Academy of sciences* **2006**, *103* (30), 11206-11210.
15. Patil, A.; Taji, S., Effect of oxygenated fuel additive on diesel engine performance and emission: A review. *IOSR Journal of Mechanical and Civil Engineering (IOSR-JMCE)* **2013**, 30-35.
16. Wang, J.; Wu, F.; Xiao, J.; Shuai, S., Oxygenated blend design and its effects on reducing diesel particulate emissions. *Fuel* **2009**, *88* (10), 2037-2045.
17. Démolis, A.; Essayem, N.; Rataboul, F., Synthesis and applications of alkyl levulinates. *ACS Sustainable Chemistry & Engineering* **2014**, *2* (6), 1338-1352.

18. Rakopoulos, D.; Rakopoulos, C.; Giakoumis, E.; Dimaratos, A.; Kyritsis, D., Effects of butanol–diesel fuel blends on the performance and emissions of a high-speed DI diesel engine. *Energy Convers. Manage.* **2010**, *51* (10), 1989-1997.
19. Association, R. F., Ethanol Industry Outlook. 36 pp. Available on line in <http://www.ethanolrfa.org/pages/annual-industry-outlook> **2015**.
20. Administrator, U. S. E. P. A. O. o. t.; Board, U. S. E. A., *Environmental Administrative Decisions: Decisions of the United States Environmental Protection Agency*. US Environmental Protection Agency: 2006; Vol. 13.
21. Demirbas, A., *Biodiesel*. Springer: 2008.
22. Bozell, J. J.; Petersen, G. R., Technology development for the production of biobased products from biorefinery carbohydrates—the US Department of Energy’s “Top 10” revisited. *Green Chemistry* **2010**, *12* (4), 539-554.
23. Zhang, J.; Wu, S.; Li, B.; Zhang, H., Advances in the catalytic production of valuable levulinic acid derivatives. *ChemCatChem* **2012**, *4* (9), 1230-1237.
24. Leonard, R. H., Levulinic acid as a basic chemical raw material. *Industrial & Engineering Chemistry* **1956**, *48* (8), 1330-1341.
25. Bozell, J. J.; Moens, L.; Elliott, D.; Wang, Y.; Neuenschwander, G.; Fitzpatrick, S.; Bilski, R.; Jarnefeld, J., Production of levulinic acid and use as a platform chemical for derived products. *Resources, conservation and recycling* **2000**, *28* (3-4), 227-239.
26. Thomas, J.; Barile, R., Conversion of cellulose hydrolysis products to fuels and chemical feedstocks. *Biomass Wastes* **1985**, *8*, 1461-1494.
27. Tiong, Y. W.; Yap, C. L.; Gan, S.; Yap, W. S. P., Conversion of biomass and its derivatives to levulinic acid and levulinate esters via ionic liquids. *Industrial & Engineering Chemistry Research* **2018**, *57* (14), 4749-4766.
28. Rackemann, D. W.; Doherty, W. O., The conversion of lignocellulosics to levulinic acid. *Biofuels, Bioproducts and Biorefining* **2011**, *5* (2), 198-214.
29. Bart, H. J.; Reidetschlager, J.; Schatka, K.; Lehmann, A., Kinetics of esterification of levulinic acid with n-butanol by homogeneous catalysis. *Industrial & engineering chemistry research* **1994**, *33* (1), 21-25.
30. Van Gerpen, J. In *Cetane number testing of biodiesel*, Proceedings, third liquid fuel conference: liquid fuel and industrial products from renewable resources, American Society of Agricultural Engineers St. Joseph, MI: 1996; pp 197-206.
31. Christensen, E.; McCormick, R. L.; Williams, A.; Yanowitz, J.; Paul, S.; Burton, S., Chemical and performance properties of levulinate esters as fuel blend components. *American Chemical Society, Division of Fuel Chemistry* **2011**, *56*, 501-502.
32. Christensen, E.; Yanowitz, J.; Ratcliff, M.; McCormick, R. L., Renewable oxygenate blending effects on gasoline properties. *Energy & Fuels* **2011**, *25* (10), 4723-4733.
33. Shrivastav, G.; Khan, T. S.; Agarwal, M.; Haider, M. A., Reformulation of gasoline to replace aromatics by biomass-derived alkyl levulinate. *ACS Sustainable Chemistry & Engineering* **2017**, *5* (8), 7118-7127.
34. Sharma, Y. C.; Singh, B.; Korstad, J., Advancements in solid acid catalysts for ecofriendly and economically viable synthesis of biodiesel. *Biofuels, Bioproducts and Biorefining* **2011**, *5* (1), 69-92.
35. Dharme, S.; Bokade, V. V., Esterification of levulinic acid to n-butyl levulinate over heteropolyacid supported on acid-treated clay. *Journal of Natural Gas Chemistry* **2011**, *20* (1), 18-24.

36. Ramli, N. A. S.; Hisham, N. I.; Amin, N. A. S., Esterification of levulinic acid to levulinate esters in the presence of sulfated silica catalyst. *Sains Malaysiana* **2018**, *47* (6), 1131-1138.
37. Tejero, M.; Ramírez, E.; Fité, C.; Tejero, J.; Cunill, F., Esterification of levulinic acid with butanol over ion exchange resins. *Applied Catalysis A: General* **2016**, *517*, 56-66.
38. Barrer, R. M., *Zeolites and clay minerals as sorbents and molecular sieves*. 1978.
39. Corma, A., Preparation and catalytic properties of new mesoporous materials. *Top. Catal.* **1997**, *4* (3-4), 249-260.
40. Millini, R.; Zou, X.; Strohmaier, K.; Schwieger, W.; Eliasova, P.; Morris, R. E.; Weckhuysen, B.; Zhou, W.; Abdo, S.; Martinez, A., *Zeolites in catalysis: properties and applications*. Royal Society of Chemistry: 2017.
41. Corma, A.; Iborra, S.; Velty, A., Chemical routes for the transformation of biomass into chemicals. *Chemical reviews* **2007**, *107* (6), 2411-2502.
42. Domine, M. E.; van Veen, A. C.; Schuurman, Y.; Mirodatos, C., Coprocessing of oxygenated biomass compounds and hydrocarbons for the production of sustainable fuel. *ChemSusChem: Chemistry & Sustainability Energy & Materials* **2008**, *1* (3), 179-181.
43. Blasco, T.; Corma, A.; Navarro, M.; Pariente, J. P., Synthesis, characterization, and catalytic activity of Ti-MCM-41 structures. *J. Catal.* **1995**, *156* (1), 65-74.
44. Perot, G.; Guisnet, M., Advantages and disadvantages of zeolites as catalysts in organic chemistry. *J. Mol. Catal.* **1990**, *61* (2), 173-196.
45. Yaghi, O. M.; O'Keeffe, M.; Ockwig, N. W.; Chae, H. K.; Eddaoudi, M.; Kim, J., Reticular synthesis and the design of new materials. *Nature* **2003**, *423* (6941), 705-714.
46. Ockwig, N. W.; Delgado-Friedrichs, O.; O'Keeffe, M.; Yaghi, O. M., Reticular chemistry: occurrence and taxonomy of nets and grammar for the design of frameworks. *Acc. Chem. Res.* **2005**, *38* (3), 176-182.
47. Zhou, H.-C.; Long, J. R.; Yaghi, O. M., Introduction to metal-organic frameworks. ACS Publications: 2012.
48. Farha, O. K.; Eryazici, I.; Jeong, N. C.; Hauser, B. G.; Wilmer, C. E.; Sarjeant, A. A.; Snurr, R. Q.; Nguyen, S. T.; Yazaydin, A. O. z. r.; Hupp, J. T., Metal-organic framework materials with ultrahigh surface areas: is the sky the limit? *Journal of the American Chemical Society* **2012**, *134* (36), 15016-15021.
49. Hmadeh, M.; Lu, Z.; Liu, Z.; Gándara, F.; Furukawa, H.; Wan, S.; Augustyn, V.; Chang, R.; Liao, L.; Zhou, F., New porous crystals of extended metal-catecholates. *Chemistry of Materials* **2012**, *24* (18), 3511-3513.
50. Furukawa, H.; Cordova, K. E.; O'Keeffe, M.; Yaghi, O. M., The chemistry and applications of metal-organic frameworks. *Science* **2013**, *341* (6149).
51. Li, J.; Liu, Y.; Wang, X.; Zhao, G.; Ai, Y.; Han, B.; Wen, T.; Hayat, T.; Alsaedi, A.; Wang, X., Experimental and theoretical study on selenate uptake to zirconium metal-organic frameworks: Effect of defects and ligands. *Chemical Engineering Journal* **2017**, *330*, 1012-1021.
52. Gu, Y.; Xie, D.; Ma, Y.; Qin, W.; Zhang, H.; Wang, G.; Zhang, Y.; Zhao, H., Size modulation of zirconium-based metal organic frameworks for highly efficient phosphate remediation. *ACS applied materials & interfaces* **2017**, *9* (37), 32151-32160.
53. Wang, C.; Liu, X.; Chen, J. P.; Li, K., Superior removal of arsenic from water with zirconium metal-organic framework UiO-66. *Scientific reports* **2015**, *5*, 16613.

54. Atallah, H.; Mahmoud, M. E.; Jelle, A.; Lough, A.; Hmadeh, M., A highly stable indium based metal organic framework for efficient arsenic removal from water. *Dalton Transactions* **2018**, 47 (3), 799-806.
55. Wong-Foy, A. G.; Matzger, A. J.; Yaghi, O. M., Exceptional H₂ saturation uptake in microporous metal–organic frameworks. *Journal of the American Chemical Society* **2006**, 128 (11), 3494-3495.
56. Eddaoudi, M.; Kim, J.; Rosi, N.; Vodak, D.; Wachter, J.; O'Keeffe, M.; Yaghi, O. M., Systematic design of pore size and functionality in isoreticular MOFs and their application in methane storage. *Science* **2002**, 295 (5554), 469-472.
57. Giménez-Marqués, M.; Hidalgo, T.; Serre, C.; Horcajada, P., Nanostructured metal–organic frameworks and their bio-related applications. *Coordination Chemistry Reviews* **2016**, 307, 342-360.
58. Freund, P.; Mielewczyk, L.; Rauche, M.; Senkovska, I.; Ehrling, S.; Brunner, E.; Kaskel, S., MIL-53(Al)/Carbon Films for CO₂-Sensing at High Pressure. *ACS Sustainable Chemistry & Engineering* **2019**, 7 (4), 4012-4018.
59. Moussa, Z.; Hmadeh, M.; Abiad, M. G.; Dib, O. H.; Patra, D., Encapsulation of curcumin in cyclodextrin-metal organic frameworks: Dissociation of loaded CD-MOFs enhances stability of curcumin. *Food chemistry* **2016**, 212, 485-494.
60. Katz, M. J.; Brown, Z. J.; Colón, Y. J.; Siu, P. W.; Scheidt, K. A.; Snurr, R. Q.; Hupp, J. T.; Farha, O. K., A facile synthesis of UiO-66, UiO-67 and their derivatives. *Chemical Communications* **2013**, 49 (82), 9449-9451.
61. Stock, N.; Biswas, S., Synthesis of metal-organic frameworks (MOFs): routes to various MOF topologies, morphologies, and composites. *Chemical reviews* **2012**, 112 (2), 933-969.
62. Lee, Y.-R.; Kim, J.; Ahn, W.-S., Synthesis of metal-organic frameworks: A mini review. *Korean J. Chem. Eng.* **2013**, 30 (9), 1667-1680.
63. Jhung, S. H.; Lee, J. H.; Yoon, J. W.; Serre, C.; Férey, G.; Chang, J. S., Microwave synthesis of chromium terephthalate MIL-101 and its benzene sorption ability. *Advanced Materials* **2007**, 19 (1), 121-124.
64. Friščić, T.; Reid, D. G.; Halasz, I.; Stein, R. S.; Dinnebier, R. E.; Duer, M. J., Ion- and liquid-assisted grinding: improved mechanochemical synthesis of metal–organic frameworks reveals salt inclusion and anion templating. *Angewandte Chemie* **2010**, 122 (4), 724-727.
65. Mueller, U.; Schubert, M.; Teich, F.; Puetter, H.; Schierle-Arndt, K.; Pastre, J., Metal–organic frameworks—prospective industrial applications. *J. Mater. Chem.* **2006**, 16 (7), 626-636.
66. Son, W.-J.; Kim, J.; Kim, J.; Ahn, W.-S., Sonochemical synthesis of MOF-5. *Chemical Communications* **2008**, (47), 6336-6338.
67. Weyna, D. R.; Shattock, T.; Vishweshwar, P.; Zaworotko, M. J., Synthesis and structural characterization of cocrystals and pharmaceutical cocrystals: mechanochemistry vs slow evaporation from solution. *Cryst. Growth Des.* **2009**, 9 (2), 1106-1123.
68. Al-Ghoul, M.; Issa, R.; Hmadeh, M., Synthesis, size and structural evolution of metal–organic framework-199 via a reaction–diffusion process at room temperature. *CrystEngComm* **2017**, 19 (4), 608-612.
69. Saliba, D.; Ammar, M.; Rammal, M.; Al-Ghoul, M.; Hmadeh, M., Crystal growth of ZIF-8, ZIF-67, and their mixed-metal derivatives. *Journal of the American Chemical Society* **2018**, 140 (5), 1812-1823.

70. Dey, C.; Kundu, T.; Biswal, B. P.; Mallick, A.; Banerjee, R., Crystalline metal-organic frameworks (MOFs): synthesis, structure and function. *Acta Crystallographica Section B: Structural Science, Crystal Engineering and Materials* **2014**, *70* (1), 3-10.
71. Hardacre, C.; Parvulescu, V., *Catalysis in ionic liquids: from catalyst synthesis to application*. Royal society of chemistry: 2014; Vol. 15.
72. Caskey, S. R.; Matzger, A. J., Selected Applications of Metal-Organic Frameworks in Sustainable Energy Technologies. *Mater. Matters* **2009**, *4*, 111.
73. Rabenau, A., The role of hydrothermal synthesis in preparative chemistry. *Angewandte Chemie International Edition in English* **1985**, *24* (12), 1026-1040.
74. Klinowski, J.; Paz, F. A. A.; Silva, P.; Rocha, J., Microwave-assisted synthesis of metal-organic frameworks. *Dalton Transactions* **2011**, *40* (2), 321-330.
75. Ni, Z.; Masel, R. I., Rapid production of metal-organic frameworks via microwave-assisted solvothermal synthesis. *Journal of the American Chemical Society* **2006**, *128* (38), 12394-12395.
76. Hoogenboom, R.; Fijten, M. W.; Thijs, H. M.; van Lankvelt, B. M.; Schubert, U. S., Microwave-assisted synthesis and properties of a series of poly (2-alkyl-2-oxazoline)s. *Designed monomers and polymers* **2005**, *8* (6), 659-671.
77. Friščić, T., Metal-organic frameworks: mechanochemical synthesis strategies. *Encyclopedia of inorganic and bioinorganic chemistry* **2011**, 1-19.
78. Boldyrev, V.; Tkáčová, K., Mechanochemistry of solids: past, present, and prospects. *J. Mater. Synth. Process.* **2000**, *8* (3-4), 121-132.
79. Beyer, M. K.; Clausen-Schaumann, H., Mechanochemistry: the mechanical activation of covalent bonds. *Chemical Reviews* **2005**, *105* (8), 2921-2948.
80. Garay, A. L.; Pichon, A.; James, S. L., Solvent-free synthesis of metal complexes. *Chem. Soc. Rev.* **2007**, *36* (6), 846-855.
81. Pichon, A.; Lazuen-Garay, A.; James, S. L., Solvent-free synthesis of a microporous metal-organic framework. *CrystEngComm* **2006**, *8* (3), 211-214.
82. Chen, B.; Qian, G., *Metal-organic frameworks for photonics applications*. Springer: 2014; Vol. 157.
83. Klimakow, M.; Klobes, P.; Thunemann, A. F.; Rademann, K.; Emmerling, F., Mechanochemical synthesis of metal-organic frameworks: a fast and facile approach toward quantitative yields and high specific surface areas. *Chemistry of Materials* **2010**, *22* (18), 5216-5221.
84. Sachdeva, S.; Pustovarenko, A.; Sudhölter, E. J.; Kapteijn, F.; de Smet, L. C.; Gascon, J., Control of interpenetration of copper-based MOFs on supported surfaces by electrochemical synthesis. *CrystEngComm* **2016**, *18* (22), 4018-4022.
85. Al-Kutubi, H.; Gascon, J.; Sudhölter, E. J.; Rassaei, L., Electrosynthesis of metal-organic frameworks: challenges and opportunities. *ChemElectroChem* **2015**, *2* (4), 462-474.
86. Majedi, A.; Davar, F.; Abbasi, A., Metal-organic framework materials as nano photocatalyst. *International Journal of Nano Dimension* **2016**, *7* (1), 1-14.
87. Martinez Joaristi, A.; Juan-Alcañiz, J.; Serra-Crespo, P.; Kapteijn, F.; Gascon, J., Electrochemical synthesis of some archetypical Zn²⁺, Cu²⁺, and Al³⁺ metal organic frameworks. *Crystal Growth & Design* **2012**, *12* (7), 3489-3498.
88. Bang, J. H.; Suslick, K. S., Applications of ultrasound to the synthesis of nanostructured materials. *Advanced materials* **2010**, *22* (10), 1039-1059.
89. Li, Z.-Q.; Qiu, L.-G.; Xu, T.; Wu, Y.; Wang, W.; Wu, Z.-Y.; Jiang, X., Ultrasonic synthesis of the microporous metal-organic framework Cu₃(BTC)₂ at ambient

temperature and pressure: an efficient and environmentally friendly method. *Mater. Lett.* **2009**, *63* (1), 78-80.

90. Mason, T. J.; Peters, D., *Practical sonochemistry: Power ultrasound uses and applications*. Woodhead Publishing: 2002.

91. Li, H.; Eddaoudi, M.; Groy, T. L.; Yaghi, O., Establishing microporosity in open metal-organic frameworks: gas sorption isotherms for Zn (BDC)(BDC= 1, 4-benzenedicarboxylate). *Journal of the American Chemical Society* **1998**, *120* (33), 8571-8572.

92. Yaghi, O.; Li, H.; Eddaoudi, M.; O’Keeffe, M., Design and synthesis of an exceptionally stable and highly porous metal-organic framework. *Nature* **1999**, *402* (6759), 276-279.

93. Furukawa, H.; Miller, M. A.; Yaghi, O. M., Independent verification of the saturation hydrogen uptake in MOF-177 and establishment of a benchmark for hydrogen adsorption in metal-organic frameworks. *J. Mater. Chem.* **2007**, *17* (30), 3197-3204.

94. Chae, H. K.; Siberio-Perez, D. Y.; Kim, J.; Go, Y.; Eddaoudi, M.; Matzger, A. J.; O’Keeffe, M.; Yaghi, O. M., A route to high surface area, porosity and inclusion of large molecules in crystals. *Nature* **2004**, *427* (6974), 523-527.

95. Walton, K. S.; Snurr, R. Q., Applicability of the BET method for determining surface areas of microporous metal-organic frameworks. *Journal of the American Chemical Society* **2007**, *129* (27), 8552-8556.

96. Furukawa, H.; Ko, N.; Go, Y. B.; Aratani, N.; Choi, S. B.; Choi, E.; Yazaydin, A. Ö.; Snurr, R. Q.; O’Keeffe, M.; Kim, J., Ultrahigh porosity in metal-organic frameworks. *Science* **2010**, *329* (5990), 424-428.

97. Hönicke, I. M.; Senkowska, I.; Bon, V.; Baburin, I. A.; Bönisch, N.; Raschke, S.; Evans, J. D.; Kaskel, S., Balancing mechanical stability and ultrahigh porosity in crystalline framework materials. *Angewandte Chemie International Edition* **2018**, *57* (42), 13780-13783.

98. Farha, O. K.; Wilmer, C. E.; Eryazici, I.; Hauser, B. G.; Parilla, P. A.; O’Neill, K.; Sarjeant, A. A.; Nguyen, S. T.; Snurr, R. Q.; Hupp, J. T., Designing higher surface area metal-organic frameworks: are triple bonds better than phenyls? *Journal of the American Chemical Society* **2012**, *134* (24), 9860-9863.

99. Park, K. S.; Ni, Z.; Côté, A. P.; Choi, J. Y.; Huang, R.; Uribe-Romo, F. J.; Chae, H. K.; O’Keeffe, M.; Yaghi, O. M., Exceptional chemical and thermal stability of zeolitic imidazolate frameworks. *Proceedings of the National Academy of Sciences* **2006**, *103* (27), 10186-10191.

100. Furukawa, H.; Müller, U.; Yaghi, O. M., “Heterogeneity within Order” in Metal-Organic Frameworks. *Angewandte Chemie International Edition* **2015**, *54* (11), 3417-3430.

101. Wang, L. J.; Deng, H.; Furukawa, H.; Gándara, F.; Cordova, K. E.; Peri, D.; Yaghi, O. M., Synthesis and characterization of metal-organic framework-74 containing 2, 4, 6, 8, and 10 different metals. *Inorganic chemistry* **2014**, *53* (12), 5881-5883.

102. Lu, W.; Wei, Z.; Gu, Z.-Y.; Liu, T.-F.; Park, J.; Park, J.; Tian, J.; Zhang, M.; Zhang, Q.; Gentle Iii, T.; Bosch, M.; Zhou, H.-C., Tuning the structure and function of metal-organic frameworks via linker design. *Chemical Society Reviews* **2014**, *43* (16), 5561-5593.

103. Li, M.; Li, D.; O’Keeffe, M.; Yaghi, O. M., Topological analysis of metal-organic frameworks with polytopic linkers and/or multiple building units and the minimal transitivity principle. *Chemical reviews* **2014**, *114* (2), 1343-1370.

104. Evans, J. D.; Sumbly, C. J.; Doonan, C. J., Post-synthetic metalation of metal–organic frameworks. *Chem. Soc. Rev.* **2014**, *43* (16), 5933-5951.
105. Ricco, R.; Malfatti, L.; Takahashi, M.; Hill, A. J.; Falcaro, P., Applications of magnetic metal–organic framework composites. *Journal of Materials Chemistry A* **2013**, *1* (42), 13033-13045.
106. Buso, D.; Jasieniak, J.; Lay, M. D. H.; Schiavuta, P.; Scopece, P.; Laird, J.; Amenitsch, H.; Hill, A. J.; Falcaro, P., Highly Luminescent Metal–Organic Frameworks Through Quantum Dot Doping. *Small* **2012**, *8* (1), 80-88.
107. Buso, D.; Nairn, K. M.; Gimona, M.; Hill, A. J.; Falcaro, P., Fast synthesis of MOF-5 microcrystals using sol–gel SiO₂ nanoparticles. *Chemistry of materials* **2011**, *23* (4), 929-934.
108. Sugikawa, K.; Nagata, S.; Furukawa, Y.; Kokado, K.; Sada, K., Stable and functional gold nanorod composites with a metal–organic framework crystalline shell. *Chemistry of Materials* **2013**, *25* (13), 2565-2570.
109. He, L.; Liu, Y.; Liu, J.; Xiong, Y.; Zheng, J.; Liu, Y.; Tang, Z., Core–Shell Noble-Metal@ Metal-Organic-Framework Nanoparticles with Highly Selective Sensing Property. *Angewandte Chemie* **2013**, *125* (13), 3829-3833.
110. Zhu, Q.-L.; Li, J.; Xu, Q., Immobilizing metal nanoparticles to metal–organic frameworks with size and location control for optimizing catalytic performance. *Journal of the American chemical society* **2013**, *135* (28), 10210-10213.
111. Petit, C.; Bandosz, T. J., MOF–graphite oxide composites: combining the uniqueness of graphene layers and metal–organic frameworks. *Advanced Materials* **2009**, *21* (46), 4753-4757.
112. Lu, G.; Li, S.; Guo, Z.; Farha, O. K.; Hauser, B. G.; Qi, X.; Wang, Y.; Wang, X.; Han, S.; Liu, X., Imparting functionality to a metal–organic framework material by controlled nanoparticle encapsulation. *Nature chemistry* **2012**, *4* (4), 310-316.
113. Marx, A.; Yamamoto, H., Aluminum bis (trifluoromethylsulfonyl) amides: New highly efficient and remarkably versatile catalysts for C–C bond formation reactions. *Angewandte Chemie International Edition* **2000**, *39* (1), 178-181.
114. Fujita, M.; Kwon, Y. J.; Washizu, S.; Ogura, K., Preparation, clathration ability, and catalysis of a two-dimensional square network material composed of cadmium (II) and 4, 4'-bipyridine. *Journal of the American Chemical Society* **1994**, *116* (3), 1151-1152.
115. Hu, Z.; Zhao, D., Metal–organic frameworks with Lewis acidity: synthesis, characterization, and catalytic applications. *CrystEngComm* **2017**, *19* (29), 4066-4081.
116. Sun, Y.; Sun, L.; Feng, D.; Zhou, H. C., An in situ one-pot synthetic approach towards multivariate zirconium MOFs. *Angewandte Chemie* **2016**, *128* (22), 6581-6585.
117. Liang, W.; Coghlan, C. J.; Ragon, F.; Rubio-Martinez, M.; D'Alessandro, D. M.; Babarao, R., Defect engineering of UiO-66 for CO₂ and H₂O uptake—a combined experimental and simulation study. *Dalton Transactions* **2016**, *45* (11), 4496-4500.
118. Trickett, C. A.; Gagnon, K. J.; Lee, S.; Gándara, F.; Bürgi, H. B.; Yaghi, O. M., Definitive molecular level characterization of defects in UiO-66 crystals. *Angewandte Chemie International Edition* **2015**, *54* (38), 11162-11167.
119. Cliffe, M. J.; Wan, W.; Zou, X.; Chater, P. A.; Kleppe, A. K.; Tucker, M. G.; Wilhelm, H.; Funnell, N. P.; Coudert, F.-X.; Goodwin, A. L., Correlated defect nanoregions in a metal–organic framework. *Nature communications* **2014**, *5* (1), 1-8.
120. Olah, G. A.; Prakash, G. S.; Sommer, J.; Molnar, A., *Superacid chemistry*. John Wiley & Sons: 2009.

121. Jiang, J.; Yaghi, O. M., Brønsted acidity in metal–organic frameworks. *Chemical reviews* **2015**, *115* (14), 6966-6997.
122. Ponomareva, V. G.; Kovalenko, K. A.; Chupakhin, A. P.; Dybtsev, D. N.; Shutova, E. S.; Fedin, V. P., Imparting high proton conductivity to a metal–organic framework material by controlled acid impregnation. *Journal of the American Chemical Society* **2012**, *134* (38), 15640-15643.
123. Du, D.-Y.; Qin, J.-S.; Li, S.-L.; Su, Z.-M.; Lan, Y.-Q., Recent advances in porous polyoxometalate-based metal–organic framework materials. *Chem. Soc. Rev.* **2014**, *43* (13), 4615-4632.
124. Juan-Alcañiz, J.; Gascon, J.; Kapteijn, F., Metalorganic frameworks as scaffolds for the encapsulation of active species: state of the art and future perspectives. *J. Mater. Chem. Journal of Materials Chemistry* **2012**, *22* (20), 10102.
125. Jiao, L.; Wang, Y.; Jiang, H. L.; Xu, Q., Metal–organic frameworks as platforms for catalytic applications. *Advanced Materials* **2018**, *30* (37), 1703663.
126. Katz, M. J.; Brown, Z. J.; Colón, Y. J.; Siu, P. W.; Scheidt, K. A.; Snurr, R. Q.; Hupp, J. T.; Farha, O. K., A facile synthesis of UiO-66, UiO-67 and their derivatives. *Chemical communications (Cambridge, England)* **2013**, *49* (82), 9449-51.
127. Biswas, S.; Liu, Y. Y.; Van Der Voort, P.; Zhang, J.; Li, Z.; Sun, L.; Grzywa, M.; Volkmer, D., Enhanced selectivity of CO₂ over CH₄ in sulphonate-, carboxylate- and iodo-functionalized UiO-66 frameworks. *Dalton Trans. Dalton Transactions* **2013**, *42* (13), 4730-4737.
128. Jemal, A.; Bray, F.; Center, M. M.; Ferlay, J.; Ward, E.; Forman, D., Global cancer statistics. *CA: a cancer journal for clinicians* **2011**, *61* (2), 69-90.
129. Huang, X.; Brazel, C. S., On the importance and mechanisms of burst release in matrix-controlled drug delivery systems. *J. Controlled Release* **2001**, *73* (2-3), 121-136.
130. Taylor, K. M.; Jin, A.; Lin, W., Surfactant-Assisted Synthesis of Nanoscale Gadolinium Metal–Organic Frameworks for Potential Multimodal Imaging. *Angewandte Chemie International Edition* **2008**, *47* (40), 7722-7725.
131. Keskin, S.; Kızılel, S., Biomedical applications of metal organic frameworks. *Industrial & Engineering Chemistry Research* **2011**, *50* (4), 1799-1812.
132. Erucar, I.; Keskin, S., Efficient storage of drug and cosmetic molecules in biocompatible metal organic frameworks: A molecular simulation study. *Industrial & Engineering Chemistry Research* **2016**, *55* (7), 1929-1939.
133. Huxford, R. C.; Della Rocca, J.; Lin, W., Metal–organic frameworks as potential drug carriers. *Curr. Opin. Chem. Biol.* **2010**, *14* (2), 262-268.
134. Deng, K.; Hou, Z.; Li, X.; Li, C.; Zhang, Y.; Deng, X.; Cheng, Z.; Lin, J., Aptamer-mediated up-conversion core/MOF shell nanocomposites for targeted drug delivery and cell imaging. *Scientific reports* **2015**, *5*, 7851.
135. Horcajada, P.; Serre, C.; Vallet-Regí, M.; Sebban, M.; Taulelle, F.; Férey, G., Metal–organic frameworks as efficient materials for drug delivery. *Angewandte chemie* **2006**, *118* (36), 6120-6124.
136. Doonan, C.; Riccò, R.; Liang, K.; Bradshaw, D.; Falcaro, P., Metal–organic frameworks at the biointerface: synthetic strategies and applications. *Acc. Chem. Res.* **2017**, *50* (6), 1423-1432.
137. Sene, S.; Marcos-Almaraz, M. T.; Menguy, N.; Scola, J.; Volatron, J.; Rouland, R.; Greneche, J.-M.; Miraux, S.; Menet, C.; Guillou, N., Maghemite-nanoMIL-100 (Fe) bimodal nanovector as a platform for image-guided therapy. *Chem* **2017**, *3* (2), 303-322.

138. Schroeder, H. A.; Balassa, J. J., Abnormal trace metals in man: zirconium. *Journal of Chronic Diseases* **1966**, *19* (5), 573-586.
139. DeCoste, J. B.; Peterson, G. W.; Jasuja, H.; Glover, T. G.; Huang, Y.-g.; Walton, K. S., Stability and degradation mechanisms of metal–organic frameworks containing the Zr₆O₄(OH)₄ secondary building unit. *Journal of Materials Chemistry A* **2013**, *1* (18), 5642-5650.
140. Abánades Lázaro, I.; Forgan, R. S., Application of zirconium MOFs in drug delivery and biomedicine. *Coordination Chemistry Reviews* **2019**, *380*, 230-259.
141. Wilmer, C. E.; Farha, O. K.; Yildirim, T.; Eryazici, I.; Krungleviciute, V.; Sarjeant, A. A.; Snurr, R. Q.; Hupp, J. T., Gram-scale, high-yield synthesis of a robust metal–organic framework for storing methane and other gases. *Energy & Environmental Science* **2013**, *6* (4), 1158-1163.
142. Ma, S.; Zhou, H.-C., Gas storage in porous metal–organic frameworks for clean energy applications. *Chemical Communications* **2010**, *46* (1), 44-53.
143. Rowsell, J. L.; Yaghi, O. M., Strategies for hydrogen storage in metal–organic frameworks. *Angewandte Chemie International Edition* **2005**, *44* (30), 4670-4679.
144. Rosi, N. L.; Eckert, J.; Eddaoudi, M.; Vodak, D. T.; Kim, J.; O'Keeffe, M.; Yaghi, O. M., Hydrogen storage in microporous metal-organic frameworks. *Science* **2003**, *300* (5622), 1127-1129.
145. Colón, Y. J.; Gómez-Gualdrón, D. A.; Snurr, R. Q., Topologically guided, automated construction of metal–organic frameworks and their evaluation for energy-related applications. *Crystal Growth & Design* **2017**, *17* (11), 5801-5810.
146. Zhang, X.; Lin, R. B.; Wang, J.; Wang, B.; Liang, B.; Yildirim, T.; Zhang, J.; Zhou, W.; Chen, B., Optimization of the Pore Structures of MOFs for Record High Hydrogen Volumetric Working Capacity. *Advanced Materials* **2020**, *32* (17), 1907995.
147. Collins, D. J.; Zhou, H.-C., Hydrogen storage in metal–organic frameworks. *J. Mater. Chem.* **2007**, *17* (30), 3154-3160.
148. He, Y.; Zhou, W.; Qian, G.; Chen, B., Methane storage in metal–organic frameworks. *Chem. Soc. Rev.* **2014**, *43* (16), 5657-5678.
149. Ding, M.; Flaig, R. W.; Jiang, H.-L.; Yaghi, O. M., Carbon capture and conversion using metal–organic frameworks and MOF-based materials. *Chem. Soc. Rev.* **2019**, *48* (10), 2783-2828.
150. Meyer, L.; Schönfeld, F.; Müller-Buschbaum, K., Lanthanide based tuning of luminescence in MOFs and dense frameworks—from mono- and multimetal systems to sensors and films. *Chemical Communications* **2014**, *50* (60), 8093-8108.
151. Dang, S.; Zhang, J.-H.; Sun, Z.-M., Tunable emission based on lanthanide (III) metal–organic frameworks: an alternative approach to white light. *J. Mater. Chem.* **2012**, *22* (18), 8868-8873.
152. Zhang, H.; Zhou, L.; Wei, J.; Li, Z.; Lin, P.; Du, S., Highly luminescent and thermostable lanthanide-carboxylate framework materials with helical configurations. *J. Mater. Chem.* **2012**, *22* (39), 21210-21217.
153. Cui, Y.; Chen, B.; Qian, G., Lanthanide metal-organic frameworks for luminescent sensing and light-emitting applications. *Coordination Chemistry Reviews* **2014**, *273-274*, 76-86.
154. Assaad, N.; Sabeh, G.; Hmadeh, M., Defect Control in Zr-Based Metal Organic Framework Nanoparticles for Arsenic Removal from Water. *ACS Applied Nano Materials* **2020**.

155. Li, S.; Chen, Y.; Pei, X.; Zhang, S.; Feng, X.; Zhou, J.; Wang, B., Water purification: adsorption over metal-organic frameworks. *Chin. J. Chem.* **2016**, *34* (2), 175-185.
156. Abu Tarboush, B. J.; Chouman, A.; Jonderian, A.; Ahmad, M.; Hmadeh, M.; Al-Ghoul, M., Metal-organic framework-74 for ultratrace arsenic removal from water: experimental and density functional theory studies. *ACS Applied Nano Materials* **2018**, *1* (7), 3283-3292.
157. Zhu, L.; Liu, X.-Q.; Jiang, H.-L.; Sun, L.-B., Metal-organic frameworks for heterogeneous basic catalysis. *Chemical reviews* **2017**, *117* (12), 8129-8176.
158. Kang, Y.-S.; Lu, Y.; Chen, K.; Zhao, Y.; Wang, P.; Sun, W.-Y., Metal-organic frameworks with catalytic centers: from synthesis to catalytic application. *Coordination Chemistry Reviews* **2019**, *378*, 262-280.
159. Zhang, Y.; Yang, X.; Zhou, H.-C., Synthesis of MOFs for heterogeneous catalysis via linker design. *Polyhedron* **2018**, *154*, 189-201.
160. Doonan, C. J.; Sumby, C. J., Metal-organic framework catalysis. *CrystEngComm* **2017**, *19* (29), 4044-4048.
161. Dhakshinamoorthy, A.; Heidenreich, N.; Lenzen, D.; Stock, N., Knoevenagel condensation reaction catalysed by Al-MOFs with CAU-1 and CAU-10-type structures. *CrystEngComm* **2017**, *19* (29), 4187-4193.
162. Islam, D.; Acharya, H., Magnetically separable palladium nanocluster supported iron based metal-organic framework (MIL-88B) catalyst in efficient hydrogenation reactions. *RSC Advances* **2015**, *5* (58), 46583-46588.
163. Cirujano, F. G.; Corma, A.; Llabrés i Xamena, F. X., Conversion of levulinic acid into chemicals: Synthesis of biomass derived levulinate esters over Zr-containing MOFs. *Chemical Engineering Science* **2015**, *124*, 52-60.
164. Wang, F.; Chen, Z.; Chen, H.; Goetjen, T. A.; Li, P.; Wang, X.; Alayoglu, S.; Ma, K.; Chen, Y.; Wang, T., Interplay of Lewis and Brønsted Acid Sites in Zr-Based Metal-Organic Frameworks for Efficient Esterification of Biomass-Derived Levulinic Acid. *ACS applied materials & interfaces* **2019**, *11* (35), 32090-32096.
165. Jrad, A.; Abu Tarboush, B. J.; Hmadeh, M.; Ahmad, M., Tuning acidity in zirconium-based metal organic frameworks catalysts for enhanced production of butyl butyrate. *Applied Catalysis A: General* **2019**, *570*, 31-41.
166. Elcheikh Mahmoud, M.; Audi, H.; Assoud, A.; Ghaddar, T. H.; Hmadeh, M., Metal-Organic Framework Photocatalyst Incorporating Bis (4'-(4-carboxyphenyl)-terpyridine) ruthenium (II) for Visible-Light-Driven Carbon Dioxide Reduction. *Journal of the American Chemical Society* **2019**, *141* (17), 7115-7121.
167. Reddy, L. H.; Arias, J. L.; Nicolas, J.; Couvreur, P., Magnetic nanoparticles: design and characterization, toxicity and biocompatibility, pharmaceutical and biomedical applications. *Chemical reviews* **2012**, *112* (11), 5818-5878.
168. Colombo, M.; Carregal-Romero, S.; Casula, M. F.; Gutiérrez, L.; Morales, M. P.; Böhm, I. B.; Heverhagen, J. T.; Prosperi, D.; Parak, W. J., Biological applications of magnetic nanoparticles. *Chem. Soc. Rev.* **2012**, *41* (11), 4306-4334.
169. Della Rocca, J.; Lin, W., Nanoscale metal-organic frameworks: magnetic resonance imaging contrast agents and beyond. *Eur. J. Inorg. Chem.* **2010**, *2010* (24), 3725-3734.
170. Doherty, C. M.; Knystautas, E.; Buso, D.; Villanova, L.; Konstas, K.; Hill, A. J.; Takahashi, M.; Falcaro, P., Magnetic framework composites for polycyclic aromatic hydrocarbon sequestration. *J. Mater. Chem.* **2012**, *22* (23), 11470-11474.

171. Figuerola, A.; Di Corato, R.; Manna, L.; Pellegrino, T., From iron oxide nanoparticles towards advanced iron-based inorganic materials designed for biomedical applications. *Pharmacol. Res.* **2010**, *62* (2), 126-143.
172. Falcaro, P.; Lapierre, F.; Marmiroli, B.; Styles, M.; Zhu, Y.; Takahashi, M.; Hill, A. J.; Doherty, C. M., Positioning an individual metal–organic framework particle using a magnetic field. *Journal of Materials Chemistry C* **2013**, *1* (1), 42-45.
173. Lee, J.; Farha, O. K.; Roberts, J.; Scheidt, K. A.; Nguyen, S. T.; Hupp, J. T., Metal–organic framework materials as catalysts. *Chem. Soc. Rev.* **2009**, *38* (5), 1450-1459.
174. Alaerts, L.; Séguin, E.; Poelman, H.; Thibault-Starzyk, F.; Jacobs, P. A.; De Vos, D. E., Probing the Lewis Acidity and Catalytic Activity of the Metal–Organic Framework [Cu₃ (btc)₂](BTC= Benzene-1, 3, 5-tricarboxylate). *Chemistry–A European Journal* **2006**, *12* (28), 7353-7363.
175. Arai, T.; Sato, T.; Kanoh, H.; Kaneko, K.; Oguma, K.; Yanagisawa, A., Organic–Inorganic Hybrid Polymer-Encapsulated Magnetic Nanobead Catalysts. *Chemistry–A European Journal* **2008**, *14* (3), 882-885.
176. Huo, S.-H.; Yan, X.-P., Facile magnetization of metal–organic framework MIL-101 for magnetic solid-phase extraction of polycyclic aromatic hydrocarbons in environmental water samples. *Analyst* **2012**, *137* (15), 3445-3451.
177. Meteku, B. E.; Huang, J.; Zeng, J.; Subhan, F.; Feng, F.; Zhang, Y.; Qiu, Z.; Aslam, S.; Li, G.; Yan, Z., Magnetic metal–organic framework composites for environmental monitoring and remediation. *Coordination Chemistry Reviews* **2020**, *413*, 213261.
178. Shekhah, O.; Wang, H.; Kowarik, S.; Schreiber, F.; Paulus, M.; Tolan, M.; Sternemann, C.; Evers, F.; Zacher, D.; Fischer, R. A., Step-by-step route for the synthesis of metal–organic frameworks. *Journal of the American Chemical Society* **2007**, *129* (49), 15118-15119.
179. Falcaro, P.; Normandin, F.; Takahashi, M.; Scopece, P.; Amenitsch, H.; Costacurta, S.; Doherty, C. M.; Laird, J. S.; Lay, M. D.; Lisi, F., Dynamic Control of MOF-5 Crystal Positioning Using a Magnetic Field. *Advanced Materials* **2011**, *23* (34), 3901-3906.
180. Sanz, R.; Martínez, F.; Orcajo, G.; Wojtas, L.; Briones, D., Synthesis of a honeycomb-like Cu-based metal–organic framework and its carbon dioxide adsorption behaviour. *Dalton Transactions* **2013**, *42* (7), 2392-2398.
181. Hui, C.; Shen, C.; Yang, T.; Bao, L.; Tian, J.; Ding, H.; Li, C.; Gao, H.-J., Large-scale Fe₃O₄ nanoparticles soluble in water synthesized by a facile method. *The Journal of Physical Chemistry C* **2008**, *112* (30), 11336-11339.
182. Caskey, S. R.; Wong-Foy, A. G.; Matzger, A. J., Dramatic tuning of carbon dioxide uptake via metal substitution in a coordination polymer with cylindrical pores. *Journal of the American Chemical Society* **2008**, *130* (33), 10870-10871.
183. Badgujar, K. C.; Badgujar, V. C.; Bhanage, B. M., A review on catalytic synthesis of energy rich fuel additive levulinate compounds from biomass derived levulinic acid. *Fuel Process. Technol.* **2020**, *197*, 106213.